Morse–Bott Theory of Free Loop Spaces

nLab Materials

October 8, 2026

Abstract

Morse–Bott theory relates the geometry of closed geodesics on a Riemannian manifold to the topology of its free loop space. The Dirichlet energy functional, playing the role of a Morse function, filters this space by subspaces of loops with bounded energy. For a closed manifold, their homotopy type can change only at critical energy levels, whose critical points are constant-speed closed geodesics, including the constant loops at energy zero.

When the critical points form smooth manifolds and the energy Hessian is nondegenerate in the transverse directions, Morse–Bott theory describes these changes by attaching disk bundles determined by the energy-decreasing directions. It thereby provides a way to build the topology of the free loop space from its closed geodesics and, conversely, to use topology to deduce the existence of geodesics. These notes develop the definitions, analytic foundations, and attachment constructions in detail, with explicit computations for round spheres and projective spaces, and comparisons of how maps between manifolds act on the resulting filtrations.

associated nLab entry: ncatlab.org/nlab/show/Morse+theory

Contents

1 Idea **3**

2 Definitions **5**
2.1 Morse–Bott theory . . . 5
2.2 Free loop spaces and the Dirichlet functional . . . 6

3 Properties **10**
3.1 Analysis of the Dirichlet functional . . . 10
3.2 The topology of energy sublevels . . . 13
3.3 Maps between filtered loop spaces . . . 15

4 Examples **19**
4.1 Round spheres . . . 21
4.1.1 The 2-sphere . . . 27
4.1.2 The 4-Sphere . . . 42
4.2 Complex projective spaces . . . 56
4.3 Filtration-respecting maps . . . 59
4.3.1 Equatorial inclusions . . . 60
4.3.2 Projective subspaces . . . 60
4.3.3 Projective quotients . . . 63
4.4 Filtration-violating maps . . . 67
4.4.1 Hopf fibrations . . . 67
4.4.2 Veronese embeddings . . . 71

References **75**

1 Idea

In general *Morse theory* reconstructs a space by increasing the allowed value of a real-valued function on it. Under suitable compactness hypotheses, the sublevel sets

$$X^{\leq a} := \{x \in X \mid f(x) \leq a\}$$

have unchanged homotopy type as a varies through an interval without critical values. The changes occur at critical points. For a nondegenerate isolated critical point of index λ, the change is, up to homotopy, the attachment of a λ-dimensional disk along its boundary. Thus differential information about a function gives a geometric construction of the topology of its domain.

Symmetries often force critical points to occur in families. *Morse–Bott theory* allows a critical submanifold K, requiring that the Hessian be nondegenerate only in the directions normal to K: its kernel at $x \in K$ is exactly T_xK. The descending directions then assemble into a vector bundle $\nu^- K \to K$. Crossing its critical value attaches the disk bundle $D\nu^- K$ along the sphere bundle $S\nu^- K$; the corresponding homotopy cofiber is the Thom space

$$\mathrm{Th}(\nu^- K) = D\nu^- K / S\nu^- K.$$

This statement replaces the attachment of a single cell. It retains the topology of the critical manifold and of its negative bundle. The attaching map is further information: critical values, indices, and bundles alone do not determine the entire filtered homotopy type. Precise hypotheses and the treatment of rank-zero bundles are given below.

For a closed Riemannian manifold M, the function of interest is the energy on its free loop space,

$$E(\gamma) = \frac{1}{2}\int_0^1 |\dot\gamma(t)|^2 \,\mathrm{d}t.$$

Its critical points are the constant loops and the parametrized closed geodesics. The circle acts by changing the starting parameter, so every nonconstant critical loop already belongs to an orbit of critical loops. On round spheres and projective spaces, larger families arise by varying the initial point and direction of a geodesic. These examples are Morse–Bott, although the energy of a general Riemannian metric need not be. The Sobolev loop space supplies the Hilbert-manifold setting, and the Palais–Smale condition supplies the compactness needed for the deformation and attachment arguments.

This text keeps the actual energy sublevels in view. They distinguish loops below the first closed-geodesic threshold from those at that threshold, and they make comparisons between different Riemannian targets precise. An isometric inclusion preserves energy; a Riemannian submersion can decrease it. Both can induce maps between corresponding filtration stages, but only additional geometric conditions ensure that critical loops map to critical loops. The projective inclusions and twistor projections below illustrate this distinction. Since all these maps commute with loop rotation, the same sublevel comparisons descend to the homotopy quotient by the circle, called cyclification here.

Sources and reading guide. The variational origins are developed in Morse's *The Calculus of Variations in the Large* [Mor34]. Bott's *Nondegenerate Critical Manifolds* [Bot54] is the original source for the critical-manifold generalization; his work on iteration of closed geodesics [Bot56] connects the variational indices of iterates with the closed-geodesic problem. Milnor's *Morse Theory* [Mil63] remains a concise entry point to the finite-dimensional

attachment picture and its applications to path spaces. For the analytic passage to Hilbert manifolds, see Palais [Pal63]; for the systematic closed-geodesic theory, see Klingenberg [Kli78]. Ziller [Zil77] treats the free loop spaces of compact globally symmetric spaces and is a principal reference for the sphere and projective-space examples.

For later survey literature, Oancea [Oan15] gives a modern account organized around Morse theory, free loop spaces, and the existence of closed geodesics. Hurtubise [Hur12] surveys three approaches to finite-dimensional Morse–Bott homology: perturbation to a Morse function, cascades, and a Morse–Bott multicomplex. These are complementary viewpoints: the present account concentrates on energy sublevels, critical manifolds, and their geometric attachments, rather than constructing a chain-level Morse–Bott complex. For the geometry of the filtration-respecting maps, the submersion formulas originate with O'Neill [ONe66]; the homogeneous projective examples also belong to the setting studied by Escobales [Esc75].

2 Definitions

We first give the general Morse–Bott definitions and then specialize to the Dirichlet energy on a free loop space. The deformation and attachment theorems are developed in § 3.

2.1 Morse–Bott theory

For a smooth function $f : X \to \mathbb{R}$, Morse theory studies how the subspaces $X^{\leq a} := \{x \in X : f(x) \leq a\}$ change as a increases. In finite dimensions, a Morse function has isolated critical points with nondegenerate Hessians. Morse–Bott theory allows critical points to occur in smooth families: the Hessian is required to be nondegenerate transverse to each critical submanifold. Under suitable compactness hypotheses, passing a critical level attaches the disk bundle of the negative Hessian directions along its sphere bundle. An isolated critical point gives the familiar attachment of a cell of dimension equal to its index; a critical manifold replaces that cell by a bundle over the manifold [Mil63; Bot54].

We use the version for smooth functions on Hilbert manifolds, with finite-dimensional critical manifolds and finite Morse indices. In this setting the Fredholm and compactness conditions must be specified explicitly. The definitions also apply in finite dimensions.

Critical points and the Morse–Bott condition. The Hessian records the quadratic behavior at a critical point. Its negative directions determine the index, while its kernel detects degeneracy.

Definition 2.1 (Hessian, index, and nullity)**.** Let f be a smooth function on a Hilbert manifold X, and let $x \in X$ be critical, meaning $df_x = 0$. The second derivative at x is a coordinate-independent continuous symmetric bilinear form $\operatorname{Hess}_x f$ on T_xX. A strong Hilbert inner product represents it by a bounded self-adjoint operator A_x:

$$\operatorname{Hess}_x f(v, w) = \langle A_x v, w\rangle.$$

The *index* $\operatorname{ind}_x f$ is the maximal dimension of a subspace on which this form is negative definite. Its *nullity* is $\operatorname{nul}_x f = \dim\ker A_x$. These quantities do not depend on the chosen equivalent Hilbert inner product. A critical point is *nondegenerate* if A_x is boundedly invertible. A function all of whose critical points are nondegenerate is a *Morse function*.

Definition 2.2 (Morse–Bott condition of finite index)**.** A critical submanifold $K \subset X$ is *Morse–Bott of finite index* if it is a finite-dimensional embedded submanifold and, for every $x \in K$, the Hessian operator is Fredholm, has finite index, and satisfies

$$\ker \operatorname{Hess}_x f = T_xK. \tag{1}$$

Locally K is required to be the whole critical set. A function is Morse–Bott if its critical set is a disjoint union of such submanifolds, locally separated from one another. For the passage-through-a-level results below we additionally require the critical manifolds in that level to be compact.

Remark 2.3 (Why Fredholm is part of the definition)*.* In a finite-dimensional normal space, absence of a kernel implies invertibility. In a Hilbert space an injective Hessian can have non-closed range. The Fredholm hypothesis makes the restriction to the orthogonal complement of the kernel boundedly invertible, which is the hypothesis needed for the Morse lemma.

Negative bundles and Thom spaces. The negative Hessian directions assemble into the bundles that enter the attachment construction.

Definition 2.4 (Negative bundle and Thom space)**.** Along a compact connected Morse–Bott critical manifold K, the negative spectral subspaces of A_x form a finite-rank vector bundle $\nu^- K \to K$, of rank $\lambda = \operatorname{ind}_K f$. The positive spectral subspaces form a Hilbert bundle $\nu^+ K$. The rank is locally constant, hence constant on K. For a finite-rank vector bundle ξ, let $D\xi$ and $S\xi$ be its unit disk and sphere bundles. Its *Thom space* is the pointed quotient

$$\operatorname{Th}(\xi) = D\xi / S\xi.$$

For a rank-zero bundle this is understood as K_+, obtained by adjoining a disjoint basepoint.

Justification of the bundle assertion. An invertible self-adjoint Fredholm operator on the normal space has a gap around zero in its spectrum. Compactness of K gives locally uniform gaps. Spectral projection onto the negative spectrum varies smoothly with the operator and has constant finite rank locally. Its images therefore define a smooth finite-rank subbundle. The positive bundle is obtained in the same way. Different choices of the strong inner product give isomorphic negative bundles, for instance by interpolating the metrics and projecting along the resulting family. □

The Palais–Smale condition. In infinite dimensions a bounded sublevel need not be compact. The following condition supplies the compactness needed for the deformation arguments in Thms. 3.8 and 3.10.

Definition 2.5 (Palais–Smale condition)**.** Fix a strong Riemannian metric on X. The function f satisfies the *Palais–Smale condition* if every sequence x_j such that $f(x_j)$ is bounded and $\|df_{x_j}\| \to 0$ has a convergent subsequence in X. The norm here is the dual Hilbert norm. In the deformation arguments one uses a complete strong metric, or a complete bounded pseudo-gradient with the corresponding compactness and descent estimates.

2.2 Free loop spaces and the Dirichlet functional

We now specialize the preceding framework to $X = L_\infty M$ and $f = E_g$, the Dirichlet energy of a loop. Throughout this application, (M, g) is a *closed* Riemannian manifold, meaning compact and without boundary; its metric and finite-dimensional manifold structure are smooth. Loops are parametrized by $t \in S^1 = \mathbb{R}/\mathbb{Z}$, and our energy convention includes a factor $1/2$. The letter $R > 0$ denotes a sphere radius, whereas R denotes the curvature tensor. We work with parametrized loops, not unparametrized geodesics, and nullity counts the whole Hessian kernel, including the loop-rotation direction.

The analytic setting is the Hilbert manifold of Sobolev H^1 loops. The basic tools assumed from analysis are the Sobolev embedding and compactness theorems on an interval, the inverse function theorem on Hilbert spaces, and existence and uniqueness for ordinary differential equations. We give proofs of the variation formulas, the compactness argument needed here, the local Morse–Bott normal form, and the explicit examples. The global handle-attachment theorem is stated with its hypotheses and its local-to-global construction; for a fully developed treatment of that machinery see [Pal63; Kli78]. The overview [Oan15] provides a guide to the wider closed-geodesic literature.

The free loop space and its Hilbert model. The Sobolev model gives the loop space a smooth Hilbert manifold structure on which the energy is defined.

Definition 2.6 (Sobolev free loop space)**.** Let (M, g) be a closed Riemannian manifold. Its *Sobolev free loop space* is

$$L_\infty M \;=\; H^1(S^1, M).$$

Using a smooth embedding $M \hookrightarrow \mathbb{R}^N$, this is the space of absolutely continuous periodic maps into M whose weak derivative is square integrable, with the induced H^1 topology. The definition is independent of the embedding. For any space X, write $LX := C^0(S^1, X)$ for the unrestricted free loop space with its compact-open topology. We write $C^\infty(S^1, M)$ for smooth loops with their usual smooth topology. The comparison in Lem. 2.8 identifies $L_\infty M$ and LM at the level of homotopy groups. The subscript ∞ indicates the absence of an energy cutoff; the Sobolev regularity is specified by the displayed definition.

Proposition 2.7 (Loop-space charts)**.** *The space $L_\infty M$ is a smooth Hilbert manifold, with*

$$T_\gamma L_\infty M \;=\; H^1(S^1, \gamma^* TM).$$

Near a smooth loop γ, choose an open neighborhood $\mathcal{U}_\gamma$ of zero in $H^1(S^1, \gamma^*TM)$ on which sections are sufficiently small in the uniform norm. The pointwise exponential map is a chart parametrization:

$$\begin{aligned} \mathcal{U}_\gamma &\longrightarrow L_\infty M \\ V &\longmapsto \Big(t \longmapsto \exp_{\gamma(t)} V(t)\Big). \end{aligned}$$

Proof. In dimension one, H^1 embeds continuously into C^0 and is a Banach algebra under multiplication. Smooth maps between finite-dimensional manifolds therefore induce smooth composition maps on H^1 on sets whose images lie in compact coordinate neighborhoods. Choose a uniform normal radius along γ. The exponential map and its inverse give mutually inverse charts by this composition property. Their derivatives at the zero section identify tangent vectors with H^1 vector fields along the loop. Smooth loops are dense by Lem. 2.8; their chart neighborhoods cover $L_\infty M$. Coordinate changes are smooth by the same composition argument. Changes of the auxiliary embedding are also smooth composition maps. □

Lemma 2.8 (Comparison with continuous and smooth loops)**.** *Smooth loops are dense in $L_\infty M$. The inclusions*

$$C^\infty(S^1, M) \;\longrightarrow\; L_\infty M \;\longrightarrow\; LM$$

induce isomorphisms on all homotopy groups, with any chosen smooth base loop.

Proof. Embed M in Euclidean space and choose a smooth tubular retraction $r : U \to M$. For a periodic loop γ, convolve its Euclidean coordinates with a periodic smooth approximate identity η_ϵ. For sufficiently small ϵ,

$$S_\epsilon \gamma \;=\; r(\eta_\epsilon * \gamma)$$

is defined and smooth. It converges to γ in H^1 for an H^1 loop, and uniformly for a continuous loop. Retraction of the straight-line interpolation supplies a homotopy between the loop and its smoothing. For a compact family of loops the same ϵ works uniformly, and these constructions are continuous in the relevant topology. For fixed positive ϵ, dependence on the original loop is continuous into the smooth topology. Apply this to a family parametrized by a sphere for surjectivity on homotopy groups, and by a disk for injectivity. On a boundary already consisting of smooth loops, the interpolation stays smooth; its collar supplies the relative adjustment. The base loop can be kept fixed by this same relative construction. □

Energy, length, and reparametrization. The functional used in the variational theory is the Dirichlet energy. Its relation to length depends on the parametrization.

Definition 2.9 (Dirichlet energy and length)**.** For $\gamma \in L_\infty M$, its *Dirichlet energy* and length are

$$E_g(\gamma) = \frac{1}{2}\int_0^1 |\dot\gamma(t)|_g^2 \,\mathrm{d}t, \qquad \ell_g(\gamma) = \int_0^1 |\dot\gamma(t)|_g \,\mathrm{d}t. \tag{2}$$

For $a \geq 0$, write

$$L_\infty^{\leq a} M = \{\gamma : E_g(\gamma) \leq a\}, \qquad L_\infty^{<a} M = \{\gamma : E_g(\gamma) < a\}. \qquad L_\infty^0 M = \{E_g = 0\}.$$

Thus $L_\infty^0 M$ is canonically the submanifold M of constant loops.

Remark 2.10 (Which topology is being filtered). Energy is smooth on the H^1 model. A general continuous loop need not have a square-integrable weak derivative, so its energy need not be finite or defined by the displayed integral. If $\dim M > 0$, even on smooth loops energy is not continuous for the uniform topology: in a unit-speed geodesic coordinate, for large n the loops $t \mapsto n^{-1}\sin(2\pi n^2 t)$ converge uniformly to a constant while their energies are $\pi^2 n^2$. Our sublevels always use the H^1 topology. The unfiltered smoothing statement does not assert preservation of an exact energy bound.

Lemma 2.11 (Elementary normalization identities)**.** *For $c > 0$, a positive integer q, and $\gamma^{(q)}(t) = \gamma(qt)$, one has*

$$\ell_g(\gamma)^2 \leq 2E_g(\gamma), \qquad E_{c^2 g}(\gamma) = c^2 E_g(\gamma), \qquad E_g(\gamma^{(q)}) = q^2 E_g(\gamma). \tag{3}$$

Equality in the first relation holds exactly when the speed is constant almost everywhere.

Proof. The first claim is Cauchy–Schwarz applied to $|\dot\gamma|$ and the constant function 1 on an interval of length 1; its equality condition is the stated one. The second follows by scaling the integrand in (2). For the third, the chain rule supplies a factor q^2 and periodicity gives $\int_0^1 |\dot\gamma(qt)|^2 \,\mathrm{d}t = \int_0^1 |\dot\gamma(t)|^2 \,\mathrm{d}t$. □

Remark 2.12. Length is invariant under smooth reparametrizations of the circle. Energy is invariant under the circle isometries $t \mapsto \pm t + \theta$, but need not be invariant under other reparametrizations. A nonconstant critical loop has constant speed, hence energy $\ell^2/2$.

The critical points of E_g are the constant-speed closed geodesics, as proved in Thm. 3.1. Rotating a nonconstant closed geodesic gives a family of critical loops; the constant loops also form a critical manifold isomorphic to M. These families explain why Morse–Bott theory is the appropriate framework. The energy is not automatically Morse–Bott for an arbitrary Riemannian metric: the transverse nondegeneracy condition must be checked. We verify it explicitly for the standard spheres and projective spaces in § 4.

The critical-energy filtration. Energy sublevels are defined for every bound. When the critical values form a discrete sequence, one can also index the filtration by its successive critical levels.

Definition 2.13 (Critical-energy filtration)**.** Suppose the distinct critical values of E_g are a discrete sequence

$$0 = c_0 < c_1 < c_2 < \cdots, \qquad c_m \longrightarrow \infty.$$

The *critical-energy stages* are the actual subspaces

$$L_m M := L_\infty^{\leq c_m} M. \tag{4}$$

Since every Sobolev loop has finite energy and $c_m \to \infty$,

$$L_0 M \subset L_1 M \subset L_2 M \subset \cdots \subset L_\infty M, \qquad \bigcup_{m \geq 0} L_m M = L_\infty M.$$

The unrestricted stage $L_\infty M$ retains its H^1 topology. Thus $L_0 M = M$ and the *first positive critical stage* $L_1 M$ includes the first positive critical level. Sublevels below that level may already contain nonconstant loops. For the standard spheres and projective spaces, Prop. 4.2 will show that $L_1 M$ is exactly the first stage with a homotopy type different from that of the constant loops. For handle arguments one can instead choose regular values $c_m < a_m < c_{m+1}$ and use $L_\infty^{\leq a_m} M$. The comparison of these two choices is addressed in Thm. 3.10. Stage number is not Morse index.

Loop rotation and cyclification. Loop rotation preserves the energy filtration. Its homotopy quotient retains both the loops and the symmetry of their parametrization.

Definition 2.14 (Rotation and filtered cyclification)**.** The circle acts on loops by $(\theta \cdot \gamma)(t) = \gamma(t + \theta)$. Its homotopy quotient is

$$\operatorname{Cyc} M := ES^1 \times_{S^1} L_\infty M, \qquad \operatorname{Cyc}_m M := ES^1 \times_{S^1} L_m M.$$

Here ES^1 is a contractible free S^1-space and $BS^1 = ES^1/S^1$. The projection to the first factor gives $\operatorname{Cyc} M \to BS^1$, and similarly for every stage. The inclusions of stages give a filtration over BS^1.

Remark 2.15 (Two technical distinctions). Rotation preserves energy by change of variable. It acts continuously on H^1 loops, and each fixed rotation acts smoothly. The joint action is generally not differentiable on H^1, since differentiating in the rotation parameter loses a derivative. No smooth joint action is needed to form the homotopy quotient.

The homotopy quotient is also not the orbit space. Constants have stabilizer S^1, and an m-fold primitive closed geodesic has stabilizer $\mathbb{Z}/m$. In particular, $\operatorname{Cyc}_0 M = M \times BS^1$, not just M.

3 Properties

We first analyze the Dirichlet functional of Def. 2.9, then explain how its critical manifolds govern the topology of its sublevels. Finally, we establish criteria for maps between Riemannian manifolds to induce maps between the resulting filtered loop spaces.

3.1 Analysis of the Dirichlet functional

We investigate the Dirichlet functional E_g of Def. 2.9: we identify its critical loops, describe its Hessian, and establish the compactness condition needed for the deformation arguments below.

Critical loops and the first variation. The first variation identifies the critical loops with closed geodesics, including the constant loops.

Theorem 3.1 (Critical points of the energy)**.** *The Dirichlet functional E_g is a smooth function on $L_\infty M$. Its differential is*

$$dE_\gamma(V) \;=\; \int_0^1 \langle D_t V, \dot\gamma\rangle \,\mathrm{d}t. \tag{5}$$

A loop is critical if and only if it is a smooth periodic geodesic, including the constant geodesics. Its velocity is periodic and its speed is constant.

Proof. In a coordinate chart the energy density is $\frac{1}{2}g_{ij}(x)\dot x^i\dot x^j$. The H^1 composition and multiplication properties used in Prop. 2.7 show that its integral depends smoothly on x. For a smooth variation $F(s,t)$, torsion-freeness gives $D_s\partial_t F = D_t\partial_s F$, hence

$$\frac{\mathrm{d}}{\mathrm{d}s}E(F(s,-))\Big|_{s=0} \;=\; \int_0^1 \langle D_t V, \dot\gamma\rangle \,\mathrm{d}t.$$

Density extends the identity to H^1 loops and fields. For a smooth periodic loop, integration by parts yields $dE_\gamma(V) = -\int_0^1\langle V, D_t\dot\gamma\rangle\,\mathrm{d}t$, with no boundary term.

Conversely, a weak critical loop satisfies, on coordinate intervals,

$$\frac{\mathrm{d}}{\mathrm{d}t}(g_{ij}(x)\dot x^j) \;=\; \frac{1}{2}\,\partial_i g_{jk}(x)\dot x^j\dot x^k$$

in the distributional sense. The right side is in L^1. Thus the momentum $g_{ij}(x)\dot x^j$ is locally $W^{1,1}$ and continuous; consequently $\dot x$ is continuous. The equation then gives $x \in C^2$, and bootstrapping gives smoothness. The weak equation across the seam $0 = 1$ makes the momentum, hence the velocity, periodic. The equation is precisely $D_t\dot\gamma = 0$. Finally, $\frac{\mathrm{d}}{\mathrm{d}t}|\dot\gamma|^2 = 2\langle D_t\dot\gamma,\dot\gamma\rangle = 0$. □

The Hessian and periodic Jacobi fields. At a critical loop, the second variation determines the negative and null directions. We fix a curvature convention before writing this Hessian as the index form.

Notation 3.2 (Curvature convention)**.** We use

$$\mathsf{R}(X,Y)Z \;=\; \nabla_X\nabla_Y Z - \nabla_Y\nabla_X Z - \nabla_{[X,Y]}Z.$$

On the sphere of radius R this convention gives

$$\mathsf{R}(V,T)T \;=\; R^{-2}\Big(|T|^2V - \langle V,T\rangle T\Big).$$

Theorem 3.3 (Index form and periodic Jacobi fields)**.** *At a closed geodesic γ, the Hessian of the Dirichlet functional E_g is*

$$\begin{aligned}\operatorname{Hess}_\gamma E_g(V,W) \;&=\; I_\gamma(V,W)\\ &=\; \int_0^1 \left(\langle D_tV, D_tW\rangle - \langle \mathsf{R}(V,\dot\gamma)\dot\gamma, W\rangle\right)\,\mathrm{d}t.\end{aligned} \tag{6}$$

Its kernel consists of the smooth solutions of

$$D_t^2V + \mathsf{R}(V,\dot\gamma)\dot\gamma \;=\; 0, \qquad V(1) \;=\; V(0), \quad D_tV(1) \;=\; D_tV(0). \tag{7}$$

The endpoint equalities are in the common tangent space at $\gamma(0) \;=\; \gamma(1)$.

Proof. Differentiate the first-variation formula at a geodesic and use the commutator identity for covariant derivatives along a two-parameter variation. Terms multiplying $D_t\dot\gamma$ vanish. The curvature symmetries and integration by parts give (6). This also shows its symmetry.

If $I_\gamma(V,W) \;=\; 0$ for all periodic W, testing with fields supported inside an interval gives the Jacobi equation weakly. It is a linear second-order ordinary differential equation with smooth coefficients, so its weak solutions are smooth. After integration by parts the remaining boundary term is $\langle D_tV(1) - D_tV(0), W(0)\rangle$; arbitrary $W(0)$ forces the second periodicity condition. The converse follows by substitution and the same integration by parts. □

Proposition 3.4 (Finite index and nullity)**.** *The Hessian of the Dirichlet functional E_g at every closed geodesic is a self-adjoint Fredholm form with finite index and nullity. In particular, a smooth finite-dimensional critical manifold is Morse–Bott once its tangent space is shown to exhaust the periodic Jacobi fields.*

Proof. On fields along γ use the Hilbert inner product

$$\langle V,W\rangle_1 \;=\; \int_0^1 \Big(\langle D_tV, D_tW\rangle + \langle V,W\rangle\Big)\,\mathrm{d}t.$$

Relative to it, (6) is represented by $A \;=\; 1-K$. Indeed, the difference from this inner product is a bounded zeroth-order bilinear form, and the embedding $H^1(\gamma^*TM) \;\hookrightarrow\; L^2(\gamma^*TM)$ is compact. The corresponding self-adjoint operator K is therefore compact. The spectral theorem for compact self-adjoint operators implies that $1-K$ has finite-dimensional kernel and only finitely many negative eigenvalues, with closed range. If the kernel is exactly tangent to a critical submanifold, the Hessian is invertible in its normal directions. The implicit function theorem applied to the normal component of the gradient then shows that this submanifold is locally the whole critical set, as required by Def. 2.2. □

Remark 3.5 (A variation of geodesics produces a Jacobi field). Differentiating a smooth family of closed geodesics gives an element of (7). Thus $TK \;\subseteq\; \ker I$ is automatic for a critical manifold K. The substantive Morse–Bott calculation is the reverse inclusion. Our nullity includes the field $\dot\gamma$ when γ is nonconstant.

Palais–Smale compactness for the Dirichlet functional. To use these local calculations in global deformation arguments, we need convergence of sequences with bounded energy and vanishing differential. Compactness of the underlying manifold supplies this Palais–Smale property.

Proposition 3.6 (Palais–Smale compactness for loop energy)**.** *For a closed Riemannian manifold, the energy on $L_\infty M$ satisfies the Palais–Smale condition for the usual strong H^1 metric.*

Proof. Let $E(\gamma_j)$ be bounded and $\|dE_{\gamma_j}\| \to 0$. Embed M in Euclidean space. Compactness of M and equivalence of the metrics on its tangent bundle make γ_j bounded in the Euclidean H^1 norm. After passage to a subsequence, γ_j converges weakly in H^1 and strongly in C^0 to an H^1 loop γ with values in M.

Choose a smooth reference loop uniformly close to γ and use an exponential chart about it. Write the loops as u_j and u in a fixed H^1 bundle of coordinate fields. They remain bounded in H^1, converge uniformly, and converge weakly in H^1. In bundle trivializations the energy density has the form

$$\frac{1}{2}a(t,u)(\dot{u},\dot{u}) + b(t,u)\dot{u} + c(t,u),$$

where a is uniformly positive definite on the compact coordinate region. The Palais–Smale assumption, tested against the bounded field $u_j - u$, gives $dE(u_j)(u_j - u) \to 0$. The terms involving a derivative of a in the u direction are bounded by $O(\|u_j - u\|_{C^0}\|\dot{u}_j\|_{L^2}^2)$ and tend to zero. The b, c terms tend to zero by uniform convergence and weak convergence of the derivatives. Consequently

$$\int_0^1 a(t,u_j)(\dot{u}_j, \dot{u}_j - \dot{u})\,\mathrm{d}t \longrightarrow 0.$$

Replace $a(t,u_j)$ by $a(t,u)$ using uniform convergence. The cross term with $\dot{u}$ vanishes by weak convergence, so uniform positivity gives $\|\dot{u}_j - \dot{u}\|_{L^2} \to 0$. This proves strong H^1 convergence.

The argument is unchanged under the coordinate changes and partitions needed to trivialize the bundle: all additional terms are of the displayed lower order. The intrinsic and coordinate H^1 norms are uniformly equivalent on these bounded sets, so the tested differentials do tend to zero. □

Remark 3.7 (A complete metric for the deformation arguments). A smooth embedding $\iota : M \hookrightarrow \mathbb{R}^N$ realizes $H^1(S^1, M)$ as a closed Hilbert submanifold of $H^1(S^1, \mathbb{R}^N)$. The induced strong metric is complete: a Cauchy sequence for its path distance is Cauchy in the ambient Hilbert norm; its limit lies in the submanifold, and a chart gives convergence also in path distance.

This embedding need not be isometric for g. For $W = d\iota_\gamma V$, the comparison of derivatives is

$$\dot{W} = d\iota_\gamma(D_t^g V) + B_\gamma(\dot{\gamma}, V), \qquad B := \nabla d\iota,$$

where B uses the given Levi-Civita connection and the Euclidean connection. Compactness of M bounds B, $d\iota$, and the inverse of $d\iota$ on its image. The one-dimensional Sobolev estimate controls $\|V\|_{C^0}$ by its intrinsic H^1 norm, and $\|W\|_{C^0}$ by its ambient H^1 norm. Applying the

displayed identity in both directions therefore gives, on each fixed energy sublevel,

$$C^{-1}\|V\|_{H^1,g} \;\le\; \|d\iota_\gamma V\|_{H^1,\mathbb{R}^N} \;\le\; C\|V\|_{H^1,g}.$$

The dual norms are equivalent there as well. Hence Prop. 3.6 also holds for this complete strong metric, which may be used in the following deformation arguments.

3.2 The topology of energy sublevels

We now explain how critical manifolds determine changes in the homotopy type of sublevels. We state the deformation and attachment results for a general smooth function f. For $f = E_g$ on the loop space of a closed Riemannian manifold, § 3.1 supplies the analytic hypotheses; the Morse–Bott condition at the critical level under consideration remains to be checked in each application.

Intervals without critical values. On a band containing no critical points, the descending flow identifies the homotopy types of the sublevels at its two ends.

Theorem 3.8 (A band without critical points)**.** *Let $f : X \to \mathbb{R}$ be smooth and satisfy Palais–Smale on a complete strong Hilbert manifold. If the compact interval $[a, b]$ contains no critical value, then $X^{\le a} \hookrightarrow X^{\le b}$ is a homotopy equivalence, in fact a deformation retract.*

Proof. There is a $\delta > 0$ with $\|\nabla f\| \ge \delta$ on $f^{-1}[a, b]$. Otherwise a sequence violating this bound has a convergent subsequence by Palais–Smale, whose limit would be a critical point in the band. The same compactness argument excludes critical values sufficiently close to $[a, b]$. On a slightly larger closed band the gradient is again bounded away from zero. There use

$$Z \;=\; -\frac{\nabla f}{\|\nabla f\|^2}.$$

A cutoff outside the larger band makes Z a bounded smooth vector field on the complete manifold. Its flow exists for the required finite times, and $df(Z) = -1$ on $[a, b]$. For $x \in X^{\le b}$ flow for time $s \max\{f(x) - a, 0\}$, $0 \le s \le 1$. The result is continuous, remains in $X^{\le b}$, fixes $X^{\le a}$, and ends in it. □

Local form near a critical manifold. Near a Morse–Bott critical manifold, normal coordinates reduce the function to a quadratic form. Its negative directions will supply the bundle attached when the critical level is crossed.

Theorem 3.9 (Morse–Bott normal form)**.** *Let K be a compact Morse–Bott critical manifold of a smooth function f, with $f|_K = c$. In a neighborhood of its zero section, there are normal-bundle coordinates in which*

$$f(x, u, v) \;=\; c - \|u\|^2 + \|v\|^2, \qquad u \in \nu_x^- K, \quad v \in \nu_x^+ K. \tag{8}$$

The coordinate map restricts to the identity on K.

Proof. Use a tubular neighborhood of K and the orthogonal normal bundle. The Hessian is invertible on each normal fiber. Its spectral splitting and its absolute value reduce it, by

a smooth fiberwise linear change, to the involution $J = -1$ on the negative summand and $+1$ on the positive summand. All inverse bounds can be chosen locally uniformly on K.

Here is the remaining nonlinear step, including its dependence on the parameter x. Taylor's formula on a normal fiber gives

$$f(x,w) - c = \frac{1}{2}\langle B(x,w)w, w\rangle, \qquad B(x,w) = 2\int_0^1 (1-s)D_w^2 f(x,sw)\,\mathrm{d}s,$$

with $B(x,0) = J$. The operators B are bounded, self-adjoint, and smooth in (x,w). On bounded self-adjoint operators C consider

$$C \longmapsto (1+JC)^* J(1+JC) = J + 2C + CJC.$$

Its derivative at 0 is $C \mapsto 2C$, an isomorphism. The inverse function theorem therefore provides a smooth $C = C(x,w)$, vanishing at $w = 0$, for which $B = (1+JC)^*J(1+JC)$. The change $w \mapsto z = (1+JC(x,w))w$ is a local diffeomorphism with identity derivative at zero, and makes the function $c + \frac{1}{2}\langle Jz, z\rangle$. Rescale z to absorb $1/2$.

These constructions are fiberwise and natural under isometric trivializations of the split normal bundle. The local solutions from the inverse function theorem agree on overlaps by uniqueness. Shrinking the neighborhood along the compact zero section yields the asserted bundle normal form. □

Crossing a critical level. Combining this local normal form with descent away from the critical manifold describes the new sublevel by attaching its negative disk bundle.

Theorem 3.10 (Passage through a Morse–Bott level)**.** *Let f be a smooth function satisfying Palais–Smale on a complete strong Hilbert manifold. Suppose that the only critical points in $f^{-1}[c-\epsilon_0, c+\epsilon_0]$ form a compact Morse–Bott manifold $K \subset f^{-1}(c)$. For sufficiently small $\epsilon > 0$, put $X^- = X^{\le c-\epsilon}$ and $X^+ = X^{\le c+\epsilon}$. Then there is an attaching map $\alpha : S(\nu^- K) \to X^-$ and a homotopy equivalence of pairs*

$$(X^+, X^-) \simeq \left(X^- \cup_\alpha D(\nu^- K), X^-\right). \tag{9}$$

In particular,

$$\operatorname{hocofib}(X^- \hookrightarrow X^+) \simeq \operatorname{Th}(\nu^- K). \tag{10}$$

The inclusion $X^{\le c} \hookrightarrow X^+$ is also a homotopy equivalence. The same assertions apply to a finite disjoint union of critical manifolds at c, with one negative bundle for each component.

Construction of the attachment. In the coordinates of Thm. 3.9, the function is $c - \|u\|^2 + \|v\|^2$. Shrinking v to zero decreases the function and preserves the negative coordinate. The new part left at this level is therefore the negative disk bundle. At $v = 0$, its sphere of radius $\sqrt{\epsilon}$ lies at $c-\epsilon$; this is the local attaching locus. Rescaling the fibers identifies it with the unit sphere bundle in the statement.

Choose nested normal neighborhoods of K. On the complement of the smaller one in the energy band, Palais–Smale gives a uniform lower bound for the gradient: a sequence with gradient tending to zero there would converge to a critical point outside that neighborhood. The descending flow therefore pushes this complement to X^- or into the normal neighborhood. In the neighborhood use the quadratic descending field $(u, -v)$, with a cutoff on its collar. A partition of unity combines it with the outside descending field; the strict inequality $df(Z) < 0$ is preserved on the overlap. Choose the local disk radii with collars so

that the outgoing boundary is in the negative direction. Flow along that boundary to X^- defines α. Contract the positive fibers and then the collars. These operations give the pair homotopy equivalence (9). This is the Hilbert-manifold handle construction: the contracted positive fibers may be infinite dimensional, whereas the retained negative bundle has finite rank.

For the last assertion there is an additional local deformation, fixing the sublevel at c: whenever $\|v\| > \|u\|$, shrink v to $(\|u\|/\|v\|)v$, and otherwise leave it fixed. The linear interpolation decreases f, is continuous also at $(0,0)$, and takes the local sublevel at $c+\epsilon$ into that at c. Combine this with descent outside the critical neighborhood, using the same collars. This proves the comparison with the exact critical sublevel. Finally, taking the homotopy cofiber of the attached pair collapses the sphere bundle and gives (10). Full collar and flow constructions in the Hilbert setting are developed in [Pal63; Kli78]. □

Relative homology and attaching maps. The Thom isomorphism computes the relative homology of this attachment. Recovering the homotopy type of the new sublevel, however, also requires the attaching map.

Corollary 3.11 (Relative homology with its orientation system)**.** *In Thm. 3.10, if K is connected and its index is λ, then*

$$H_j(X^+, X^-; \mathbb{Z}) \cong H_{j-\lambda}(K; \mathfrak{o}_{\nu^-}),$$

where $\mathfrak{o}_{\nu^-}$ is the orientation local system of the negative bundle. With coefficients in $\mathbb{F}_2$ the orientation twist disappears. It also disappears over $\mathbb{Z}$ after an orientation of ν^- is chosen.

Proof. Apply the relative Thom isomorphism to $(D\nu^-, S\nu^-)$ and use (9). □

Remark 3.12 (What the indices do not determine). The critical manifolds, their indices, and even their negative bundles do not specify the attaching maps α. Thus this theorem does not by itself split the homology of the entire loop space into critical-manifold summands. Any perfection or splitting assertion requires an additional argument. We do not assume one here.

3.3 Maps between filtered loop spaces

We next compare the filtrations under maps of Riemannian manifolds. A bound on the differential controls numerical energy sublevels. To compare the numbered critical stages of Def. 2.13, one must additionally compare the ordered critical values in source and target; the examples below make this distinction explicit.

Energy comparison under composition. The chain rule translates a pointwise bound on the differential into an energy bound for the induced map of loop spaces.

Proposition 3.13 (Maps with a differential bound)**.** *Let $F : (N,h) \to (M,g)$ be smooth and suppose $|dF_x(v)|_g \le A|v|_h$ for all tangent vectors, with $A \ge 0$. Composition defines a continuous map of loop spaces with*

$$E_g(F \circ \gamma) \le A^2 E_h(\gamma).$$

If F is an isometric immersion, the energies are equal; consequently, for every $a \geq 0$,

$$(L_\infty F)^{-1}(L_\infty^{\leq a} M) \;=\; L_\infty^{\leq a} N. \tag{11}$$

More generally, if the critical spectra are discrete and $A^2 c_m(N,h) \leq c_j(M,g)$, then composition induces $L_m N \to L_j M$ and $\mathrm{Cyc}_m N \to \mathrm{Cyc}_j M$ over BS^1.

Proof. The Sobolev chain rule gives $(F\circ\gamma)' = dF_\gamma(\dot\gamma)$ almost everywhere. Square the differential bound and integrate. For an isometric immersion the integrands are equal. Continuity of composition follows from the H^1 composition property in local charts. The threshold inequality gives the stated stage map. Composition commutes with rotation, so the same map passes to the Borel constructions. □

Riemannian submersions. For a Riemannian submersion, projection removes precisely the vertical contribution to the energy. This gives both an energy inequality and an explicit condition for equality.

Definition 3.14 (Riemannian submersion)**.** A smooth surjective submersion $p : (N,h) \to (M,g)$ is *Riemannian* if dp restricts to an isometry from $\mathcal{H}_x = (\ker dp_x)^\perp$ onto $T_{p(x)}M$. The subbundles $\mathcal{V} = \ker dp$ and $\mathcal{H}$ are called vertical and horizontal. Write $V = V^{\mathcal{H}} + V^{\mathcal{V}}$ for their orthogonal decomposition.

Proposition 3.15 (Energy and geodesics under submersion)**.** *For a Riemannian submersion $p : (N,h) \to (M,g)$ and any H^1 loop γ in N,*

$$E_g(p\gamma) \;=\; E_h(\gamma) - \frac{1}{2}\int_0^1 |\dot\gamma^{\mathcal{V}}(t)|_h^2 \,\mathrm{d}t. \tag{12}$$

In particular $L_\infty p$ preserves every numerical energy sublevel. Equality of energies holds exactly when $\dot\gamma$ is horizontal almost everywhere. These maps commute with rotation and give maps of the corresponding Borel sublevels over BS^1. If source and target have the same ordered critical values c_m, they give maps $L_m N \to L_m M$ and $\mathrm{Cyc}_m N \to \mathrm{Cyc}_m M$.

A geodesic initially tangent to $\mathcal{H}$ remains horizontal and projects to a geodesic with the same speed. In particular a closed horizontal geodesic projects to a closed geodesic with the same energy.

Proof. Since dp kills $\mathcal{V}$ and is an isometry on $\mathcal{H}$,

$$|(p\gamma)'|_g^2 \;=\; |\dot\gamma^{\mathcal{H}}|_h^2 \;=\; |\dot\gamma|_h^2 - |\dot\gamma^{\mathcal{V}}|_h^2$$

almost everywhere. Integration proves (12), including its equality condition. Composition is continuous by Prop. 3.13 and commutes with rotation.

For the geodesic assertion, recall the horizontal connection identity: for horizontal lifts X, Y of vector fields $\overline{X}, \overline{Y}$ on the base, $(\nabla^N_X Y)^{\mathcal{H}}$ is the lift of $\nabla^M_{\overline{X}}\overline{Y}$. This follows from the Koszul formula, since the inner products of such fields are pulled back from the base. The same formula gives $(\nabla^N_X X)^{\mathcal{V}} = 0$: for a vertical field V, both $V(h(X,X))$ and $h([X,V],X)$ vanish. Consequently the local horizontal lift of a base geodesic is a geodesic. Uniqueness of the geodesic equation proves the assertion for every initially horizontal geodesic, continued over its interval of definition. These are the basic submersion identities of [ONe66]. □

Remark 3.16 (Sublevels versus critical loci). A Riemannian submersion need not send a general closed geodesic to a closed geodesic. Even when the critical-value spectra agree, a critical loop can move to a lower energy or to a noncritical loop. Also, the horizontal lift of a closed base geodesic need not itself be closed. The proposition asserts maps of filtered spaces, without asserting fibrations of individual stages or maps of their Morse–Bott negative bundles.

Totally geodesic inclusions and fixed loci. An isometric inclusion preserves energy. If it is also totally geodesic, it preserves critical loops and identifies their Hessians on the included tangent directions.

Definition 3.17 (Totally geodesic inclusion)**.** For an isometric immersion $F : N \to M$, the second fundamental form is the normal-valued symmetric bilinear form

$$\mathrm{II}(V, W) \;=\; \nabla^{M}_{dF(V)} dF(W) - dF(\nabla^{N}_{V} W).$$

The immersion is *totally geodesic* if $\mathrm{II} = 0$.

Proposition 3.18 (Critical loops and Hessians under inclusion)**.** *A totally geodesic isometric immersion sends closed geodesics to closed geodesics with the same parametrization and energy. At a closed geodesic of N,*

$$I^{N}_{\gamma}(V, W) \;=\; I^{M}_{F\gamma}(dF(V), dF(W)), \qquad \mathrm{ind}_{N}(\gamma) \;\le\; \mathrm{ind}_{M}(F\gamma).$$

If the two manifolds have the same ordered critical values c_m, it induces $L_m N \to L_m M$ for every m. It also induces $\mathrm{Cyc}_m N \to \mathrm{Cyc}_m M$ over BS^1.

Proof. The acceleration formula is

$$D^{M}_{t}(F\gamma)' \;=\; dF(D^{N}_{t}\dot{\gamma}) + \mathrm{II}(\dot{\gamma}, \dot{\gamma}).$$

This proves the assertion about geodesics. Differentiate $E_M \circ L_\infty F = E_N$ twice at the critical loop. The term involving the first derivative of E_M vanishes, so the Hessians agree on the included tangent space. Every negative subspace for the source is therefore negative in the target. The stage assertion follows from Prop. 3.13. Finally composition commutes with rotation, hence gives the asserted maps of Borel constructions. □

Remark 3.19. Isometry alone already preserves every numerical energy sublevel. Total geodesy is needed to preserve the critical loops. Identifying the *ordinal* stages additionally requires comparing the two critical-value spectra. An increase of Morse index in the target does not change the critical energy.

Fixed loci of isometric group actions provide a useful source of totally geodesic inclusions, and their loop spaces can be identified directly inside the ambient filtered loop space.

Proposition 3.20 (Fixed loci and filtered loops)**.** *Let a compact group G act isometrically on M. Every connected component of the fixed locus M^G is a totally geodesic submanifold with its induced metric. For the pointwise action on loops,*

$$(L^{\le a}_{\infty} M)^{G} \;=\; L^{\le a}_{\infty}(M^{G}).$$

This is an equality of subspaces; it concerns ordinary fixed points, not homotopy fixed points.

Proof. At a fixed point, the exponential map is equivariant and identifies the fixed tangent vectors with the nearby fixed locus. A geodesic with fixed initial point and fixed initial velocity is fixed for all time by uniqueness of the geodesic equation. This proves total geodesy. A loop is fixed by the pointwise action exactly when every value is fixed, and the energy then equals its energy in the induced metric. □

4 Examples

The central comparison question in these examples is whether a map $f : X \to Y$ preserves the *first stage beyond constant loops*:

$$(L_\infty f)(L_1 X) \;\subseteq\; L_1 Y \;? \tag{13}$$

For the standard spheres and projective spaces below, $L_1 M = \{E_M \le c_1(M)\}$ is exactly the first stage whose homotopy type differs from that of the constant loops M. We call it the *small-loop stage*; for spheres this is the stage used in the small-cyclification construction of [GSS26]. The question concerns the induced composition map on these subspaces, and is independent of the units used for energy.

Stage numbers and metric scale. In stage-comparison statements we write S^n and $\mathbb{F}P^n$, suppressing scale parameters on *both* sides. These spaces always carry their standard round or projective metrics, up to positive constant rescaling. This does not allow an arbitrary change of metric. The notation S^n_R is reserved for a sphere explicitly realized with radius R in Euclidean space, and $g_{\mathbb{F},R} = 4R^2 g_{\mathbb{F},\mathrm{quot}}$ records the projective metric when a quantitative calculation needs it (Def. 4.52). Radial homotheties identify all the sphere models. The following lemma justifies suppressing these scales when comparing stages.

Lemma 4.1 (Constant rescaling leaves the stages unchanged)**.** *Suppose that (M, g) has the discrete critical values $c_m(g)$ of Def. 2.13, and let $g' = \lambda^2 g$, $\lambda > 0$. Under the identity on the underlying loop space,*

$$E_{g'} = \lambda^2 E_g, \qquad c_m(g') = \lambda^2 c_m(g), \qquad L_m(M, g') = L_m(M, g). \tag{14}$$

The last equality is an equality of subspaces with their inclusion maps, not merely an equality of homotopy types. The critical manifolds, Morse indices, and nullities are unchanged. The same holds for the cyclified filtration. Consequently, for a fixed smooth map between two such manifolds, its correspondence between numbered stages is unchanged by independent constant rescalings of the source and target metrics.

Proof. The energy identity follows from its definition. Its first and second derivatives are multiplied by the same positive constant, preserving the critical loci and Hessian signs. Multiplication by λ^2 preserves the order of the critical values. Thus

$$\{E_{g'} \le c_m(g')\} = \{\lambda^2 E_g \le \lambda^2 c_m(g)\} = \{E_g \le c_m(g)\}.$$

The two Sobolev topologies agree, and rotation acts in the same way on these identical subspaces. This proves the assertions for the filtered spaces and their Borel constructions. Applying the result separately on source and target proves the last claim. □

For the spaces below the critical energies satisfy $c_m(M) = m^2 c_1(M)$. Thus the dimensionless energy

$$\varepsilon_M(\gamma) := \frac{E_M(\gamma)}{c_1(M)}, \qquad L_m M = \{\gamma : \varepsilon_M(\gamma) \le m^2\}, \tag{15}$$

is a scale-independent way to specify the same subspaces. In particular the small-loop condition is $\varepsilon_M \le 1$, whatever the numerical value of $c_1(M)$.

Proposition 4.2 (The first stage is the first homotopy change)**.** *Let M be a round S^N, $N \geq 1$, or a standard $\mathbb{F}P^n$, $n \geq 1$, with $\mathbb{F} \in \{\mathbb{R}, \mathbb{C}, \mathbb{H}\}$. For every $0 < a < c_1(M)$, the inclusion of constant loops $M \hookrightarrow \{E_M \leq a\}$ is a homotopy equivalence. In contrast, L_1M is not homotopy equivalent to M. Consequently the stage numbered 1 is the first nontrivial stage in this homotopy-theoretic sense.*

Proof. The constant loops are Morse–Bott minima, and there are no further critical points below $c_1(M)$. Apply Thm. 3.10 at energy zero, where the negative bundle has rank zero and the lower sublevel is empty. This gives the homotopy equivalence from the constants to a small positive sublevel. Then Thm. 3.8 extends it to every $a < c_1(M)$. The critical-manifold and index computations in Thms. 4.4, 4.5 and 4.63 show that the first positive critical manifold is $K_1 \cong STM$, the unit tangent bundle, with index

$$\lambda = \begin{cases} N-1, & M = S^N, \\ 0, & M = \mathbb{R}P^n, \\ 1, & M = \mathbb{C}P^n, \\ 3, & M = \mathbb{H}P^n. \end{cases}$$

For S^1 the same computation has no normal directions: the two orientations of a once-traversed circle give $K_1 \cong STS^1$ with index zero. The Morse–Bott attachment and the Thom isomorphism, Thm. 3.10 and Cor. 3.11, give

$$H_j(L_1M, M; \mathbb{F}_2) \cong H_{j-\lambda}(K_1; \mathbb{F}_2). \tag{16}$$

Here passage from a sublevel just below c_1 to M uses the first assertion, and coefficients modulo two remove every orientation twist. Evaluation at 0,

$$\begin{array}{ccc} L_1M & \xrightarrow{e_0} & M \\ \gamma & \longmapsto & \gamma(0), \end{array}$$

retracts the inclusion of constant loops. That inclusion is therefore injective on homology in every degree. The long exact sequence of the pair splits into short exact sequences, so (16) implies

$$\dim_{\mathbb{F}_2} H_\lambda(L_1M; \mathbb{F}_2) = \dim_{\mathbb{F}_2} H_\lambda(M; \mathbb{F}_2) + \dim_{\mathbb{F}_2} H_0(K_1; \mathbb{F}_2) > \dim_{\mathbb{F}_2} H_\lambda(M; \mathbb{F}_2).$$

These dimensions are finite, and K_1 is nonempty. Thus even the abstract homotopy types differ. □

Sublevels below c_1 already contain nonconstant loops; their homotopy type, rather than the presence of such loops, is what distinguishes the first nontrivial stage. We use the *whole* free loop space throughout. In particular, for $\mathbb{R}P^n$ the first change includes noncontractible loops; restricting to the contractible component and renumbering its stages would ask a different question (Rem. 4.64).

First-stage comparisons. The results proved below give the following guide. Here $\mathbb{F} \subseteq \mathbb{K}$ are chosen from $\mathbb{R} \subset \mathbb{C} \subset \mathbb{H}$, $r = \dim_{\mathbb{F}} \mathbb{K}$, and $d = \dim_{\mathbb{R}} \mathbb{F}$; projective dimensions are positive. In the quotient row the field inclusion is proper. In the Veronese row, $q > 1$ is the polynomial degree and $N_q = \binom{n+q}{q} - 1$.

Map	Stage correspondence	Preserves L_1?
$S^p \hookrightarrow S^q$ (equatorial)	$m \mapsto m$	yes
$\mathbb{F}P^k \hookrightarrow \mathbb{K}P^n$ $(k \le n)$	$m \mapsto m$	yes
$\mathbb{F}P^{r(n+1)-1} \to \mathbb{K}P^n$	$m \mapsto m$	yes
$S^{d(n+1)-1} \to \mathbb{F}P^n$ (Hopf)	$m \mapsto 2m$ (sharp)	no
$\mathbb{C}P^n \hookrightarrow \mathbb{C}P^{N_q}$ (Veronese)	$m \mapsto \lceil m\sqrt{q} \rceil$ (sharp)	no

The proofs are Prop. 4.59 and Thms. 4.65, 4.69, 4.76 and 4.86. All these maps commute with loop rotation, giving the same stage correspondences after cyclification over BS^1. In particular the first three rows preserve small cyclification. The Hopf row requires the second target stage, while a degree-q Veronese embedding requires stage $\lceil \sqrt{q} \rceil$.

4.1 Round spheres

Notation 4.3. For $n \ge 1$, let $S^n_R := \{x \in \mathbb{R}^{n+1} : |x| = R\}$ with the induced metric. Let $V_2(\mathbb{R}^{n+1})$ denote the manifold of ordered orthonormal pairs (u, v). The unit tangent bundle of a Riemannian manifold is denoted $STM = \{(x, w) : |w| = 1\}$.

Theorem 4.4 (Closed geodesics of a round sphere)**.** *The critical manifolds of $E : L_\infty S^n_R \to \mathbb{R}$ are the constants $K_0 = S^n_R$, at energy zero, and, for $m \ge 1$,*

$$K_m = \left\{\gamma_{u,v,m}(t) = R\Big(\cos(2\pi mt)u + \sin(2\pi mt)v\Big) : (u, v) \in V_2(\mathbb{R}^{n+1})\right\}. \tag{17}$$

There are diffeomorphisms $K_m \cong V_2(\mathbb{R}^{n+1}) \cong STS^n_R$, and

$$c_m = E(K_m) = 2\pi^2 R^2 m^2, \qquad \ell(K_m) = 2\pi R m. \tag{18}$$

The dimension of K_m is $2n - 1$.

Proof. For a geodesic on the sphere, its Euclidean acceleration is normal to the sphere. Twice differentiating $|\gamma|^2 = R^2$ gives

$$\ddot\gamma = -\frac{|\dot\gamma|^2}{R^2}\gamma.$$

Its speed is constant. A nonconstant solution therefore has the form $R(\cos(\omega t)u + \sin(\omega t)v)$ with an orthonormal pair (u, v) and $\omega > 0$. Periodicity of the position and velocity is equivalent to $\omega = 2\pi m$ for a positive integer m. The speed is $2\pi mR$, giving (18). The frame is recovered by continuous linear Fourier coefficients:

$$u = \frac{2}{R}\int_0^1 \gamma(t)\cos(2\pi mt)\,\mathrm{d}t, \qquad v = \frac{2}{R}\int_0^1 \gamma(t)\sin(2\pi mt)\,\mathrm{d}t.$$

These formulas exhibit the finite-dimensional family as a smooth embedded submanifold of the Sobolev loop space. Sending (u, v) to (Ru, v) identifies it with STS^n_R, of dimension $2n - 1$. For $n = 1$, it has two components, one for each orientation. □

Theorem 4.5 (Sphere index, nullity, and negative bundle)**.** *The energy on $L_\infty S^n_R$ is Morse–Bott. At its critical manifolds,*

$$\begin{aligned} \operatorname{ind}(K_0) &= 0, & \operatorname{nul}(K_0) &= n, \\ \operatorname{ind}(K_m) &= (2m-1)(n-1), & \operatorname{nul}(K_m) &= 2n-1 \quad (m \ge 1). \end{aligned} \tag{19}$$

Let $\xi \to V_2(\mathbb{R}^{n+1})$ be the rank-$(n-1)$ bundle with fiber $\xi_{(u,v)} = \langle u, v\rangle^{\perp}$. As an ordinary real vector bundle, the negative bundle is

$$\nu^{-} K_m \cong \xi^{\oplus(2m-1)}. \tag{20}$$

Proof. Fix the loop (17). Its unit tangent $e_0(t) = \dot\gamma(t)/(2\pi m R)$ is parallel. Any fixed Euclidean vector in $\langle u, v\rangle^{\perp}$ is a parallel tangent field along γ. Choose an orthonormal basis $e_1, \dots, e_{n-1}$ of this orthogonal complement and write a periodic field as $V = f_0 e_0 + \sum_{\alpha=1}^{n-1} f_\alpha e_\alpha$. The curvature formula and (6) give

$$I_\gamma(V, V) = \int_0^1 \left(|\dot f_0|^2 + \sum_{\alpha=1}^{n-1} \Big(|\dot f_\alpha|^2 - (2\pi m)^2 |f_\alpha|^2 \Big) \right) \mathrm{d}t. \tag{21}$$

For the real periodic Fourier basis $1, \cos(2\pi k t), \sin(2\pi k t)$, $k \geq 1$, the tangential operator $-\mathrm{d}^2/\mathrm{d}t^2$ has no negative mode and one zero mode. For each normal direction the operator is $-\mathrm{d}^2/\mathrm{d}t^2 - (2\pi m)^2$. Its negative modes are the constant mode and the two modes for each $1 \leq k < m$, giving $1 + 2(m-1) = 2m - 1$. Its zero modes are the two modes at $k = m$. This proves the index and nullity for $m \geq 1$. These are spectral values of the Jacobi operator on L^2; the representing operator on H^1 has the same signs and kernel, as required for the Morse–Bott condition.

Variation of (u, v) gives tangent vectors to K_m in the kernel. The dimension just computed is exactly $\dim K_m$, so the kernel has no further directions. At a constant loop the form is $\int_0^1 |D_t V|^2 \, \mathrm{d}t$ in a fixed tangent space; its kernel consists of the constant fields. This proves the assertion also at K_0. Fredholmness follows from Prop. 3.4.

Finally a negative field is uniquely a trigonometric polynomial of frequencies $0, \dots, m-1$ with coefficients in $\langle u, v\rangle^{\perp}$:

$$V(t) = w_0 + \sum_{k=1}^{m-1} \Big(w_k^c \cos(2\pi k t) + w_k^s \sin(2\pi k t) \Big).$$

There are $2m - 1$ such coefficients, proving the bundle identification (20). □

Remark 4.6 (Comparison with the literature). The sphere computation is classical; see [Kli78; Zil77] and the index formulas recalled in [Şir24, Thm. 3.1]. The Fourier proof above fixes the parametrization, the factor $1/2$ in energy, and the convention that nullity includes loop rotation. The bundle isomorphism (20) does not declare the rotation action on its summands trivial: rotation changes the frame and mixes Fourier modes.

Corollary 4.7 (The sphere filtration)**.** *The stages are*

$$\begin{gathered} S^n_R = L_0 S^n_R \hookrightarrow L_1 S^n_R \hookrightarrow L_2 S^n_R \hookrightarrow \cdots, \\ L_m S^n_R = \{E \leq 2\pi^2 R^2 m^2\}. \end{gathered} \tag{22}$$

For $m \geq 1$, their successive homotopy cofibers are

$$\operatorname{hocofib}(L_{m-1} S^n_R \to L_m S^n_R) \simeq \operatorname{Th}\Big(\xi^{\oplus(2m-1)}\Big). \tag{23}$$

Every positive sublevel strictly below c_1 is homotopy equivalent to the constant loops.

Proof. The critical values and manifolds are given by Thms. 4.4 and 4.5, and the Palais–Smale condition by Prop. 3.6. Choose regular values immediately before and after c_m. Apply Thm. 3.10 at c_m, and Thm. 3.8 in the adjoining gaps. The exact-critical-sublevel comparison

identifies the preceding regular sublevel with $L_{m-1}S^n_R$ and the following one with $L_mS^n_R$. This gives (23). At energy zero, Thm. 3.10 attaches the rank-zero bundle of the constants to the empty sublevel. The regular-band theorem extends this equivalence through the entire interval below c_1. □

Remark 4.8 (At the threshold and below it). The first stage in (22) contains the entire first critical manifold and its negative attachment. The open sublevel $\{E < c_1\}$ also has the homotopy type of the constants. For example, fix $0 < a < c_1$ and use the normalized descending field $-\nabla E/\|\nabla E\|^2$ on $a \le E < c_1$. A loop of energy $E(\gamma) > a$ reaches level a in time $E(\gamma) - a$. Each such trajectory stays in a closed regular band, where Palais–Smale ensures existence for that time. The time depends continuously on the loop; stopping at level a gives a deformation onto $\{E \le a\} \simeq S^n_R$. Consequently replacing $E \le c_1$ by $E < c_1$ changes the problem. The first-stage attaching map and a finite-dimensional homotopy model are computed below.

Proposition 4.9 (Rotation on the sphere critical manifolds). *On $K_m \cong V_2(\mathbb{R}^{n+1})$, rotation of the loop parameter rotates the ordered frame through angle $2\pi m\theta$. Its stabilizer is $\mathbb{Z}/m$, and its orbit space is the oriented Grassmannian $\mathrm{Gr}_2^+(\mathbb{R}^{n+1})$. The map from the Borel construction to this orbit space has homotopy fiber $B(\mathbb{Z}/m)$:*

$$B(\mathbb{Z}/m) \longrightarrow (K_m)_{hS^1} \longrightarrow \mathrm{Gr}_2^+(\mathbb{R}^{n+1}).$$

For $m = 1$, the fiber is contractible.

Proof. Expand $\gamma(t+\theta)$ in the sine and cosine basis. The new frame is $u' = \cos(2\pi m\theta)u + \sin(2\pi m\theta)v$, $v' = -\sin(2\pi m\theta)u + \cos(2\pi m\theta)v$. This proves the action and stabilizer claims. An oriented plane is exactly a frame modulo this rotation. Over a local trivialization of the frame bundle, the Borel construction has fiber $ES^1 \times_{S^1} (S^1/(\mathbb{Z}/m)) \simeq B(\mathbb{Z}/m)$. □

The first-stage homotopy pushout. The negative bundle in Thm. 4.5 specifies what is attached at the first positive critical value. For a round sphere one can also identify the attaching map explicitly. The following homotopy-pushout description makes explicit the attaching geometry of Klingenberg's round-circle model and Morse–Bott decomposition [Kli78, §§ 2.3–2.5, especially Thm. 2.4.10, Cor. 2.4.11, and Prop. 2.5.3]. Its cyclified form for the four-sphere is stated in [GSS26, Lem. 3.4]; here we spell out the construction for arbitrary round spheres of dimension $n \ge 2$. We give the parametrized-loop version first, then pass to the homotopy quotient.

Notation 4.10 (Frames, poles, and the first negative bundle). Continue to use $\xi_{(u,v)} = \langle u, v\rangle^\perp$ over $V_2(\mathbb{R}^{n+1})$. Its unit sphere bundle is $S\xi = V_3(\mathbb{R}^{n+1})$, the space of ordered orthonormal triples. Write

$$\begin{array}{ccc} V_3(\mathbb{R}^{n+1}) \xrightarrow{p_n} V_2(\mathbb{R}^{n+1}) & \qquad & V_3(\mathbb{R}^{n+1}) \xrightarrow{\alpha_n} S^n_R \\ (u,v,w) \longmapsto (u,v) & & (u,v,w) \longmapsto Rw. \end{array} \tag{24}$$

Here (u, v) parametrizes an oriented great circle, and Rw, perpendicular to its plane, is a chosen pole. The pole is extra data: for a given great circle its choices form an S^{n-2}.

Lemma 4.11 (An explicit descending disk)**.** *For $(u, v, z) \in D\xi$, define*

$$\begin{aligned} D\xi &\xrightarrow{\Phi_R} L_1 S^n_R \\ (u, v, z) &\longmapsto \Phi_{u,v,z} \\ \Phi_{u,v,z}(t) &= R\Big(z + \sqrt{1-|z|^2}\Big(\cos(2\pi t)u + \sin(2\pi t)v\Big)\Big)\,. \end{aligned} \tag{25}$$

This is continuous in the H^1 topology, is smooth near the zero section, and satisfies

$$E(\Phi_{u,v,z}) = c_1(1-|z|^2), \qquad c_1 = 2\pi^2 R^2. \tag{26}$$

It maps the zero section to the first critical manifold and the sphere bundle to constant loops by α_n. Its derivative in the disk direction at $z = 0$ is the constant normal field Rz, identifying the disk tangent with the negative space. In particular, for a unit $w \perp u, v$, the loops

$$H_\theta(u, v, w)(t) = R\Big(\cos\theta\Big(\cos(2\pi t)u + \sin(2\pi t)v\Big) + \sin\theta\, w\Big)\,, \qquad 0 \le \theta \le \frac{\pi}{2}, \tag{27}$$

give a homotopy from the great circle to the pole, with energy $c_1 \cos^2\theta$.

Proof. Orthogonality gives $|\Phi_{u,v,z}(t)|^2 = R^2$. Its velocity has constant norm $2\pi R\sqrt{1-|z|^2}$, proving the energy identity. Both its values and its t-derivatives depend continuously on (u, v, z) even at $|z| = 1$; this proves H^1 continuity. The square root is smooth near $z = 0$, where differentiating gives Rz. By Thm. 4.5 these constant normal fields are exactly the first negative space. Finally put $z = \sin\theta\, w$ to obtain (27). □

Theorem 4.12 (The first-stage homotopy pushout for round spheres)**.** *For every $n \ge 2$, the following square, with the homotopy (27), is a homotopy pushout:*

$$\begin{array}{ccc} V_3(\mathbb{R}^{n+1}) & \xrightarrow{p_n} & V_2(\mathbb{R}^{n+1}) \\ {\scriptstyle \alpha_n}\downarrow & & \downarrow{\scriptstyle \text{great circles}} \\ S^n_R & \xrightarrow[\text{constant loops}]{} & L_1 S^n_R\,. \end{array} \tag{28}$$

Equivalently, with the maps of (24),

$$L_1 S^n_R \simeq \operatorname{hocolim}\Big(V_2(\mathbb{R}^{n+1}) \xleftarrow{p_n} V_3(\mathbb{R}^{n+1}) \xrightarrow{\alpha_n} S^n_R\Big)\,. \tag{29}$$

More concretely, Φ_R and the constant loops induce a homotopy equivalence of pairs

$$(S^n_R \cup_{\alpha_n} D\xi,\ S^n_R) \longrightarrow (L_1 S^n_R,\ S^n_R)\,. \tag{30}$$

The union here glues $S\xi \subset D\xi$ to S^n_R by α_n.

Proof. The first critical manifold is $K_1 = V_2(\mathbb{R}^{n+1})$ with negative bundle ξ. By Cor. 4.7 and Thm. 3.10, the first stage is obtained, up to homotopy, by attaching $D\xi$ to a sublevel $X_a := \{E \le a\}$ with $0 < a < c_1$. The constant-loop inclusion $S^n_R \to X_a$ is a homotopy equivalence. We identify the attachment after this equivalence and verify the specific comparison map (30).

First take a sufficiently small radius $\varepsilon > 0$ in the disk of Lem. 4.11. This disk supplies the local negative handle germ. Here is why its explicit form can be used in the Morse–Bott attachment theorem. In a normal-form chart write $E = c_1 - \|v^-\|^2 + \|v^+\|^2$. Projection of Φ_R onto the critical-manifold coordinate and the negative coordinate has invertible derivative

along the zero section. After shrinking the disk, the inverse function theorem therefore writes its image as a graph $v^+ = h(x, v^-)$ over the negative bundle. Here $h(x, 0) = 0$ and its derivative in the negative direction vanishes at zero. Compactness of K_1 permits a uniform radius. Replacing h by $(1 - s)h$, $0 \le s \le 1$, decreases energy and fixes the zero section. Thus this disk germ is homotopic through descending disk germs to the standard negative disk of the Morse–Bott normal form.

On the boundary of the small disk, the attachment is represented by $\Phi_{u,v,\varepsilon w}$, at energy $a_\varepsilon = c_1(1 - \varepsilon^2) < c_1$. For $\varepsilon \le r \le 1$, the path $\Phi_{u,v,rw}$ stays in X_{a_ε} and ends at the constant loop Rw. Evaluation at 0 is a homotopy inverse to the constant-loop inclusion $S^n_R \to X_{a_\varepsilon}$. Applying it to this path identifies the attaching map, up to homotopy, with α_n. The radius interval $[\varepsilon, 1]$ provides the attaching homotopy itself. Consequently the handle-attachment construction, using the disk germ just verified and this homotopy, gives precisely the comparison map induced by Φ_R in (30). It is a homotopy equivalence of pairs.

The inclusion $S\xi \hookrightarrow D\xi$ is a cofibration, so its pushout along α_n is a homotopy pushout. Radial contraction $D\xi \simeq V_2(\mathbb{R}^{n+1})$ replaces the sphere-bundle inclusion by its projection p_n. Homotopy invariance of the pushout now gives (29). In its double mapping-cylinder model the comparison homotopy is exactly (27). This is the first sphere attachment in the Morse theory of [Kli78, §§ 2.3–2.5], with its attaching map displayed explicitly. □

Proposition 4.13 (A model by parametrized round circles)**.** *Let $A^n_R \subset L_1 S^n_R$ consist of the constant loops and the loops traversing a round circle once at constant speed, with a chosen initial point and orientation (cf. Fig. 1). Here a round circle is the intersection of S^n_R with an affine two-plane, and the one-point intersections are included as constant loops. Then Φ_R induces a homeomorphism*

$$S^n_R \cup_{\alpha_n} D\xi \;\cong\; A^n_R,$$

and the actual inclusion

$$A^n_R \xhookrightarrow{\sim} L_1 S^n_R \tag{31}$$

is a homotopy equivalence relative to the constant loops. It is S^1-equivariant for loop rotation.

Proof. For $|z| < 1$, the loop $\Phi_{u,v,z}$ traverses the circle centered at Rz in the affine plane $Rz + \langle u, v\rangle$, with radius $R\sqrt{1 - |z|^2}$. Conversely, a nonconstant parametrized round circle uniquely determines its center Rz, its radius $\rho > 0$, and the frame

$$u = \frac{\gamma(0) - Rz}{\rho}, \qquad v = \frac{\dot\gamma(0)}{2\pi\rho}.$$

Thus Φ_R is one-to-one on the open disk bundle, and its only identifications on the boundary are the constant-loop identifications prescribed by α_n. The resulting continuous bijection from the compact pushout to the Hausdorff space A^n_R is a homeomorphism. Its inclusion in the first stage is the underlying homotopy equivalence established in Thm. 4.12.

Rotation acts on (u, v) by the frame rotation of Prop. 4.9 with $m = 1$, and leaves z fixed. This makes Φ_R equivariant. In particular, its underlying homotopy equivalence induces a weak equivalence of Borel constructions. This last conclusion needs only the continuous circle action, not a jointly smooth action on the Sobolev loop space; compare Rem. 2.15. □

Corollary 4.14 (The cyclified homotopy pushout)**.** *Let*

$$G_n = \mathrm{Gr}_2^+(\mathbb{R}^{n+1}), \qquad F_n = \{(P, w) : P \in G_n,\ |w| = 1,\ w \perp P\}.$$

Thus G_n parametrizes oriented great circles, and F_n parametrizes an oriented great circle together with a pole. Let $c_n : G_n \to BS^1$ classify the principal circle bundle of rigid parametrizations $V_2(\mathbb{R}^{n+1}) \to G_n$. Define

$$\begin{array}{ccc} F_n \xrightarrow{q_n} G_n & \qquad & F_n \xrightarrow{a_n} S^n_R \times BS^1 \\ (P, w) \longmapsto P & & (P, w) \longmapsto (Rw, c_n(P)). \end{array} \tag{32}$$

There is a homotopy pushout

$$\begin{array}{ccc} F_n & \xrightarrow{q_n} & G_n \\ {\scriptstyle a_n}\downarrow & & \downarrow \\ S^n_R \times BS^1 & \longrightarrow & \mathrm{Cyc}_1\, S^n_R. \end{array} \tag{33}$$

This is also a homotopy pushout over BS^1, using $c_n q_n$, c_n, and the projection on the three input corners.

Proof. The disk-bundle model and its attaching map are S^1-equivariant. Its boundary inclusion has an invariant radial collar, so it is an equivariant cofibration. Taking the Borel construction preserves the resulting homotopy pushout. By Prop. 4.13 its output is equivalent to $\mathrm{Cyc}_1\, S^n_R$.

The action on $V_2(\mathbb{R}^{n+1})$ is free, with quotient G_n. On $V_3(\mathbb{R}^{n+1})$ it rotates (u, v) while fixing w; this action is free too, with quotient F_n. Their homotopy quotients are therefore equivalent to these ordinary quotients. Moreover the principal circle bundle $V_3(\mathbb{R}^{n+1}) \to F_n$ is the pullback along q_n of $V_2(\mathbb{R}^{n+1}) \to G_n$: choosing a frame of P together with w is exactly choosing the triple (u, v, w). Its classifying map is consequently $c_n q_n$. Since rotation fixes all constant loops, their homotopy quotient is $S^n_R \times BS^1$, and the attaching map into it has components Rw and $c_n(P)$, as stated. All the Borel maps retain their projections to BS^1, which proves the sliced assertion. □

Remark 4.15 (The four-sphere and the classifying component). At $n = 4$ the two presentations read

$$L_1 S^4_R \simeq \mathrm{hocolim}\Big(V_2(\mathbb{R}^5) \longleftarrow V_3(\mathbb{R}^5) \longrightarrow S^4_R\Big),$$
$$\mathrm{Cyc}_1\, S^4_R \simeq \mathrm{hocolim}\left(\frac{\mathrm{SO}(5)}{\mathrm{SO}(2)\times\mathrm{SO}(3)} \longleftarrow \frac{\mathrm{SO}(5)}{\mathrm{SO}(2)\times\mathrm{SO}(2)} \longrightarrow S^4_R \times BS^1\right).$$

The second description is the precise form of [GSS26, Lem. 3.4]: the left map forgets the pole, while the right map remembers both the pole and the bundle of parametrizations. The BS^1-component is essential; replacing it by a constant map specifies a different diagram. In particular, the ordinary orbit space of round circles has points for degenerate circles, whereas cyclification retains a copy of BS^1 at every such point.

Remark 4.16 (Naturality, the cofiber, and the one-sphere). The construction is natural under linear isometric inclusions $\mathbb{R}^{p+1} \hookrightarrow \mathbb{R}^{q+1}$: the frame inclusions commute with p_n, α_n, and with the explicit descending disks. Thus these models also represent the maps of first stages induced by equatorial inclusions. Collapsing the constant-loop corner recovers $\mathrm{hocofib}(S^n_R \to L_1 S^n_R) \simeq \mathrm{Th}(\xi)$, in agreement with (23).

For $n = 1$ the same formula is interpreted with $V_3(\mathbb{R}^2) = \varnothing$ and a rank-zero negative bundle. One obtains

$$L_1 S^1_R \simeq S^1 \sqcup S^1 \sqcup S^1, \qquad \mathrm{Cyc}_1 S^1_R \simeq (S^1 \times BS^1) \sqcup * \sqcup *.$$

Indeed the energy bound permits precisely winding numbers $0, 1, -1$. In winding ± 1, the energy–length inequality forces constant speed at the bound, giving the two freely rotating families of great circles. In winding zero, linear contraction of a periodic real lift to its mean decreases energy and retracts onto the constant loops.

4.1.1 The 2-sphere

For the round two-sphere, the first negative bundle is a trivial line bundle. Its two boundary components are attached to the same sphere of constant loops. We now use this description to compute the fundamental group, keeping track of a geometric generator. Throughout, c_x denotes the constant loop with value $x \in S^2_R$. The computation then proceeds in three steps: determine the second homotopy group and the action of this generator; apply the outer evaluation fibration to obtain the fundamental groups of $LL_1S^2_R$; and compare them with the unrestricted torus mapping groups. A final discussion relates both calculations to Samelson products. All stages retain the parametrization of their loops; no quotient by loop rotation is taken here.

Theorem 4.17 (Fundamental group of the first two-sphere stage)**.** *For every $R > 0$, the first critical-energy stage*

$$L_1 S^2_R = \left\{ \gamma \in H^1(S^1, S^2_R) \,\middle|\, E(\gamma) \leq 2\pi^2 R^2 \right\}$$

is path-connected and has infinite cyclic fundamental group. For a constant base loop c_{x_0}, a presentation is

$$\pi_1\big(L_1 S^2_R, c_{x_0}\big) \cong \mathbb{Z}\,. \tag{34}$$

A representative sweeps a family of round latitude circles from one pole to the opposite pole, then returns through constant loops, as specified in (39).

Proof. The two boundary components. Fix the standard orientation of $\mathbb{R}^3$ and put $K = V_2(\mathbb{R}^3)$. The cross product gives a global unit section of the first negative line bundle:

$$\xi_{(u,v)} = \mathbb{R}(u \times v).$$

Thus $D\xi \cong K \times [-1, 1]$ and $S\xi \cong K \sqcup K$, with the two copies corresponding to $z = -(u \times v)$ and $z = u \times v$. There are identifications

$$\begin{aligned} K &\xrightarrow{\cong} \mathrm{SO}(3) \\ (u, v) &\longmapsto (u, v, u \times v), \end{aligned} \qquad V_3(\mathbb{R}^3) = \mathrm{O}(3) \cong K \sqcup K.$$

Under these identifications, the projection p_2 restricts to the identity on each copy of K. The two attaching maps are

$$\begin{aligned} K &\xrightarrow{q_\pm} S^2_R \\ (u, v) &\longmapsto \pm R(u \times v). \end{aligned} \tag{35}$$

Consequently Thm. 4.12 becomes the homotopy pushout

$$\begin{array}{ccc} K \sqcup K & \xrightarrow{\text{fold}} & K \\ {\scriptstyle q_- \sqcup q_+}\downarrow & & \downarrow \\ S^2_R & \longrightarrow & L_1 S^2_R. \end{array} \tag{36}$$

Its disk-bundle model is the space

$$P_R \;=\; \Big(S^2_R \sqcup (K \times [-1,1])\Big)\Big/\Big((k,-1) \sim q_-(k),\ (k,1) \sim q_+(k)\Big). \tag{37}$$

The explicit map of (25) gives a homotopy equivalence $P_R \to L_1 S^2_R$ fixing the constant loops. Since S^2_R and K are path-connected and both ends of the cylinder meet S^2_R, the model is path-connected.

The one- and two-dimensional attachments. We apply van Kampen through the relative cell structure of P_R; the cell-attachment form of the theorem is recalled in [Hat02, Prop. 1.26]. Conjugation on imaginary quaternions identifies SO(3) with the quotient of the unit quaternions S^3 by $\{1,-1\}$, hence with $\mathbb{R}P^3$. The filtration $\mathbb{R}P^0 \subset \mathbb{R}P^1 \subset \mathbb{R}P^2 \subset \mathbb{R}P^3$ gives K one cell e^j in each dimension $j = 0,1,2,3$: each $\mathbb{R}P^j$ is obtained from a closed hemisphere by identifying antipodal boundary points, with its interior as the new cell [Hat02, Ex. 0.4]. Choose its zero-cell to be $k_0 = (u,v)$.

Relative to S^2_R, the model (37) therefore has one cell in each dimension $1,2,3,4$. Indeed, a characteristic disk D^j for e^j contributes $D^j \times [-1,1]$, a $(j+1)$-cell: its side boundary maps to the earlier cylinder cells, while its two end faces map to S^2_R by q_- and q_+. Let $P^{[r]}_R$ denote the subspace after the relative cells of dimension at most r have been attached. The first step is

$$P^{[1]}_R \;=\; S^2_R \cup \Big(\{k_0\} \times [-1,1]\Big),$$

with the interval joining the distinct points $q_-(k_0)$ and $q_+(k_0)$. Attaching one interval to a path-connected space adds one free generator to its fundamental group. Here the initial space is simply connected, so van Kampen gives $\pi_1(P^{[1]}_R) \cong \mathbb{Z}$. The generator traverses the new interval from $q_+(k_0)$ to $q_-(k_0)$ and returns along any path in S^2_R. All such return paths are homotopic relative to their endpoints.

It remains to check whether the two-cell imposes a relation. Let $\chi : [0,1] \to K$ be the characteristic path of the one-cell of K, with $\chi(0) = \chi(1) = k_0$. The attaching boundary of the rectangle $[0,1] \times [-1,1]$ consists of the two loops $q_-\chi$ and $q_+\chi$ in S^2_R, together with two oppositely oriented traversals of the interval $\{k_0\} \times [-1,1]$. The first two loops are nullhomotopic in S^2_R. After these contractions, the attaching loop goes down the interval and immediately back up it. Its word in the generator is $ww^{-1} = 1$. Thus the two-cell imposes no relation, and

$$\pi_1\Big(P^{[2]}_R\Big) \;\cong\; \langle w \rangle\,.$$

The remaining cells have dimensions 3 and 4 and cannot change the fundamental group. This proves (34).

A representative within the energy bound. Write $n = u \times v$ and take $x_0 = Rn$. For $s,t \in [0,1]$, set

$$\Gamma_s(t) \;=\; R\Big(\cos(\pi s)n + \sin(\pi s)\Big(\cos(2\pi t)u + \sin(2\pi t)v\Big)\Big)\,. \tag{38}$$

This is a continuous path of H^1 loops from c_{Rn} to c_{-Rn}, with

$$E(\Gamma_s) \;=\; 2\pi^2 R^2 \sin^2(\pi s) \;\le\; 2\pi^2 R^2.$$

It passes through a once-traversed great circle at $s = 1/2$. Let $\sigma(s) = R(-\cos(\pi s)n + \sin(\pi s)u)$, a path from $-Rn$ to Rn on the sphere. Then

$$\beta = \Gamma * \big(s \longmapsto c_{\sigma(s)}\big), \qquad w = [\beta] \in \pi_1(L_1 S^2_R, c_{Rn}), \tag{39}$$

where $*$ means path concatenation in the displayed order. The return path consists of zero-energy loops. In (37), the first path is exactly the interval $\{k_0\} \times [-1, 1]$, traversed from 1 to -1 by $r = \cos(\pi s)$. Thus β represents the generator obtained in the cell calculation, rather than a nontrivial multiple of it. Choose $n = x_0/R$ to obtain any prescribed basepoint. □

Remark 4.18 (Why the disconnected boundary matters). The critical manifold alone has $\pi_1(K) = \pi_1(\mathrm{SO}(3)) \cong \mathbb{Z}/2$. It is not the whole first stage. Moreover the upper-left corner of (36) has two connected components. Replacing that diagram by a pushout of groups based in just one component would lose the generator w. Geometrically, w enters the cylinder at one boundary component and leaves it at the other. The relative cell calculation above accounts for both components and shows why the result is infinite cyclic, with no residual element of order two.

Corollary 4.19 (Comparison with the unrestricted free loop space)**.** *Inclusion of the first stage induces an isomorphism*

$$\pi_1(L_1 S^2_R, c_{x_0}) \xrightarrow{\cong} \pi_1(L_\infty S^2_R, c_{x_0}) \cong \mathbb{Z}. \tag{40}$$

In particular, the loop β of (39) also generates the unrestricted fundamental group.

Proof. For $m \geq 2$, the negative bundle of $K_m \cong \mathrm{SO}(3)$ has rank $2m-1 \geq 3$, by Thm. 4.5. It is trivial because ξ is trivial. The corresponding Morse–Bott attachment has relative cells of dimensions $2m-1, 2m, 2m+1, 2m+2$, all at least 3. These are cells in the attachment model of the pair, rather than a claim that the Sobolev sublevel is itself a CW complex. By van Kampen and Thm. 3.10, each inclusion $L_{m-1}S^2_R \hookrightarrow L_m S^2_R$ therefore induces an isomorphism on π_1.

Finally, energy is continuous in the H^1 topology. Every based loop in $L_\infty S^2_R$, and every homotopy of such loops, has compact parameter space and hence bounded energy. It therefore lies in some finite stage. Thus passage to the whole free loop space introduces neither new generators nor new relations, proving the assertion. □

The second homotopy group and its monodromy. To compute the fundamental groups after applying the free-loop functor once more, we also need $\pi_2(L_1 S^2_R)$ and the action on it of the generator w. An alternative description of the round-circle model makes both of these accessible to integral homology calculations. This continues the first-stage attachment calculation of Thm. 4.17: we use the actual round-circle inclusion of Prop. 4.13, so that the generators remain compatible with inclusion into the unrestricted loop space.

Lemma 4.20 (An evaluation-coordinate model)**.** *Let S^2 in the second factor below have radius one, and put*

$$Q_R := \big(S^2_R \times S^2\big) \big/ \big((x, x/R) \sim (x, -x/R)\big). \tag{41}$$

Thus the diagonal section $D_+ = \{(x, x/R)\}$ is identified pointwise with the antipodal section $D_- = \{(x, -x/R)\}$. Only the indicated pairs of section points are identified; neither section

is collapsed to a point. The formula

$$\begin{array}{ccc} S^2_R \times S^2 & \longrightarrow & L_1 S^2_R \\ (x,n) & \longmapsto & \gamma_{x,n} \end{array} \tag{42}$$

$$\gamma_{x,n}(t) \;=\; \langle x,n\rangle n + \cos(2\pi t)\Big(x - \langle x,n\rangle n\Big) + \sin(2\pi t)(n\times x)$$

induces a homeomorphism from Q_R onto the round-circle model A^2_R of Prop. 4.13. Consequently $Q_R \simeq L_1 S^2_R$ (cf. Fig. 1). Evaluation at $t = 0$ corresponds to projection onto x; the identified sections correspond to the constant loops.

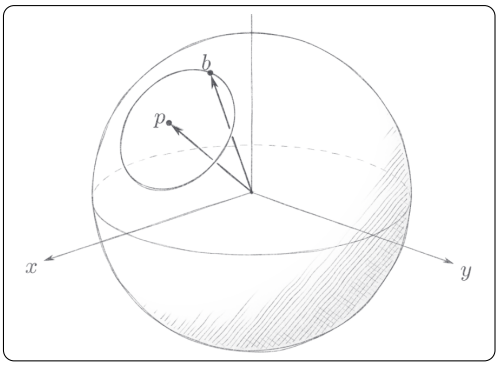


Figure 1: The space $L_1 S^2 \subset LS^2$ (22) of *small loops* in the sphere is homotopy equivalent (by Prop. 4.13) to its further subspace of loops that trace out round circles on S^2, once at constant rate.
These in turn are equivalently determined (Lem. 4.20) by their base point $b \in S^2$ and by the oriented rotation axis $p \in S^2 \subset \mathbb{R}^3$ that they are encircling clockwise. Here constant loops are included, regarded as circles of vanishing radius that as such may be regarded as oriented either by the axis $p = b$ or $p = -b$.

Proof. The vectors $x - \langle x,n\rangle n$ and $n \times x$ are orthogonal and have the same squared norm $R^2 - \langle x,n\rangle^2$. They are perpendicular to $\langle x,n\rangle n$. It follows that $|\gamma_{x,n}(t)| = R$, that $\gamma_{x,n}(0) = x$, and that

$$E(\gamma_{x,n}) \;=\; 2\pi^2\Big(R^2 - \langle x,n\rangle^2\Big) \;\leq\; 2\pi^2 R^2.$$

For $n \neq \pm x/R$ this is a once-traversed round circle whose oriented unit normal is n and whose initial point is x. These data determine each nonconstant round circle uniquely. For $n = \pm x/R$ the formula is the constant loop c_x, and these are its only degeneracies. The formula and its t-derivative depend continuously on (x,n), so it defines a continuous map into the H^1 loop space. The induced bijection from the compact quotient Q_R to the Hausdorff space A^2_R is a homeomorphism. The last assertions follow from evaluation and Prop. 4.13. □

Proposition 4.21 (The second homotopy group as a module)**.** *Put $Y = L_1 S^2_R$, based at a constant loop, and let τ denote the action of the generator $w \in \pi_1(Y)$ chosen in (39). As an abelian group,*

$$M \;:=\; \pi_2(Y) \;\cong\; \mathbb{Z}\alpha \;\oplus \bigoplus_{i\in\mathbb{Z}} \mathbb{Z} z_i. \tag{43}$$

Here α is the class of the constant-loop sphere. The class z_i is the negative of the usual second-factor sphere class in the ith sheet of the universal cover described below. With this orientation convention, the action is

$$\tau(\alpha) \;=\; \alpha + 2z_0, \qquad \tau(z_i) \;=\; z_{i+1}. \tag{44}$$

Equivalently, with t acting by τ, this is the $\mathbb{Z}[t,t^{-1}]$-module

$$M \;\cong\; \frac{\mathbb{Z}[t,t^{-1}]\{\alpha, z_0\}}{\Big\langle (t-1)\alpha - 2z_0 \Big\rangle}. \tag{45}$$

The first-factor sphere and the constant-loop sphere retain their usual orientations. Only the chosen generators z_i reverse the second-factor orientation in (41); the maps themselves are unchanged. This convention will give $[W_a, W_b] = \zeta_0^2$ when a labels the inner circle and b the outer circle.

Proof. The universal cover. For each $i \in \mathbb{Z}$, take a copy $E_i = S^2_R \times S^2$, with its two sections $D_{+,i}$ and $D_{-,i}$. Form a chain by making the identifications

$$\widetilde{Q}_R = \left(\coprod_{i\in\mathbb{Z}} E_i\right) \Big/ \big((x, -x/R)_i \sim (x, x/R)_{i+1}\big). \tag{46}$$

Each copy maps to Q_R by its quotient map. Away from the sections this is a disjoint union of copies of the identity. Near their image, a neighborhood in Q_R is obtained by identifying the zero sections of disjoint tubular neighborhoods of D_+ and D_-. Each lift of that neighborhood joins $D_{-,i}$ to $D_{+,i+1}$ in exactly the same way. These neighborhoods verify the covering-space condition. The shift $E_i \to E_{i+1}$ is a deck transformation.

Every finite subchain is simply connected: its pieces E_i are simply connected and adjacent pieces meet in a simply connected sphere. Apply van Kampen using tubular neighborhoods of the attaching sections. To pass to the whole chain, note that the formulas

$$h_i(x, n) = i + \frac{1 - \langle x/R, n\rangle}{2}$$

agree on the identified sections. They define a continuous height function whose bounded inverse images lie in finite subchains. Hence any loop has image in a finite subchain and is nullhomotopic there. The connected covering (46) is therefore the universal cover.

The representative β starts on $D_{+,0}$, traverses E_0 to $D_{-,0} = D_{+,1}$, and returns through the constant section. Its lift ends in the next sheet. Thus the deck shift represents the action τ of the specified generator, with the convention that conjugation uses $w(-)w^{-1}$. To view this as an action on based π_2, join the two lifted basepoints by the lifted path. Such basepoint changes are unambiguous in the simply connected cover.

Integral homology of the chain. In $H_2(E_i;\mathbb{Z})$ write b_i for the usual first-factor class and z_i for the negative of the usual second-factor class. Projection to the two factors shows that the section classes are

$$[D_{+,i}] = b_i - z_i, \qquad [D_{-,i}] = b_i + z_i. \tag{47}$$

The diagonal has second-factor degree $+1$, hence coefficient -1 in the chosen z_i basis; the antipodal section has degree -1, hence coefficient $+1$. For each finite subchain, Mayer–Vietoris presents H_2 as the direct sum of the $H_2(E_i)$ modulo the identifications of these section classes: there is no further term because $H_1(S^2) = 0$. Passing to the union gives

$$H_2(\widetilde{Q}_R;\mathbb{Z}) = \left(\bigoplus_i (\mathbb{Z}b_i \oplus \mathbb{Z}z_i)\right) \Big/ \Big\langle b_i + z_i = b_{i+1} - z_{i+1} \ : \ i \in \mathbb{Z}\Big\rangle.$$

Put $\alpha_i = b_i - z_i$, the class of $D_{+,i}$. The relations become

$$\alpha_{i+1} = \alpha_i + 2z_i \qquad (i \in \mathbb{Z}). \tag{48}$$

They eliminate every α_i except α_0, without imposing any relation on α_0 or the z_i. Thus the resulting abelian group is precisely the direct sum in (43), with $\alpha = \alpha_0$. Explicitly, the eliminations are

$$\alpha_i = \begin{cases} \alpha + 2\sum_{j=0}^{i-1} z_j, & i > 0, \\ \alpha - 2\sum_{j=i}^{-1} z_j, & i < 0. \end{cases}$$

Substitution into the section relations gives an inverse to the homomorphism from the free abelian group on α and the z_i, verifying that no relations are lost. All sums here have finite support.

Since the universal cover is simply connected, the Hurewicz map in degree two is an isomorphism. Covering-space invariance and Lem. 4.20 identify this homology group with $\pi_2(Y)$. The deck shift sends α_i to α_{i+1} and z_i to z_{i+1}. Equation (48) therefore proves the action and the module presentation. For later use, inner evaluation $\varepsilon : Y \to S^2_R$, $\varepsilon(\delta) = \delta(0)$, sends these classes to

$$\varepsilon_*(\alpha) = [\mathrm{id}_{S^2_R}], \qquad \varepsilon_*(z_i) = 0. \tag{49}$$

Indeed, by Lem. 4.20, evaluation is first-factor projection. The class α is represented by the diagonal section of constant loops, while z_i is represented in the cover by the second-factor sphere in E_i with its orientation reversed, and a path from the chosen basepoint to that sheet. In particular, z_0 is the negative of the based class of $n \mapsto \gamma_{x_0,n}$ from (42), based at $n = x_0/R$. An actual based representative is obtained by precomposing this map with a reflection of S^2 fixing x_0/R. □

The fundamental groups of the iterated free loop space. We now consider the *ordinary* free loop space $LY = C^0(S^1, Y)$, with the compact-open topology, of the *small* loop space $Y = L_1 S^2_R$, hence we consider the subspace

$$LL_1S^2 \subset LLS^2 \simeq \mathrm{Map}(T^2, S^2) \tag{50}$$

We label the inner (small) circle by a and the outer (ordinary) circle by b. The order of loop iteration is consequently outer b, inner a. Its path components correspond to conjugacy classes in $\pi_1(Y) = \langle w \rangle \cong \mathbb{Z}$, hence are indexed by an integer C. Write $(LY)_C$ for the component of

$$\gamma_C(t) = \beta(Ct), \tag{51}$$

where β is regarded as a period-one loop in Y. This convention also covers $C = 0$ and negative C.

The integer C is the degree of the adjoint torus map $(s,t) \mapsto \gamma(s)(t)$ to S^2_R, with the outer parameter first in the orientation. In the coordinate labels just fixed this is the orientation of $S^1_b \times S^1_a$, or (k_y, k_x) in the band-theory interpretation. It is the negative of the (k_x, k_y) orientation; the component label C is kept in the outer-first convention throughout. Indeed, for $\gamma = \beta$ the latitude sweep (38) covers the sphere once with positive orientation, and its constant-loop return has zero area. More explicitly, for normalized area form ω with $\int_{S^2_R} \omega = 1$,

$$\int_{[0,1]^2} \Gamma^* \omega = \int_0^1 \int_0^1 \frac{\pi}{2} \sin(\pi s)\, \mathrm{d}t\, \mathrm{d}s = 1.$$

Concatenation adds degrees, and degree is invariant under free homotopy. This identifies the component label with the usual degree label for torus maps.

The generator notation in the following theorem records these two directions. Evaluation at the outer loop's basepoint is

$$\begin{aligned} (LL_1S^2_R)_C &\xrightarrow{\mathrm{ev}_0} L_1S^2_R \\ \gamma &\longmapsto \gamma(0). \end{aligned}$$

The generator W_a maps to $w \in \pi_1(L_1S^2_R)$, hence corresponds to the *inner, bounded-energy* loop direction. The generator W_b comes from the constant-loop sphere $\alpha \in \pi_2(L_1S^2_R)$ of

Prop. 4.21, via the based-loop adjunction and translation to the component of γ_C. It lies in the kernel of $(\mathrm{ev}_0)_*$ and corresponds to the *outer, unrestricted* loop direction. In particular,

$$W_a \quad \longleftrightarrow \quad a = x = \text{inner } L_1, \qquad W_b \quad \longleftrightarrow \quad b = y = \text{outer } L.$$

Here "direction" refers to the torus coordinate on which the associated family of sphere maps varies. For instance, at $C = 0$, W_b is represented by a family independent of the inner coordinate, whereas the representative $B_0(s)(t) = \beta(s)$ of W_a is independent of the outer coordinate t. Here s parametrizes the loop representing an element of the fundamental group.

Theorem 4.22 (Fundamental groups of $LL_1S^2_R$)**.** *The space LL_1S^2 (50) has*

(i) *connected components $C \in \mathbb{Z}$:*

$$\pi_0\big(LL_1S^2\big) \simeq \mathbb{Z}\,, \tag{52}$$

(ii) *fundamental groups*

(a) *for $C = 0$:*

$$\pi_1\big(LL_1S^2, 0\big) \cong \left\langle \begin{array}{c} W_a, \\ W_b, \\ \{\zeta_i\}_{i\in\mathbb{Z}} \end{array} \middle| \begin{array}{rcl} [W_a, W_b] &=& \zeta_0^2, \\ [W_a, \zeta_i] &=& \zeta_{i+1}\zeta_i^{-1}, \\ [W_b, \zeta_i] &=& 1, \\ [\zeta_i, \zeta_j] &=& 1 \end{array} \begin{array}{l} \\ \\ \text{for} \\ i,j\in\mathbb{Z} \\ \\ \end{array} \right\rangle, \tag{53}$$

(b) *for $C \neq 0$:*

$$\pi_1\big(LL_1S^2, C\big) \cong \left\langle \begin{array}{r} W_a, \\ W_b, \\ \zeta_0\,, \\ \vdots\,, \\ \zeta_{|C|-1} \end{array} \middle| \begin{array}{rcl} [W_a, W_b] &=& \zeta_0^2, \\ [W_a, \zeta_i] &=& \zeta_{i+1}\zeta_i^{-1}, \\ [W_b, \zeta_i] &=& 1, \\ [\zeta_i, \zeta_j] &=& 1, \\ \zeta_0^2\zeta_1^2\cdots\zeta_{|C|-1}^2 &=& 1 \end{array} \begin{array}{l} \\ \\ \\ \\ \text{for} \\ i,j\in\mathbb{Z}_{/C} \end{array} \right\rangle. \tag{54}$$

More succinctly, these are semidirect products

$$\pi_1\big(LL_1S^2, C\big) \cong A_C \rtimes_\tau \mathbb{Z}\langle W_a\rangle, \qquad A_C = \begin{cases} \mathbb{Z}\alpha \oplus \dfrac{\bigoplus_{i=0}^{N-1}\mathbb{Z}z_i}{\langle 2\sum_{i=0}^{N-1} z_i\rangle}, & \text{if } C \neq 0, \\ \mathbb{Z}\alpha \oplus \displaystyle\bigoplus_{i\in\mathbb{Z}} \mathbb{Z}z_i, & \text{if } C = 0, \end{cases} \tag{55}$$

where W_b and ζ_i are the multiplicative forms of α and z_i, and $\tau(\alpha) = \alpha + 2z_0$, $\tau(z_i) = z_{i+1}$.

Proof. [1] *The evaluation fibration.* By Lem. 4.20, Y has the homotopy type of the finite gluing model Q_R; in particular, the usual based and free-loop homotopy calculations apply. Write $y_0 = c_{x_0}$, and let $PY = C^0([0,1], Y)$. The endpoint map $PY \to Y \times Y$ is a fibration, and its pullback along the diagonal is

$$\begin{array}{ccc} LY & \longrightarrow & PY \\ {\scriptstyle \mathrm{ev}_0}\downarrow & & \downarrow{\scriptstyle (\mathrm{ev}_0, \mathrm{ev}_1)} \\ Y & \xrightarrow[\Delta]{} & Y \times Y. \end{array}$$

[1] A formalization of the proof of Thm. 4.22 in `Lean 4` is available at ncatlab.org/nlab/show/Materials#MorseBottOfLoopSpaces. The equivalence $Q_1 \simeq L_1S^2$ (Lem. 4.20) assumed in this proof is currently not covered by this formalization.

Thus evaluation gives the free-loop fibration

$$\Omega Y \longrightarrow LY \xrightarrow{\mathrm{ev}_0} Y.$$

Here ΩY consists of loops based at y_0. The chosen loop γ_C represents w^C, by (39) and (51). Transport around a loop representing w^k conjugates the component label to $w^k w^C w^{-k}$. Since Thm. 4.17 identifies $\pi_1(Y)$ with $\mathbb{Z}$, this label does not change. Consequently the restriction to $(LY)_C$ has the connected fiber $\Omega_C Y$, and evaluation is surjective on fundamental groups. Its homotopy exact sequence has the segment

$$M \xrightarrow{1-\tau^C} M \longrightarrow G_C \xrightarrow{(\mathrm{ev}_0)_*} \mathbb{Z} \longrightarrow 0, \qquad M = \pi_2(Y). \tag{56}$$

The module M and the action τ are precisely those of Prop. 4.21. The second copy of M is $\pi_1(\Omega_C Y, \gamma_C)$, identified with $\pi_2(Y)$ by translation to the identity component of the based loop space, specified in (58) below. To identify the first arrow, first consider the endpoint fibration based at the path γ_C. A pair of spheres at its endpoints represents $(m_0, m_1) \in M \oplus M$. Its boundary compares the two spheres after transporting the second along γ_C. With right translation by γ_C and the boundary orientation chosen here, this is

$$\partial_{\mathrm{end}}(m_0, m_1) = m_0 - \tau^C m_1.$$

The diagonal sends a sphere of basepoints m to (m, m). Naturality of the boundary under the displayed pullback therefore gives $\partial(m) = m - \tau^C m$. Changing the sign of this boundary convention does not change its image. These are the evaluation-fibration calculations underlying the general centralizer description of free-loop fundamental groups; compare [Bro10, Thm. 1.5]. The same boundary is described by component Samelson products in Prop. 4.28 below.

In particular, it is the quotient by the differences $m - \tau^C m$ that enters $\pi_1((LY)_C)$, not the subgroup of elements fixed by τ^C. Thus (56) gives the short exact sequence

$$1 \longrightarrow M/(\tau^C - 1)M \longrightarrow G_C \longrightarrow \mathbb{Z} \longrightarrow 1. \tag{57}$$

For precision, denote the map from the second copy of M in (56) by $\iota_C : M \to G_C$. It is the composite

$$\begin{gathered} \pi_2(Y, y_0) \cong \pi_1(\Omega_0 Y, c_{y_0}) \xrightarrow{(T_C)_*} \pi_1(\Omega_C Y, \gamma_C) \longrightarrow \pi_1((LY)_C, \gamma_C), \\ \Omega_0 Y \xrightarrow{T_C} \Omega_C Y \\ \omega \longmapsto \omega * \gamma_C. \end{gathered} \tag{58}$$

The standard unit reparametrization identifies $c_{y_0} * \gamma_C$ with γ_C. The inverse translation uses the reversed loop γ_C^{-1}, so T_C is a homotopy equivalence. The generators in the abelian kernel are, by definition,

$$W_b = \iota_C(\alpha), \qquad \zeta_i = \iota_C(z_i).$$

Thus W_b comes from the constant-loop sphere and the ζ_i from the orientation-reversed second-factor spheres in the universal cover, as described in (49).

Splitting and conjugation. The extension (57) splits as an extension of groups: a lift of the generator of $\mathbb{Z}$ is the loop in $(LY)_C$ given explicitly by

$$B_C(s)(t) = \beta(s + Ct), \qquad W_a = [B_C]. \tag{59}$$

Indeed, $B_C(0) = B_C(1) = \gamma_C$ and $B_C(s)(0) = \beta(s)$. Sending an integer k to W_a^k is a section of the surjection on fundamental groups. This does not assert a section of the evaluation fibration over every point of Y in the component C. Conjugation by W_a on the kernel is

transport around w, with the conjugation convention used in Prop. 4.21. More explicitly,

$$W_a\, \iota_C(m)\, W_a^{-1} \;=\; \iota_C(\tau m).$$

This follows by moving the basepoint of the representing sphere along $\mathrm{ev}_0 B_C = \beta$ in (58). The action is independent of the lift of w, since two lifts differ by an element of the abelian kernel. This proves

$$G_C \;\cong\; \Big(M/(\tau^C - 1)M\Big) \rtimes_\tau \mathbb{Z}.$$

Computing the quotient integrally. For $C = 0$, the endomorphism $\tau^C - 1$ is zero, so the kernel is the whole group in (43). For $C \neq 0$, the images of $\tau^C - 1$ and $\tau^N - 1$ are the same, where $N = |C|$: for $C = -N$ use $\tau^{-N} - 1 = -\tau^{-N}(\tau^N - 1)$ and invariance of the latter image under τ. On the displayed generators of M,

$$(\tau^N - 1)z_i \;=\; z_{i+N} - z_i, \qquad (\tau^N - 1)\alpha \;=\; 2\sum_{i=0}^{N-1} z_i. \tag{60}$$

Because α and the z_i freely generate M as an abelian group, these generate the entire image of $\tau^N - 1$. They impose exactly periodicity of the z_i and the single relation $2\sum_i z_i = 0$. This is A_C in (55). The action descends: shifting the sum leaves it fixed, and $\tau^N(\alpha) = \alpha + 2\sum_i z_i = \alpha$ in this quotient. This calculation takes place over $\mathbb{Z}$: the relation $2\sum_i z_i = 0$ does not permit cancellation of the factor 2.

The group presentation. The kernel A_C is abelian, so W_b commutes with all ζ_i, and the ζ_i commute with one another. The action of W_a gives

$$W_a W_b W_a^{-1} \;=\; W_b \zeta_0^2, \qquad W_a \zeta_i W_a^{-1} \;=\; \zeta_{i+1}.$$

The first identity is equivalent to $[W_a, W_b] = \zeta_0^2$ with the stated convention. For $C \neq 0$, the remaining additive relation becomes $(\prod_i \zeta_i)^2 = 1$. Conversely, these relations move every W_a to the right of a word, yielding a pair (u, k) with $u \in A_C$ and $k \in \mathbb{Z}$. The multiplication is

$$(u, k)(v, l) \;=\; (u + \tau^k v, k + l).$$

The semidirect product with this multiplication satisfies all the relations and receives the displayed generators. The resulting homomorphisms in both directions fix every generator and are therefore mutually inverse. Hence there are no further defining relations. □

Proposition 4.23 (Inclusion into the unrestricted torus mapping space)**.** *Let $j : L_1 S^2_R \hookrightarrow L S^2_R$ be the inclusion, using the continuous loop space of Def. 2.6, and let*

$$\begin{array}{ccc} LL_1 S^2_R & \xrightarrow{J := Lj} & LLS^2_R \;\cong\; \mathrm{Map}(T^2, S^2_R) \\ \gamma & \longmapsto & j \circ \gamma. \end{array} \tag{61}$$

Write $\bar\gamma_C = J(\gamma_C)$ and $H_C = \pi_1((LLS^2_R)_C, \bar\gamma_C)$. The map J preserves the degree C and induces a bijection on path components. For each $C \in \mathbb{Z}$, there are generators $\overline{W}_a, \overline{W}_b, \zeta$ for which

$$H_C \;\cong\; \Big\langle \overline{W}_a, \overline{W}_b, \zeta \;\Big|\; [\overline{W}_a, \zeta] = [\overline{W}_b, \zeta] = 1, \quad [\overline{W}_a, \overline{W}_b] = \zeta^2, \quad \zeta^{2C} = 1 \Big\rangle. \tag{62}$$

For $C = 0$, the last relation is vacuous and ζ has infinite order; for $C \neq 0$, its order is exactly $2|C|$. The induced homomorphism is surjective and is specified on the generators of

Thm. 4.22 by

$$\begin{aligned} G_C &\xrightarrow{J_*} H_C \\ W_a &\longmapsto \overline{W}_a \\ W_b &\longmapsto \overline{W}_b \\ \zeta_i &\longmapsto \zeta. \end{aligned} \tag{63}$$

Thus all the ζ_i have the same image, a central generator originating in $\pi_3(S^2)$. More precisely, the kernel is the normal subgroup generated by $\zeta_i\zeta_0^{-1}$ and, as an abstract group, is

$$\ker J_* \cong \begin{cases} \mathbb{Z}^{|C|-1}, & C \neq 0, \\ \bigoplus_{i\in\mathbb{Z}-\{0\}} \mathbb{Z}, & C = 0. \end{cases} \tag{64}$$

In particular, J_* is an isomorphism exactly for $C = 1$ and $C = -1$.

Proof. The unrestricted inner loop space. Put $Y = L_1S^2_R$ and $X = LS^2_R$, with the same constant base loop. The map j factors as

$$Y \hookrightarrow L_\infty S^2_R \longrightarrow X.$$

By Lem. 2.8 and Cor. 4.19, it induces an isomorphism on π_1, taking w to $\bar{w} = [j\beta]$. Free-loop components are conjugacy classes, so this proves the assertion about components. It also preserves their degree label, since the adjoint torus map itself is unchanged.

Evaluation on the inner loop space has the constant-loop section:

$$\Omega S^2_R \longrightarrow X \xrightarrow{\varepsilon} S^2_R, \qquad s(x) = c_x, \qquad \varepsilon s = \mathrm{id}.$$

The section makes the connecting homomorphisms in the homotopy exact sequence zero. Hence

$$\pi_1(X) \cong \pi_2(S^2_R) \cong \mathbb{Z}, \qquad M' := \pi_2(X) \cong \mathbb{Z}\alpha' \oplus \mathbb{Z}\eta, \tag{65}$$

where $\alpha' = s_*[\mathrm{id}_{S^2_R}]$ and the second summand is the image of $\pi_2(\Omega S^2_R) = \pi_3(S^2_R)$. The Hopf fibration $S^1 \to S^3 \to S^2$ identifies this last group with $\pi_3(S^3) = \mathbb{Z}$, generated by the Hopf map; see [Hat02, Ex. 4.51]. We fix the sign of η below.

The map on π_2 and the primitive Hopf class. The homomorphism $j_* : M \to M'$ is surjective. Indeed, the proof of Cor. 4.19 uses Thms. 3.10 and 4.5 to build every later stage by relative cells of dimension at least three. Cellular approximation therefore makes each map on π_2 surjective: in the attachment model of the pair, a two-dimensional sphere can be moved into the earlier stage, since every new cell has dimension at least three. Such cells may nevertheless impose relations on π_2, so injectivity is not being asserted. Every compact family of Sobolev loops has bounded energy, by continuity of (2), and so lies in a finite stage of Def. 2.13. The assertion follows for $L_\infty S^2_R$, and then for X by Lem. 2.8.

Let τ' be the action of $\bar{w}$ on M'. It is trivial on the fiber summand $\mathbb{Z}\eta$. To see this, note that $\pi_1(\Omega S^2_R) \to \pi_1(X)$ is an isomorphism, again by the section and the exact sequence. The path-connected loop space ΩS^2_R is an H-space, and its fundamental group acts trivially on its higher homotopy groups. Explicitly, multiplication of a sphere by a loop in this H-space gives a homotopy whose basepoint traces that loop and whose initial and final spheres agree. Naturality transfers this trivial action to the fiber summand in M'.

The constant-loop sections agree under j, so $j_*(\alpha) = \alpha'$. By (49), every $j_*(z_i)$ lies in the fiber summand. Naturality of the fundamental-group action and (44) now give

$$j_*(z_i) = j_*(\tau^i z_0) = (\tau')^i j_*(z_0) = j_*(z_0).$$

Initially write their common value as $d\eta$ for an arbitrary Hopf generator. Since α, z_i generate M and j_* is surjective onto $\mathbb{Z}\alpha' \oplus \mathbb{Z}\eta$, one must have $d = 1$ or $d = -1$. Choose the Hopf generator's sign so that $j_*(z_0) = \eta$. This proves, without an undetermined integer multiple,

$$j_*(\alpha) = \alpha', \qquad j_*(z_i) = \eta \quad (i \in \mathbb{Z}), \qquad \tau'(\alpha') = \alpha' + 2\eta, \qquad \tau'(\eta) = \eta. \tag{66}$$

The formula for $\tau'(\alpha')$ follows by applying j_* to (44). Thus the sign convention is inherited from the geometric generators already chosen, rather than imposed separately.

Naturality of the outer evaluation calculation. Apply the evaluation-fibration argument in the proof of Thm. 4.22 to X and $\bar{\beta} = j\beta$. It gives

$$H_C \cong A'_C \rtimes_{\tau'} \mathbb{Z}, \qquad A'_C = \frac{M'}{((\tau')^C - 1)M'} \cong \mathbb{Z}\alpha' \oplus \big(\mathbb{Z}\eta/\langle 2C\eta\rangle\big). \tag{67}$$

Here $(\tau')^C(\alpha') = \alpha' + 2C\eta$ for every integer C, including negative C. The generators $\overline{W}_b$ and ζ are the images of α' and η under the analogue of (58). The generator $\overline{W}_a$ is represented by $\bar{B}_C(s)(t) = \bar{\beta}(s + Ct)$, the image of (59). The action in (66) therefore gives exactly (62), including the asserted order of ζ.

All maps just used commute with j, so there is a commutative diagram of split short exact sequences

$$\begin{array}{ccccccccc} 1 & \longrightarrow & A_C & \longrightarrow & G_C & \longrightarrow & \mathbb{Z} & \longrightarrow & 1 \\ & & \downarrow{\scriptstyle \bar{j}_*} & & \downarrow{\scriptstyle J_*} & & \| & & \\ 1 & \longrightarrow & A'_C & \longrightarrow & H_C & \longrightarrow & \mathbb{Z} & \longrightarrow & 1. \end{array} \tag{68}$$

On the left, $\bar{j}_*$ is induced by (66); the splittings are also preserved since $J \circ B_C = \bar{B}_C$. This proves the three generator formulas and surjectivity.

The kernel. By the diagram, $\ker J_* = \ker \bar{j}_*$. For $C \neq 0$, let $N = |C|$ and put $s = \sum_{i=0}^{N-1} z_i$. The coefficient of α is preserved, and on the remaining summand the map is

$$\begin{aligned} \mathbb{Z}^N/\langle 2s\rangle &\longrightarrow \mathbb{Z}/(2N) \\ [\textstyle\sum_i q_i z_i] &\longmapsto \textstyle\sum_i q_i \pmod{2N}. \end{aligned}$$

Every element of its kernel has a unique representative whose coefficients sum to zero: subtract the appropriate multiple of $2s$, whose coefficient sum is $2N$. The subgroup of such representatives is freely generated by $z_i - z_0$ for $1 \leq i < N$. For $C = 0$, the same argument uses finite-support integer sequences and their ordinary sum, with no quotient relation; the basis is $z_i - z_0$ for $i \neq 0$. In multiplicative notation these bases are $\zeta_i\zeta_0^{-1}$. Their subgroups are invariant under the shift action of W_a, hence are already normal in G_C. This proves (64) and the final assertion. □

In degree zero, (62) is the integral Heisenberg-type presentation with commutator $[\overline{W}_a, \overline{W}_b] = \zeta^2$. The Samelson-product proof of this unrestricted presentation in [KSS26, Thms. 3.3 and 3.5] is related to the present generators in Rem. 4.27 and Prop. 4.28. The nonzero-degree groups are its central quotients by $\zeta^{2C} = 1$. Thus inclusion identifies the indexed Hopf generators with a single central generator; it preserves the two loop-direction generators.

Corollary 4.24 (Torsion, cyclic action, and the smallest sectors)**.** *For $C \neq 0$ and $N = |C|$, the abelian kernel is $A_C \cong \mathbb{Z}^N \oplus \mathbb{Z}/2$. The element*

$$\kappa = \prod_{i=0}^{N-1} \zeta_i$$

is central and has order exactly two. Under Prop. 4.23, its image is $J_*(\kappa) = \zeta^N$, also of order exactly two. The action of W_a on A_C has order N, and W_a^N is central. The subgroup generated by A_C and W_a^N is abelian of index N. For $C = 1$ or $C = -1$,

$$G_C \cong \mathbb{Z}^2 \oplus \mathbb{Z}/2.$$

For $|C| \geq 2$, and also for $C = 0$, the group is nonabelian.

Proof. The vector $\sum_i z_i$ is primitive in $\mathbb{Z}^N$, so quotienting by twice that vector gives $\mathbb{Z}^{N-1} \oplus \mathbb{Z}/2$. Adding $\mathbb{Z}\alpha$ proves the assertion about A_C, and shows that κ has exact order two. The inclusion formula follows from (63), and its image has order two since ζ has order $2N$. The cyclic shift fixes this sum, hence κ is central. Equation (60) shows that $\tau^N = 1$ on A_C. If $0 < k < N$, the vector $z_k - z_0$ is not a multiple of $2\sum_i z_i$, so $\tau^k \neq 1$; the order is exactly N. The claims about W_a^N and the subgroup index now follow from the semidirect product.

For $N = 1$ the relation is $\zeta_0^2 = 1$, and the action is trivial, giving the stated abelian group. For $N \geq 2$, $2z_0$ is nonzero modulo $\langle 2\sum_i z_i \rangle$, so $[W_a, W_b] = \zeta_0^2 \neq 1$. For $C = 0$, the same commutator is nontrivial because z_0 has infinite order in the free abelian kernel. □

Samelson products and the unrestricted comparison. The preceding computation has a complementary description by Samelson products. Kallel–Sati–Schreiber use these to compute the unrestricted torus mapping groups [KSS26, §§ 2.2–3.2]. Here and in the following pinpoints we use their revised manuscript dated August 13, 2026. We first recall the source of the factor two, then identify the additional Samelson products that retain the bounded-stage information in Thm. 4.22.

Definition 4.25 (Samelson products and components)**.** Let Z be a pointed connected space of CW homotopy type. The based-loop space ΩZ is an H-group under concatenation. Its commutator, with convention $uvu^{-1}v^{-1}$, induces up to homotopy a map

$$\begin{aligned} \Omega Z \wedge \Omega Z &\xrightarrow{[-,-]_{\mathrm{Sam}}} \Omega Z \\ u \wedge v &\longmapsto uvu^{-1}v^{-1}. \end{aligned}$$

One may use a topological-group model of ΩZ to make the unit cancellations and passage to the smash product literal. Composing with representatives on S^p and S^q gives the *Samelson product*

$$[-,-]_{\mathrm{Sam}} : \pi_p(\Omega Z) \times \pi_q(\Omega Z) \longrightarrow \pi_{p+q}(\Omega Z).$$

For $p, q \geq 1$ it is the usual bilinear product. The same commutator construction also applies when one index is zero, using S^0 to represent a component. In that case it records conjugation by that component; bilinearity in the component variable is not asserted.

Under suspension–loop adjunction, the positive-degree Samelson product corresponds, with the suspension sign convention, to the Whitehead product. The latter is defined using the attaching map of the top cell of $S^{p+1} \times S^{q+1}$ to $S^{p+1} \vee S^{q+1}$. See [KSS26, Defs. 2.5–2.6 and Prop. 2.7].

Lemma 4.26 (The two-sphere square)**.** *Let $\iota = [\mathrm{id}_{S^2}]$ and let $h \in \pi_3(S^2)$ be the Hopf generator of Hopf invariant one. With compatible Whitehead and adjunction orientations,*

$$[\iota, \iota]_{\mathrm{Wh}} = 2h, \qquad [e, e]_{\mathrm{Sam}} = 2\tilde{h}, \quad e = \tilde{\iota} \in \pi_1(\Omega S^2), \quad \tilde{h} \in \pi_2(\Omega S^2). \tag{69}$$

In particular, the coefficient is integral and is exactly two.

Proof. The Hopf fibration and its homotopy exact sequence identify $\pi_3(S^2)$ with $\mathbb{Z}h$, as recalled in the proof of Prop. 4.23. The Hopf invariant is a homomorphism on this group and sends h to one. We compute it on the Whitehead square.

Write $C_{[\iota,\iota]}$ for its mapping cone. The fold map $S^2 \vee S^2 \to S^2$ extends over the top cell to a map $F : S^2 \times S^2 \to C_{[\iota,\iota]}$ of degree one on that cell. If x and y are the degree-two and degree-four generators of the cone's integral cohomology, and u, v are the two factor classes of the product, then

$$F^*x = u + v, \qquad F^*y = uv, \qquad (u+v)^2 = 2uv.$$

Thus $x^2 = 2y$, which is the definition of Hopf invariant two. Since h generates $\pi_3(S^2)$, this proves the first identity. The adjunction identifies its adjoint with the displayed Samelson square, proving the second. This is the $k = 1$ case of [KSS26, Prop. 2.9]. □

Remark 4.27 (The unrestricted commutator). Here is how Lem. 4.26 gives the commutator in (62). Write $T^2 = S^1_b \times S^1_a$, with a the inner and b the outer parameter, as fixed before Thm. 4.22. Let

$$\begin{aligned} T^2 = S^1_b \times S^1_a &\xrightarrow{q_{ab}} S^1_a \wedge S^1_b \cong S^2 \\ (t_b, t_a) &\longmapsto t_a \wedge t_b. \end{aligned}$$

collapse the two coordinate circles, after ordering the coordinates as (a, b). The smash sphere on the right has the (a, b) orientation, so q_{ab} has degree -1 relative to the outer-first (b, a) orientation used for the component label C. In the component of the constant map, adjunction gives an isomorphism of groups

$$\pi_1 \operatorname{Map}_{*,0}(T^2, S^2) \cong [T^2, \Omega S^2]_*. \tag{70}$$

The multiplication on the right is induced by pointwise loop concatenation. Consider the three representatives

$$U_a = e \circ \mathrm{pr}_a, \qquad U_b = e \circ \mathrm{pr}_b, \qquad V = \widetilde{h} \circ q_{ab}.$$

Here e and $\widetilde{h}$ also denote chosen based maps representing the classes in Lem. 4.26. Their first commutator is the composite

$$T^2 \xrightarrow{q_{ab}} S^1_a \wedge S^1_b \xrightarrow{e \wedge e} \Omega S^2 \wedge \Omega S^2 \xrightarrow{[-,-]_{\mathrm{Sam}}} \Omega S^2, \tag{71}$$

so $[U_a, U_b] = V^2$. The mixed commutators with V factor through maps $T^2 \to S^1 \wedge S^2 = S^3$, which are nullhomotopic by cellular approximation. Thus V is central. This is the two-sphere specialization of [KSS26, Thm. 3.3].

To see that these are all generators and relations, restrict to $A = S^1_a \vee S^1_b$. The cofiber sequence $A \to T^2 \xrightarrow{q_{ab}} S^2 \to \Sigma A$ gives

$$1 \longrightarrow \pi_2(\Omega S^2) \xrightarrow{q^*_{ab}} [T^2, \Omega S^2]_* \longrightarrow \pi_1(\Omega S^2)^2 \longrightarrow 1.$$

Indeed, the connecting map $S^2 \to \Sigma A$ is the suspension of the torus attaching commutator and is nullhomotopic. Thus q^*_{ab} is injective; restriction is surjective because the classes U_a, U_b lift the two standard generators. The image of the generator under q^*_{ab} is V, so every element has a unique expression $U_a^p U_b^q V^r$, with $p, q, r \in \mathbb{Z}$. Together with the commutators this proves the complete presentation. Equivalently, $\Sigma T^2 \simeq S^2 \vee S^2 \vee S^3$ supplies three integer coordinates, but this is not a splitting of suspension cogroups and hence does not make the group abelian.

Forgetting the based condition induces an isomorphism on fundamental groups in degree zero, because evaluation has the constant-map section and S^2 is simply connected. With

compatible choices of orientations and lifts, the classes above are $\overline{W}_a, \overline{W}_b, \zeta$ of Prop. 4.23. In particular, the Hopf generator's sign is calibrated by the already fixed ordered commutator $[\overline{W}_a, \overline{W}_b] = \zeta^2$. The sign reversal in q_{ab} relative to the outer-first ordering agrees with the orientation-reversed classes z_i chosen in Prop. 4.21. Thus the positive Hopf generator h in the Whitehead-square lemma is unchanged; its torus representative uses the ordered smash (a, b) and has the sign required by ζ.

Proposition 4.28 (Samelson products recover the bounded-stage action)**.** *Put $Y = L_1 S^2_R$ and retain $M = \pi_2(Y)$, w, and τ from Prop. 4.21. Let $u \in \pi_0(\Omega Y)$ be the component represented by β, so u corresponds to $w \in \pi_1(Y)$. For $m \in M$ write $m^\flat \in \pi_1(\Omega_0 Y)$ for its loop adjoint. Then, for every $r \in \mathbb{Z}$,*

$$[m^\flat, u^r]_{\mathrm{Sam}} = \Big((1-\tau^r)m\Big)^\flat, \qquad [u^r, m^\flat]_{\mathrm{Sam}} = \Big((\tau^r-1)m\Big)^\flat. \tag{72}$$

In particular,

$$[u, \alpha^\flat]_{\mathrm{Sam}} = (2z_0)^\flat, \qquad [u, z_i^\flat]_{\mathrm{Sam}} = (z_{i+1} - z_i)^\flat. \tag{73}$$

Under the homomorphism $\iota_C : M \to G_C$ of (58), these become

$$[W_a, W_b] = \zeta_0^2, \qquad [W_a, \zeta_i] = \zeta_{i+1}\zeta_i^{-1}.$$

For $j : Y \to X := LS^2_R$, the naturality of these products is expressed, before taking coinvariants, by

$$\begin{array}{ccc} M & \xrightarrow{\tau^r - 1} & M \\ {\scriptstyle j_*}\downarrow & & \downarrow{\scriptstyle j_*} \\ M' & \xrightarrow[(\tau')^r - 1]{} & M', \end{array} \qquad M' = \pi_2(X). \tag{74}$$

For $m = \alpha$ and $r = 1$, the top output $2z_0$ maps to 2η; the shift differences $z_{i+1} - z_i$ map to zero. Here η is the image in $\pi_2(X)$ of the Hopf generator, as in (66).

Proof. Choose a representative loop $f_m : S^1 \to \Omega_0 Y$ of $m^\flat$. The commutator with a representative of u^r is the loop

$$t \longmapsto f_m(t)\, \beta^r\, f_m(t)^{-1}\, \beta^{-r}.$$

In the abelian group $\pi_1(\Omega_0 Y) = M$, its class is the sum of m and the negative of the conjugated class $\tau^r m$. Reversing the order of the two commutator factors gives $\tau^r m - m$. This proves (72). Substituting the action (44) gives (73).

To pass to G_C, the splitting (59) represents u by W_a, and conjugation acts on the abelian kernel by τ, as proved in Thm. 4.22. Thus the commutator of $\iota_C(m)$ with W_a^r is $\iota_C((1-\tau^r)m)$, and similarly in the reverse order. This gives the two claimed group commutators.

Finally Ωj preserves concatenation and inverses up to homotopy, hence preserves Samelson products. Equivalently, $j_*\tau = \tau' j_*$; this proves the commutative square. Its values follow from (66). The value 2η is therefore the same Hopf coefficient detected by the ordinary Samelson square in Rem. 4.27. □

This formulation also identifies the relation imposed by the component C. For $r > 0$, telescoping gives

$$(\tau^r - 1)\alpha = 2\sum_{i=0}^{r-1} z_i, \qquad j_*\Big((\tau^r - 1)\alpha\Big) = 2r\eta. \tag{75}$$

For $r = -N < 0$ the first expression is $-2\sum_{i=-N}^{-1} z_i$, and the second remains $2r\eta$. The evaluation boundary in (56) is $1 - \tau^C$, the negative of the displayed operator at $r = C$.

These operators have the same image, so the boundary kills these component Samelson products. For $C \neq 0$, it also kills $(1-\tau^C)z_i = z_i - z_{i+C}$. Together these are exactly the periodicity and product relations in (60). After applying j_*, they become the single relation $2C\eta = 0$ of (67).

Remark 4.29 (The pointed fiber and the second appearance of two). The revised argument in [KSS26, Lems. 3.8–3.9 and Prop. 3.10] recovers the same relation using restriction to the coordinate wedge $A = S^1_a \vee S^1_b \subset T^2$. Choose a degree-$C$ torus map constant on A, using the outer-first orientation. Under the identification by q_{ab} above, its induced map from the smash sphere has degree $-C$. The fiber of restriction over the constant map on A is the *pointed* mapping space

$$\mathrm{Map}_{*,C}(T^2/A, S^2) \cong \mathrm{Map}_{*,-C}(S^2, S^2),$$

where the component label on T^2/A uses the orientation inherited from T^2, while S^2 has the (a,b) smash orientation. This pointed mapping space has fundamental group $\mathbb{Z}h$. It is not the unpointed sphere mapping space. Evaluation and its constant-map section give

$$\pi_2 \mathrm{Map}(A, S^2) \cong \underbrace{\mathbb{Z}^2}_{\pi_3(S^2)\oplus\pi_3(S^2)} \oplus \underbrace{\mathbb{Z}}_{\pi_2(S^2)}, \qquad \pi_1 \mathrm{Map}(A, S^2) \cong \mathbb{Z}^2.$$

The corresponding exact sequence is

$$\mathbb{Z}^2 \oplus \mathbb{Z} \xrightarrow{\partial_C} \mathbb{Z}h \longrightarrow H_C \longrightarrow \mathbb{Z}^2 \longrightarrow 1, \qquad \partial_C(p,q,r) = -2Cr\,h. \tag{76}$$

Here are the two ingredients in the boundary computation. For the based-circle summands, use the pointed restriction fibration. It is modeled by the homotopy fiber of

$$\begin{aligned} \Omega S^2 \times \Omega S^2 &\xrightarrow{\quad c \quad} \Omega S^2 \\ (\alpha, \beta) &\longmapsto \alpha\beta\alpha^{-1}\beta^{-1}. \end{aligned}$$

The map c is nullhomotopic on either factor, hence c_* vanishes on their direct sum π_2. This gives zero boundary on the first two summands. Changing the nullhomotopy of the attaching loop to the choice representing the torus component C does not alter this vanishing: the resulting transport acts through $\pi_1(\Omega S^2)$, whose action on higher homotopy groups is trivial, as explained in Prop. 4.23.

For the last summand, pull back restriction along the constant-map section $S^2 \to \mathrm{Map}(A, S^2)$. A torus map constant on A factors through $T^2/A = S^2$, so this pullback is the sphere evaluation fibration

$$\mathrm{Map}_{*,-C}(S^2, S^2) \longrightarrow \mathrm{Map}_{-C}(S^2, S^2) \longrightarrow S^2.$$

Its boundary on $r\iota$ is $[-C\iota, r\iota]_{\mathrm{Wh}} = -2Crh$, with the boundary orientation chosen in (76). Geometrically, extending the corresponding family of degree-$(-C)$ spheres with moving basepoint over a parameter two-sphere requires extending the map on $S^2 \vee S^2$ over $S^2 \times S^2$; the top-cell obstruction is precisely this Whitehead product. This proves the displayed boundary formula and recovers the subgroup generated by ζ, already shown to be central, as $\mathbb{Z}/(2C)$ (meaning $\mathbb{Z}$ if $C = 0$). In the iterated evaluation calculation this same integer appears as $(1-(\tau')^C)\alpha' = -2C\eta$. Reversing the boundary orientation reverses both signs, without changing the quotient relation $\zeta^{2C} = 1$. Thus the Heisenberg coefficient two and the order $2|C|$ of its central generator when $C \neq 0$ are two consequences of the same Whitehead square.

Remark 4.30 (What the energy bound retains). The component products in (73) contain

more information than the ordinary Samelson square in ΩS^2: they distinguish the indexed classes z_i. On the subgroup $\bigoplus_i \mathbb{Z} z_i \subset M$, inclusion is the summation map $\sum_i q_i z_i \mapsto (\sum_i q_i)\eta$. It kills every shift difference, but does not make the entire action trivial: $\tau'(\alpha') = \alpha' + 2\eta$ survives. This explains simultaneously the centrality of the single unrestricted Hopf generator and the surviving Heisenberg commutator.

The auxiliary H-group used here is ΩY, whose components are indexed by $\pi_1(Y) = \mathbb{Z}$. Conjugation by these components can act nontrivially. This is compatible with the trivial action of the fundamental group of the *connected* H-space ΩS^2 used in Prop. 4.23. No closure of $L_1 S^2$ under concatenating its inner loops is assumed. The first-stage Morse–Bott geometry is still needed to compute M and τ; the Samelson description then interprets their commutators and their loss of information under inclusion.

Remark 4.31 (Scope of the two-sphere formula). The corrected [KSS26, Prop. 2.9] retains torsion terms in the higher-dimensional squares:

$$[\iota_4, \iota_4]_{\mathrm{Wh}} = 2h_{\mathbb{H}} - \kappa_{\mathbb{H}}, \qquad [\iota_8, \iota_8]_{\mathrm{Wh}} = 2h_{\mathbb{O}} - \kappa_{\mathbb{O}}.$$

Here the torsion generators have orders 12 and 120, respectively. Hence those integral identities cannot be obtained from the Hopf invariant alone. For the present two-sphere computation, $\pi_3(S^2) = \mathbb{Z}$ has no torsion, so (69) is an exact integral identity. In particular, these corrections do not change Thm. 4.22 and Prop. 4.23.

4.1.2 The 4-Sphere

For the four-sphere the first stage is simply connected, so Sullivan models provide a direct description of its rational homotopy groups. We compute the model through generators of degree ten in Thm. 4.36 below. Its small-cyclification counterpart is stated and proved in Cor. 4.39. We use the generator names and normalizations of [GSS26, Prop. 3.10 and Rem. 3.11]: H_3, H_7 and $F_2, F_4, F_6, F_8, F_{10}$, with subscripts indicating degrees. In particular, the quadratic term in $\mathrm{d}H_7$ has coefficient $\frac{1}{2}$. The proof uses the first-stage attachment to compute cohomology, then the later attachments to compare with the full loop space. That comparison supplies information not determined by the cohomology groups alone.

For the following model calculations put $Y = L_1 S^4_R$ and $X = L S^4_R$, and work over $\mathbb{Q}$. The subsequent lifting discussion returns to integral coefficients. Constant rescaling does not change the answer, by Lem. 4.1.

Sullivan models and the meaning of the degree bound. We recall the algebraic conventions before doing the calculation; see [FH17, §§ 2–4] for the general theory.

Definition 4.32 (Minimal Sullivan models and their generator stages)**.** For a positively graded rational vector space V, write $\mathbb{Q}[V]$ for the *free graded-commutative algebra*: even generators commute and admit arbitrary powers, while odd generators anticommute and have square zero. A differential d has degree $+1$ and obeys

$$d(ab) = (da)b + (-1)^{|a|} a\, db.$$

A *minimal Sullivan algebra* is such an algebra with an ordering of its generators for which each differential is a sum of products of at least two earlier generators. For simply connected spaces the generators may be ordered by degree and all have degree at least two.

A *minimal Sullivan model* of a simply connected space Z of finite rational type is a quasi-isomorphism

$$\mathcal{M}(Z) \;=\; (\mathbb{Q}[V], d) \;\longrightarrow\; A_{\mathrm{PL}}(Z),$$

where A_{PL} denotes rational piecewise-polynomial forms on singular simplices, with its usual face compatibility, and $H^*(A_{\mathrm{PL}}(Z)) \;\cong\; H^*(Z;\mathbb{Q})$. A quasi-isomorphism is a map inducing isomorphisms on cohomology. Such a minimal model exists and is unique up to isomorphism. Its subalgebra generated by $V^{\leq n}$ is denoted $\mathcal{M}_{\leq n}(Z)$. The bound here is on *generator degrees*, not on total degrees of monomials: in particular, the differentials of degree-n generators still take values in degree $n+1$.

Lemma 4.33 (Recognizing a generator stage)**.** *Let A be a minimal Sullivan algebra with generators of degrees $2,\dots,n$, and let $f : A \to A_{\mathrm{PL}}(Z)$ induce isomorphisms in cohomology through degree n and an injection in degree $n+1$. Then A extends to a minimal model of Z by adjoining only generators of degree at least $n+1$. Consequently it is the full generator stage $\mathcal{M}_{\leq n}(Z)$ for a choice of minimal model.*

Proof. This is the degree-by-degree construction of a minimal model. Here are the steps needed to check the stated cutoff. At the next degree $r \;=\; n+1$, first adjoin closed generators whose images represent a basis of the cokernel of $H^r(f)$. The map on H^r is then an isomorphism. Next choose cocycles representing a basis of the kernel in degree $r+1$, and adjoin degree-r generators whose differentials are those cocycles. Their images can be chosen as primitives, because the cocycles map to exact forms on Z. There are no degree-one elements, so these new generators cannot enter a product of degree $r+1$. The independent kernel classes therefore introduce no additional degree-r cohomology and remove precisely that kernel in degree $r+1$. Every prescribed differential is decomposable: at this point there is no generator of degree $r+1$. The resulting map is an isomorphism through degree r and injective in degree $r+1$. Repeat with $r+1, r+2, \dots$ and take the union. The resulting minimal algebra maps by a quasi-isomorphism to $A_{\mathrm{PL}}(Z)$, and no generator of degree at most n has been added or changed. □

The cohomological input from Morse–Bott theory. The attachment computation gives all the rational cohomology of Y, not just a range of degrees.

Proposition 4.34 (Cohomology and the comparison in degree ten)**.** *The space $Y \;=\; L_1 S^4_R$ is 2-connected and has the homotopy type of a finite CW complex of dimension at most ten. Its rational cohomology is*

$$H^k(Y;\mathbb{Q}) \;\cong\; \begin{cases} \mathbb{Q}, & k \;=\; 0,3,4,10, \\ 0, & \textit{otherwise.} \end{cases} \tag{77}$$

Every product of two positive-degree cohomology classes is zero. For the inclusion $j : Y \hookrightarrow X \;=\; LS^4_R$,

$$j^* \;:\; H^{10}(X;\mathbb{Q}) \;\xrightarrow{\;\cong\;}\; H^{10}(Y;\mathbb{Q}). \tag{78}$$

More generally, the relative rational homology and cohomology of the pair are one-dimensional in degree 9 and vanish in all other degrees at most 13.

Proof. The critical manifold and its negative bundle. By Thm. 4.5, the first critical manifold is $K \;=\; V_2(\mathbb{R}^5) \;=\; STS^4_R$, and its negative bundle is the oriented rank-three bundle ξ.

Its orientation is induced by that of $\mathbb{R}^5$ and the ordered frame spanning its orthogonal complement. The first-stage model of Thm. 4.12 attaches its disk bundle to S^4_R. A finite CW structure on the seven-dimensional manifold K gives relative cells of dimensions $3+j$, $0 \le j \le 7$. Thus the resulting model is finite and at most ten-dimensional. No relative cell has dimension below three. Since S^4 is 2-connected, cellular approximation shows that the result is still 2-connected.

The sphere bundle $S^3 \to STS^4_R \to S^4_R$ has Euler class $e(TS^4) = 2\iota_4$, where ι_4 is an orientation class: its evaluation on the fundamental class is $\chi(S^4) = 2$. In its rational Gysin sequence, multiplication by this Euler class is an isomorphism from $H^0(S^4;\mathbb{Q})$ to $H^4(S^4;\mathbb{Q})$. It removes the possible classes in degrees three and four of the total space, since the relevant segment is

$$0 \longrightarrow H^3(K;\mathbb{Q}) \longrightarrow \mathbb{Q} \xrightarrow{\times 2} \mathbb{Q} \longrightarrow H^4(K;\mathbb{Q}) \longrightarrow 0.$$

The unit and the top class remain, so

$$H^k(K;\mathbb{Q}) \cong \begin{cases} \mathbb{Q}, & k = 0, 7, \\ 0, & \text{otherwise.} \end{cases} \tag{79}$$

The first attachment. The Thom isomorphism for the oriented rank-three negative bundle, using (30) and Cor. 3.11, gives

$$H^k(Y, S^4_R;\mathbb{Q}) \cong H^{k-3}(K;\mathbb{Q}).$$

Here and below a negative cohomological degree means zero. Evaluation $\varepsilon : Y \to S^4_R$ retracts the constant-loop inclusion $s : S^4_R \to Y$. Thus s^* is surjective in every degree, and the long exact sequence of the pair splits into short exact sequences

$$0 \longrightarrow H^{k-3}(K;\mathbb{Q}) \longrightarrow H^k(Y;\mathbb{Q}) \xrightarrow{s^*} H^k(S^4_R;\mathbb{Q}) \longrightarrow 0.$$

This proves (77). The assertion about products follows because no sum of two positive degrees in $\{3, 4, 10\}$ supports cohomology.

The later attachments. The next two Morse indices are 9 and 15. All these negative bundles are oriented, by (20) and the orientation of ξ. The second attachment therefore has relative rational cohomology

$$H^k(L_2S^4_R, L_1S^4_R;\mathbb{Q}) \cong H^{k-9}(K;\mathbb{Q}),$$

which is concentrated in degrees 9 and 16. Over $\mathbb{Q}$ the same calculation holds in homology. Every subsequent relative cell has dimension at least 15. The exact sequence of the triple consequently identifies this relative homology with that of $(L_\infty S^4_R, L_1S^4_R)$ through degree 13. Passage to all finite stages is legitimate because compact families of Sobolev loops have bounded energy: each singular chain, and each chain witnessing a boundary, occurs in some finite stage. The smoothing comparison Lem. 2.8 then identifies these groups with those for (X, Y). The corresponding cohomology statement follows over $\mathbb{Q}$ by universal coefficients. In particular, the groups adjacent to j^* in

$$H^{10}(X, Y;\mathbb{Q}) \longrightarrow H^{10}(X;\mathbb{Q}) \xrightarrow{j^*} H^{10}(Y;\mathbb{Q}) \longrightarrow H^{11}(X, Y;\mathbb{Q})$$

both vanish. This proves (78). □

A model of the unrestricted loop space. We will extend the following algebra to model the first stage. We include the path-space calculation, which also fixes the normalizations of H_7 and F_6.

Lemma 4.35 (The free-loop model of the four-sphere)**.** *A minimal model of* $X = LS^4_R$ *is*

$$B = \big(\mathbb{Q}[H_3, F_4, F_6, H_7], \mathrm{d}\big),$$
$$\begin{aligned} \mathrm{d}H_3 &= 0, \\ \mathrm{d}H_7 &= \tfrac{1}{2}F_4 \wedge F_4, \\ \mathrm{d}F_4 &= 0, \\ \mathrm{d}F_6 &= H_3 \wedge F_4. \end{aligned} \tag{80}$$

Through degree eleven, its nonzero cohomology groups have representatives

k	0	3	4	9	10
$H^k(B)$	$\mathbb{Q}\cdot[1]$	$\mathbb{Q}\cdot[H_3]$	$\mathbb{Q}\cdot[F_4]$	$\mathbb{Q}\cdot[H_3\wedge F_6]$	$\mathbb{Q}\cdot[z_{10}]$

$$z_{10} = F_4 \wedge F_6 + 2H_3 \wedge H_7. \tag{81}$$

All other groups in this range vanish.

Proof. In the normalization of [GSS26, § 2.2], the four-sphere has minimal model

$$A = \big(\mathbb{Q}[G_4, G_7], \mathrm{d}\big),$$
$$\begin{aligned} \mathrm{d}G_4 &= 0, \\ \mathrm{d}G_7 &= \tfrac{1}{2}G_4 \wedge G_4. \end{aligned}$$

Its cohomology is $\mathbb{Q}[G_4]/(G_4^2)$, with the orientation class represented by G_4. One constructs a model map by choosing an orientation cocycle in $A_{\mathrm{PL}}(S^4)$ and a primitive for half its square, which is exact since $H^8(S^4;\mathbb{Q}) = 0$.

The free-loop space is the homotopy pullback of the endpoint path fibration along the diagonal, as in the proof of Thm. 4.22. The Sullivan model for this pullback is the classical free-loop construction of Vigué-Poirrier–Sullivan [VS76]; see also [FH17, Thm. 14.1]. For this sphere it can be computed explicitly as follows. Write $G_{4,i}, G_{7,i}$, $i = 0, 1$, for the endpoint generators of $A \otimes A$. A relative Sullivan resolution of its multiplication map is

$$P = (A \otimes A) \otimes \mathbb{Q}[\bar{G}_3, \bar{G}_6],$$
$$\begin{aligned} \mathrm{d}G_{4,i} &= 0, \\ \mathrm{d}G_{7,i} &= \tfrac{1}{2}G_{4,i} \wedge G_{4,i}, \\ \mathrm{d}\bar{G}_3 &= G_{4,1} - G_{4,0}, \\ \mathrm{d}\bar{G}_6 &= G_{7,1} - G_{7,0} - \tfrac{1}{2}(G_{4,0} + G_{4,1}) \wedge \bar{G}_3. \end{aligned}$$

In particular,

$$\mathrm{d}^2\bar{G}_6 = \tfrac{1}{2}(G_{4,1}^2 - G_{4,0}^2) - \tfrac{1}{2}(G_{4,0} + G_{4,1})(G_{4,1} - G_{4,0}) = 0.$$

To check that this is a resolution, change variables to

$$\begin{aligned} a_4 &= G_{4,1} - G_{4,0}, \\ b_7 &= G_{7,1} - G_{7,0} - \tfrac{1}{2}(G_{4,0} + G_{4,1}) \wedge \bar{G}_3. \end{aligned}$$

The extra factors become the contractible pairs $\mathrm{d}\bar{G}_3 = a_4$ and $\mathrm{d}\bar{G}_6 = b_7$. Thus the map $P \to A$ sending both endpoints to G_4, G_7 and $\bar{G}_3, \bar{G}_6$ to zero is a quasi-isomorphism. It models the endpoint fibration, whose total path space is equivalent to S^4.

Pullback along the diagonal identifies the two endpoints. Set $F_4 = G_4$, $H_7 = G_7$, $H_3 = \bar{G}_3$ and $F_6 = -\bar{G}_6$. The differential then becomes (80). It is minimal because all differentials

are decomposable in earlier generators, ordered by degree.

For the cohomology calculation, the monomials in degrees $6, 7, 8$ are, respectively, F_6; $H_7, H_3 \wedge F_4$; and F_4^2. Their differentials show that those cohomology groups vanish. The only degree-nine monomial is $H_3 \wedge F_6$; it is closed because $H_3^2 = 0$, and no degree-eight element has that differential. In degree ten,

$$\begin{aligned} \mathrm{d}(F_4 \wedge F_6) &= H_3 \wedge F_4^2, \\ \mathrm{d}(H_3 \wedge H_7) &= -\tfrac{1}{2} H_3 \wedge F_4^2. \end{aligned}$$

Thus the closed subspace is spanned by z_{10}, and there are no nonzero boundaries in that degree. Finally the degree-eleven monomials are $F_4 \wedge H_7$ and $H_3 \wedge F_4^2$. The first has differential $\frac{1}{2} F_4^3$; the second is the boundary $\mathrm{d}(F_4 \wedge F_6)$. Together with the unit and the classes of H_3, F_4, this proves (81). □

The minimal model through generator degree ten. The inclusion $j : Y \to X$ gives a map $B \to A_{\mathrm{PL}}(Y)$ by composing a model map for X with j^*. By Prop. 4.34, this map preserves the nonzero degree-ten class while sending the degree-nine class to zero. We now extend it to a model of Y.

Theorem 4.36 (The minimal Sullivan model of $L_1 S^4_R$ through degree ten)**.** *There is a minimal Sullivan model of $Y = L_1 S^4_R$ whose generators of degree at most ten are exactly*

$$H_3, \quad F_4, \quad F_6, \quad H_7, \quad F_8, \quad F_{10}.$$

In particular there are no generators in degrees $1, 2, 5, 9$, and one in each of degrees $3, 4, 6, 7, 8, 10$. The full subalgebra generated by these elements is

$$\mathcal{M}_{\leq 10}(Y) = \big(\mathbb{Q}[H_3, F_4, F_6, H_7, F_8, F_{10}], \mathrm{d}\big), \tag{82}$$

with differential

$$\begin{aligned} \mathrm{d}H_3 &= 0, \\ \mathrm{d}H_7 &= \tfrac{1}{2} F_4 \wedge F_4, \\ \mathrm{d}F_4 &= 0, \\ \mathrm{d}F_6 &= H_3 \wedge F_4, \\ \mathrm{d}F_8 &= H_3 \wedge F_6, \\ \mathrm{d}F_{10} &= H_3 \wedge F_8. \end{aligned} \tag{83}$$

The model map can be chosen to induce cohomology isomorphisms through degree eleven. In degree ten, $H^{10}(Y; \mathbb{Q})$ is generated by the image of $[z_{10}] = [F_4 \wedge F_6 + 2H_3 \wedge H_7]$. Moreover j is modeled, in this range, by the inclusion of the subalgebra B of (80).

Proof. The initial algebra and its map. Write $f : B \to A_{\mathrm{PL}}(Y)$ for the map just described. By the relative cohomology calculation in Prop. 4.34, j^* is an isomorphism through degree seven. In degree eight both source and target cohomology vanish. It is also an isomorphism in degree ten by (78). Hence f is an isomorphism in these degrees, and

$$f_*[z_{10}] \neq 0.$$

This last fact will exclude a further generator in degree nine.

Adjoining the degree-eight generator. The class $[H_3 \wedge F_6]$ spans $H^9(B)$, whereas $H^9(Y; \mathbb{Q}) = 0$. Choose $\omega_8 \in A^8_{\mathrm{PL}}(Y)$ with $\mathrm{d}\omega_8 = f(H_3 \wedge F_6)$. Adjoin a generator

F_8 by $\mathrm{d}F_8 = H_3 \wedge F_6$ and extend f by $f(F_8) = \omega_8$. Call this intermediate algebra $B_8 = B \otimes \mathbb{Q}[F_8]$. The differential is consistent, since

$$\mathrm{d}(H_3 \wedge F_6) = -H_3 \wedge \mathrm{d}F_6 = -H_3^2 \wedge F_4 = 0.$$

It kills exactly the degree-nine cohomology class and creates no new class in degree eight: the only new degree-eight element is F_8, whose differential is nonzero.

The degree-ten monomials of B_8 are still just $F_4 \wedge F_6, H_3 \wedge H_7$. Thus $H^{10}(B_8) = \mathbb{Q} \cdot [z_{10}]$, and its map to $H^{10}(Y;\mathbb{Q})$ is an isomorphism. There is consequently neither a missing degree-nine class to represent nor a degree-ten kernel to kill. No generator of degree nine is required.

The new obstruction in degree eleven. The degree-eleven monomials of B_8 are precisely

$$H_3 \wedge F_8, \qquad F_4 \wedge H_7, \qquad H_3 \wedge F_4^2.$$

Their differentials are $0, \frac{1}{2}F_4^3, 0$, respectively. The degree-ten differentials span only $\mathbb{Q}\{H_3 \wedge F_4^2\}$. It follows that

$$H^{11}(B_8) = \mathbb{Q} \cdot [H_3 \wedge F_8]. \tag{84}$$

Since $H^{11}(Y;\mathbb{Q}) = 0$, choose a primitive ω_{10} of $f(H_3 \wedge F_8)$ in $A_{\mathrm{PL}}(Y)$. Adjoin F_{10} with $\mathrm{d}F_{10} = H_3 \wedge F_8$, and set $f(F_{10}) = \omega_{10}$. Again $\mathrm{d}^2 = 0$, because $\mathrm{d}(H_3 \wedge F_8) = -H_3^2 \wedge F_6 = 0$.

This generator does not introduce a closed degree-ten element: in that degree the possible differentials are $H_3 \wedge F_8$ and $H_3 \wedge F_4^2$, which are linearly independent monomials. Thus the closed subspace remains exactly $\mathbb{Q}\{z_{10}\}$. In degree eleven both closed monomials are now boundaries, namely $\mathrm{d}F_{10} = H_3 \wedge F_8$ and $\mathrm{d}(F_4 \wedge F_6) = H_3 \wedge F_4^2$. All lower cohomology groups are unchanged. Consequently the resulting map from the algebra in (82) is an isomorphism on cohomology through degree eleven, including the zero group in degree eleven.

Completeness and minimality. All six differentials in (83) are decomposable in generators of smaller degree. The algebra is therefore minimal, not merely a differential algebra with $\mathrm{d}^2 = 0$. By Lem. 4.33, the map just constructed extends to a full minimal model using only generators of degree at least eleven. This proves that the list contains every generator through degree ten. Since the construction extends the original map on B, the inclusion $B \hookrightarrow \mathcal{M}(Y)$ models j. □

Corollary 4.37 (Rational homotopy groups and the inclusion)**.** *For* $2 \le k \le 10$*,*

$$\pi_k(L_1 S^4_R) \otimes \mathbb{Q} \cong \begin{cases} \mathbb{Q}, & k = 3,4,6,7,8,10, \\ 0, & k = 2,5,9. \end{cases} \tag{85}$$

The inclusion into LS^4_R *is an isomorphism on rational homotopy in degrees* $3,4,6,7$ *and sends the additional classes in degrees* $8,10$ *to zero.*

Proof. For a simply connected space of finite rational type, V^k in its minimal Sullivan model is naturally dual to $\pi_k \otimes \mathbb{Q}$ [FH17, Thm. 4.1]. Apply this to the two models above. The map $B \hookrightarrow \mathcal{M}(Y)$ includes exactly the generators in degrees $3,4,6,7$; dualizing its map on indecomposables gives the stated homotopy homomorphism. □

Remark 4.38 (The degree-ten class and the first omitted generator). The generator F_{10} is *not* a cohomology class: its differential is nonzero. The surviving degree-ten cohomology class is instead the decomposable cocycle $z_{10} = F_4 \wedge F_6 + 2H_3 \wedge H_7$. Its nonvanishing uses the comparison with LS^4; it would not follow just by counting the cohomology groups of Y.

Algebraically it is precisely what allows the construction to pass degree nine without a new generator.

The displayed algebra is also not the entire minimal model. It already has an unwanted degree-twelve class

$$[F_6^2 - 2F_4 \wedge F_8], \qquad \mathrm{d}(F_6^2 - 2F_4 \wedge F_8) = 0,$$

since the two terms have the same differential $2H_3 \wedge F_4 \wedge F_6$. It is not a boundary: degree-eleven differentials span only $\mathbb{Q}\{F_4^3\}$. The degree-twelve monomials are $F_6^2, F_4 \wedge F_8, F_4^3$, so this class spans all of $H^{12}(\mathcal{M}_{\leq 10}(Y))$. Since $H^{12}(Y;\mathbb{Q}) = 0$, the next step requires exactly one degree-eleven generator, which may be chosen with differential $F_6^2 - 2F_4 \wedge F_8$. This illustrates why a cutoff on generator degrees must not discard their differentials or be mistaken for a complete model of the space.

The small-cyclification model. We now retain the circle action instead of forgetting it. The resulting degree-two generator records the map to BS^1; its appearance changes two of the preceding differential relations. This recovers the model in [GSS26, Prop. 3.10 and Rem. 3.11].

Corollary 4.39 (The minimal Sullivan model of $\mathrm{Cyc}_1 S^4_R$ through degree ten)**.** *For the rotation action of Def. 2.14, put $Z = \mathrm{Cyc}_1 S^4_R = ES^1 \times_{S^1} L_1 S^4_R$. There is a minimal Sullivan model whose full generator stage through degree ten is*

$$\mathcal{M}_{\leq 10}(Z) = \Big(\mathbb{Q}[F_2, H_3, F_4, F_6, H_7, F_8, F_{10}], \mathrm{d}\Big), \tag{86}$$

with differential

$$\begin{aligned} \mathrm{d}H_3 &= 0, \\ \mathrm{d}H_7 &= \tfrac{1}{2}F_4 \wedge F_4 - F_2 \wedge F_6, \\ \mathrm{d}F_2 &= 0, \\ \mathrm{d}F_4 &= H_3 \wedge F_2, \\ \mathrm{d}F_6 &= H_3 \wedge F_4, \\ \mathrm{d}F_8 &= H_3 \wedge F_6, \\ \mathrm{d}F_{10} &= H_3 \wedge F_8. \end{aligned} \tag{87}$$

There are no other generators of degree at most ten. The projection $Z \to BS^1$ is modeled by the inclusion of $\mathbb{Q}[F_2]$, with F_2 the degree-two generator of $H^*(BS^1;\mathbb{Q})$, oriented as in the proof. The fibre inclusion $L_1 S^4_R \to Z$ is modeled by setting $F_2 = 0$, recovering (83). The inclusion $Z \to \mathrm{Cyc}\, S^4_R$ is modeled, in this range, by inclusion of the subalgebra on F_2, H_3, F_4, F_6, H_7.

Proof. The relative model and its generator degrees. By Def. 2.14, we have the Borel fibration

$$L_1 S^4_R \longrightarrow Z \longrightarrow BS^1.$$

Its base is simply connected, and its fibre is 2-connected and of finite rational type by Prop. 4.34. The Sullivan model of a fibration [FH17, § 12, especially Thm. 12.1] therefore gives a relative model over $\mathbb{Q}[F_2]$ whose underlying algebra is $\mathbb{Q}[F_2] \otimes \mathcal{M}(Y)$ and whose differential reduces modulo (F_2) to that of $\mathcal{M}(Y)$. This total algebra is minimal: its reduction is minimal, and every additional differential term is divisible by F_2 and has degree at least four, so cannot be a linear generator. All factors in such a term have smaller degree than the generator being differentiated. Thus, through degree ten, the only generators are the six

of Thm. 4.36 together with F_2. It remains to determine the differential terms involving F_2; the fibre model by itself does not determine them.

The rotation action on the full loop space. The equivariant free-loop model of Vigué-Poirrier–Burghelea [VB85, Thm. A and (1.3)] adjoins F_2 to the free-loop model with differential $\mathrm{d}_B + F_2 s$, where s is the degree-(-1) derivation coming from loop rotation. Choose the sign of F_2 so that

$$\begin{aligned} sF_4 &= H_3, \\ sH_7 &= -F_6, \\ sH_3 &= 0, \\ sF_6 &= 0. \end{aligned}$$

These formulas follow from the suspended sphere generators: $F_4 = G_4$, $H_7 = G_7$, $H_3 = sG_4$, $F_6 = -sG_7$. They satisfy $s^2 = 0$ and $\mathrm{d}_B s + s\mathrm{d}_B = 0$; for example, on H_7 the two terms are $-H_3 \wedge F_4$ and $H_3 \wedge F_4$. The cited theorem identifies this algebra with the Borel construction, including the projection and fibre inclusion. Consequently a minimal model of $\operatorname{Cyc} S^4_R$ is

$$\begin{aligned} C &= \Big(\mathbb{Q}[F_2, H_3, F_4, F_6, H_7], \mathrm{d}\Big), \\ \mathrm{d}H_3 &= 0, \\ \mathrm{d}H_7 &= \tfrac{1}{2} F_4 \wedge F_4 - F_2 \wedge F_6, \\ \mathrm{d}F_2 &= 0, \\ \mathrm{d}F_4 &= H_3 \wedge F_2, \\ \mathrm{d}F_6 &= H_3 \wedge F_4. \end{aligned} \tag{88}$$

The later handles in the proof of Prop. 4.34 attach cells of dimension at least nine. Hence $Y \to X$ is 8-connected. The map $Z \to \operatorname{Cyc} S^4_R$ lies over the identity of BS^1; comparison of the homotopy exact sequences of the two Borel fibrations shows that it too is 8-connected. It therefore induces an isomorphism on minimal generators through degree seven. Taking the images of the generators of C as the generators of those names in $\mathcal{M}(Z)$ makes all five relations in (88) hold exactly. This choice is a valid change of generators because their linear parts are invertible and their other terms are decomposable in smaller degrees.

Removing possible corrections in the remaining degrees. We spell out why the next two relations need no additional terms. If A' is a differential subalgebra free over $\mathbb{Q}[F_2]$, then multiplication by F_2 identifies its ideal (F_2) with A' shifted upward by two degrees. Since $\mathrm{d}F_2 = 0$, this gives

$$H^{n+1}((F_2)A') \cong H^{n-1}(A'). \tag{89}$$

Suppose a degree-n generator v has prescribed differential modulo (F_2) and a proposed closed lift $\theta \in A'^{n+1}$. Then $\mathrm{d}v - \theta$ is a cocycle in $(F_2)A'$. If the group in (89) vanishes, this difference is $\mathrm{d}\eta$ for an $\eta \in (F_2)A'^n$. Replacing v by $v - \eta$ gives $\mathrm{d}v = \theta$ without changing its reduction to the fibre.

For F_8 take $A' = C$, $n = 8$ and $\theta = H_3 \wedge F_6$, which is closed. Degree seven of C has basis

$$H_7, \qquad H_3 \wedge F_4, \qquad H_3 \wedge F_2^2.$$

Only the last two can occur in a cocycle: the differential of H_7 is nonzero, while their differentials vanish. They are respectively the boundaries of F_6 and $F_2 \wedge F_4$. Thus $H^7(C) = 0$ and we can choose

$$\mathrm{d}F_8 = H_3 \wedge F_6.$$

For F_{10} take $A' = C_8 = C \otimes \mathbb{Q}[F_8]$, $n = 10$ and $\theta = H_3 \wedge F_8$, again closed. Degree nine of C_8 has basis

$$H_3 \wedge F_2^3, \qquad H_3 \wedge F_6, \qquad H_3 \wedge F_2 \wedge F_4, \qquad F_2 \wedge H_7.$$

The last element has nonzero differential and the other three are closed. Those three are the boundaries of $F_2^2 \wedge F_4$, F_8, and $F_2 \wedge F_6$, respectively. Hence $H^9(C_8) = 0$ and we can choose

$$\mathrm{d}F_{10} = H_3 \wedge F_8.$$

Both changes are by decomposable elements of lower generators. They preserve the model of the projection and reduce to the identity on the fibre. Together with the generator count already obtained from the relative model, this proves the complete stage (86) and all the assertions about its maps. □

Lifting through the small cyclification. The differential $\mathrm{d}F_8 = H_3 \wedge F_6$ suggests an obstruction to lifting a map through $\mathrm{Cyc}_1 S^4 \to \mathrm{Cyc}\, S^4$. We now prove the integral statement and classify the choices of lift in dimension nine, expanding the obstruction and twist computations of [GSS26, Thm. 3.8]. Existence requires only the first nonzero relative homotopy group; classification also sees the next group, $\mathbb{Z}/2$. We first isolate the existence obstruction, then explain the twisted stable cohomotopy group acting on the lifts.

In this discussion X denotes the *source* of a map, and we suppress the radius of the round four-sphere. All cohomology is ordinary cohomology, without compact-support or boundary conditions, unless stated otherwise.

Notation 4.40 (Maps to be lifted and their homotopies)**.** Write

$$\mathcal{C}_1 = \mathrm{Cyc}_1 S^4, \qquad \mathcal{C} = \mathrm{Cyc}\, S^4, \qquad i : \mathcal{C}_1 \longrightarrow \mathcal{C}.$$

For a map $c : X \to \mathcal{C}$, let $b : X \to BS^1$ be its projection. If $L \to BS^1$ is the universal complex line, put $L_c = b^*L$ and $f_2 = c_1(L_c) \in H^2(X;\mathbb{Z})$. A *homotopy lift* of c consists of a map $\widetilde{c} : X \to \mathcal{C}_1$ and a specified homotopy $i\widetilde{c} \simeq c$:

$$\begin{array}{ccc} & & \mathcal{C}_1 \\ & \overset{\widetilde{c}}{\nearrow} & \downarrow{\scriptstyle i} \\ X & \xrightarrow{\;c\;} & \mathcal{C} \\ & \underset{b}{\searrow} & \downarrow \\ & & BS^1. \end{array} \tag{90}$$

The homotopy is part of the data. More precisely, set

$$\mathrm{Lift}(c) = \pi_0 \,\mathrm{hofib}_c\Big(\mathrm{Map}(X, \mathcal{C}_1) \longrightarrow \mathrm{Map}(X, \mathcal{C})\Big). \tag{91}$$

Equivalently, replace i by a fibration and take homotopy classes of sections of its pullback along c, with homotopies through sections. These constructions may be performed in the homotopy slice over BS^1, keeping the circle bundle b fixed. Forgetting the specified homotopy gives a different classification problem, to which the torsor statement below does not directly apply.

Lemma 4.41 (The first two relative homotopy groups)**.** *Let $Q = \mathrm{hocofib}(L_1 S^4 \to LS^4)$. Its bottom cell induces an 11-connected map $S^9 \to Q$. The map i is 8-connected, and its homotopy fibre F satisfies*

$$\pi_k F = 0 \quad (k \le 7), \qquad \pi_8 F \cong \mathbb{Z}, \qquad \pi_9 F \cong \mathbb{Z}/2. \tag{92}$$

The local coefficient system on $\mathcal{C}$ with fibre $\pi_8 F$ is constant.

Proof. By Thm. 4.5 and Cor. 4.7, the first attachment after $L_1 S^4$ has negative rank nine over $K_2 = V_2(\mathbb{R}^5) = STS^4$; the next has negative rank fifteen. Consequently Q is obtained from $\mathrm{Th}(\nu^- K_2)$ by cells of dimension at least fifteen. The sphere bundle $S^3 \to STS^4 \to S^4$ has a CW model with one cell in each of dimensions $0, 3, 4, 7$: start with the fibre over the zero-cell of S^4, then trivialize over its open four-cell and attach the product cells using the clutching map. The Thom construction shifts these dimensions by nine. Thus its non-basepoint cells have dimensions $9, 12, 13, 16$, proving the assertion about $S^9 \to Q$.

The pair $(LS^4, L_1 S^4)$ is 8-connected, and $L_1 S^4$ is 2-connected, by the same cell description and Prop. 4.34. Homotopy excision [Hat02, Prop. 4.28] therefore identifies its relative homotopy groups with $\pi_k Q$ for $k \leq 10$ and gives a surjection for $k = 11$. In particular the groups in degrees nine and ten are $\pi_9 S^9 = \mathbb{Z}$ and $\pi_{10} S^9 = \mathbb{Z}/2$, the latter being the first stable stem, generated by the suspension of the Hopf map.

The map i is a map of Borel fibrations over the identity of BS^1. Its homotopy fibre is therefore equivalent to that of $L_1 S^4 \to LS^4$. The relative homotopy groups just computed shift downward by one to give (92). Finally LS^4 is simply connected by its evaluation fibration, and so is $\mathcal{C}$ by its Borel fibration. Thus there is no $\pi_1(\mathcal{C})$-action twisting the coefficient group $\pi_8 F$. □

Theorem 4.42 (The integral obstruction in dimension nine)**.** *After choosing an orientation of $\pi_8 F \cong \mathbb{Z}$, there is a universal class*

$$o \in H^9(\mathcal{C}; \mathbb{Z}) \tag{93}$$

such that for every CW complex X of dimension at most nine,

$$\mathrm{Lift}(c) \neq \varnothing \quad \Longleftrightarrow \quad c^* o = 0 \text{ in } H^9(X; \mathbb{Z}). \tag{94}$$

This is the only obstruction to existence *in these dimensions. In the Sullivan normalization above,*

$$o_{\mathbb{Q}} = \mu[H_3 \wedge F_6] \quad \text{for some } \mu \in \mathbb{Q}^\times. \tag{95}$$

Here $o_{\mathbb{Q}}$ is the image under change of coefficients. The nonzero scalar records the comparison of integral and rational generator normalizations; its value is not needed for the vanishing criterion on oriented nine-manifolds.

Proof. Cellular construction of the obstruction. Replace i by a fibration with fibre F and pull it back along c. A section extends over the eight-skeleton: the obstruction on a k-cell belongs to $\pi_{k-1} F$, which vanishes for $k \leq 8$. For an oriented nine-cell, trivialize the pullback over its characteristic disk. The existing boundary section gives a map $S^8 \to F$, and hence an integer in $\pi_8 F$. These integers form the obstruction cochain. The cellular extension argument shows that it is a cocycle and that changing the section on eight-cells changes it by a coboundary. Its cohomology class is therefore the primary obstruction. If it vanishes, alter the section on eight-cells to make every nine-cell obstruction zero and extend over all nine-cells. There are no higher cells to test. This also explains why $\pi_9 F$ does not provide another existence obstruction: that would lie in degree ten.

For universality, the first nontrivial Moore–Postnikov stage of i is a principal $K(\mathbb{Z}, 8)$-fibration over $\mathcal{C}$, classified by a map $o : \mathcal{C} \to K(\mathbb{Z}, 9)$ [Hat02, Thm. 4.71]. Its class is (93), and naturality of the cellular construction makes the obstruction for c exactly $c^* o$.

Its rational representative. In the full-cyclification model (88), the degree-nine monomials are

$$H_3 \wedge F_6, \quad H_3 \wedge F_2 \wedge F_4, \quad H_3 \wedge F_2^3, \quad F_2 \wedge H_7.$$

The first three are closed, the last is not, and

$$\begin{aligned} \mathrm{d}(\tfrac{1}{2} F_4 \wedge F_4) &= H_3 \wedge F_2 \wedge F_4, \\ \mathrm{d}(F_4 \wedge F_2^2) &= H_3 \wedge F_2^3. \end{aligned}$$

The degree-eight monomials are $F_2^4, F_2^2 \wedge F_4, F_2 \wedge F_6, F_4^2$; their differentials span precisely the two displayed boundaries. Thus

$$H^9(\mathcal{C}; \mathbb{Q}) = \mathbb{Q} \cdot [H_3 \wedge F_6].$$

For $\mathcal{C}_1$, the generator F_8 makes the remaining class exact, so $H^9(\mathcal{C}_1; \mathbb{Q}) = 0$ by Cor. 4.39.

To see that $o_{\mathbb{Q}}$ is *nonzero*, use the rational Serre spectral sequence of $F \to \mathcal{C}_1 \to \mathcal{C}$. Since F is 7-connected, $H^8(F; \mathbb{Q}) = \mathbb{Q}$, and the only possible differential into bidegree $(9, 0)$ is the transgression

$$d_9 : H^8(F; \mathbb{Q}) \longrightarrow H^9(\mathcal{C}; \mathbb{Q}).$$

It takes the oriented fibre generator to $o_{\mathbb{Q}}$, up to the corresponding sign convention. The target class cannot survive, since the total space has zero degree-nine cohomology. Thus d_9 is nonzero, proving (95). □

Corollary 4.43 (The de Rham criterion for oriented nine-manifolds)**.** *Let X^9 be a connected oriented smooth nine-manifold. A map $c : X^9 \to \mathcal{C}$ lifts if and only if*

$$c^*[H_3 \wedge F_6] = 0 \quad \text{in } H^9_{\mathrm{dR}}(X^9). \tag{96}$$

This is the D0-brane tadpole criterion of [GSS26, Thm. 3.8(i)]. For closed X^9 it is equivalently the vanishing of the integral of the representative nine-form over X^9. If X^9 is noncompact or has nonempty boundary, a lift always exists, without imposed conditions at infinity or on the boundary.

Proof. If X^9 is closed, orientation and Poincaré duality give $H^9(X^9; \mathbb{Z}) = \mathbb{Z}$, which injects into real cohomology. If it is noncompact or has nonempty boundary, it admits a CW model of dimension at most eight, and its ordinary degree-nine cohomology vanishes with any constant coefficients. Thus in both cases $c^* o = 0$ is equivalent to the vanishing of its real image. Apply (95) and the de Rham theorem. On a closed connected oriented manifold, integration identifies top-degree real cohomology with $\mathbb{R}$, giving the stated integral criterion. □

Remark 4.44 (What the rational model does and does not detect). For a smooth source, the symbols in (96) denote representatives obtained from a differential-form realization of the rationalized map c. In particular F_6 need not be closed; $H_3 \wedge F_6$ is closed because $\mathrm{d}F_6 = H_3 \wedge F_4$ and $H_3 \wedge H_3 = 0$. A lift supplies a primitive F_8 through $\mathrm{d}F_8 = H_3 \wedge F_6$. The integral theorem is what makes this necessary condition sufficient on oriented nine-manifolds. For a general nine-complex one must retain $c^* o$ with integral coefficients: its rational image can vanish while an integral obstruction remains. Likewise, prescribing boundary values or behaviour at infinity changes the lifting problem and generally replaces ordinary cohomology by relative or supported groups.

The twist carried by the second Morse–Bott attachment. To classify lifts we must retain $\pi_9 F = \mathbb{Z}/2$. The circle action determines how this stable Hopf class fits together with $\pi_8 F = \mathbb{Z}$ over the parameter space BS^1. This is a degree-two twist of a spectrum; the ordinary integral coefficient system remains constant.

Lemma 4.45 (The equivariant negative bundle and its characteristic class)**.** *On $K_2 = V_2(\mathbb{R}^5)$ let $\xi_{(u,v)} = \langle u, v\rangle^{\perp}$, as in Thm. 4.5, and let $\mathbb{C}_1$ be the one-dimensional complex representation of S^1 of weight one. The rank-nine negative bundle is equivariantly*

$$\nu^{-} K_2 \cong \xi \oplus (\xi \otimes_{\mathbb{R}} \mathbb{C}_1). \tag{97}$$

For its Borel bundle $\bar{\nu} \to (K_2)_{hS^1}$,

$$w_1(\bar{\nu}) = 0, \qquad w_2(\bar{\nu}) = \rho_2 t, \qquad t = c_1(L), \tag{98}$$

where classes from BS^1 are pulled back to $(K_2)_{hS^1}$, and ρ_2 denotes reduction modulo two.

Proof. The Fourier calculation in (21) has negative normal frequencies zero and one at $m = 2$. The constant field is a copy of ξ. For the other fields write $a\cos(2\pi s) + b\sin(2\pi s)$ with $a, b \in \xi$. Replacing s by $s + \theta$ sends $a - ib$ to $e^{2\pi i\theta}(a - ib)$, giving the weight-one summand in (97).

The tautological oriented plane $P = \langle u, v\rangle$ and ξ are complementary equivariant subbundles of the trivial ambient $\mathbb{R}^5$-bundle. By Prop. 4.9, its frame rotates with weight two on K_2. Thus its Borel bundle satisfies $w_1(\bar{P}) = 0$ and $w_2(\bar{P}) = \rho_2(2t) = 0$. The Whitney product formula gives $w_1(\bar{\xi}) = w_2(\bar{\xi}) = 0$.

The other summand of $\bar{\nu}$ is the underlying real bundle of the complex rank-three bundle $(\bar{\xi} \otimes_{\mathbb{R}} \mathbb{C}) \otimes L$. The complexification of an oriented real bundle has trivial determinant, so its first Chern class is zero. Tensoring by L gives first Chern class $3t$. For an underlying real complex bundle w_2 is the reduction of c_1, hence this summand contributes $\rho_2 t$. The Whitney formula now gives (98); see [MS74, §§ 4, 14] for these characteristic class identities. □

Notation 4.46 (Fibrewise cofibres and twisted stable cohomotopy)**.** The *fibrewise homotopy cofibre*

$$\mathcal{Q} = \operatorname{hocofib}_{/BS^1}(i)$$

is the homotopy pushout of $\mathcal{C} \leftarrow \mathcal{C}_1 \to BS^1$. It is pointed over BS^1 by a zero section, has fibre Q from Lem. 4.41, and receives the collapse map $q : \mathcal{C} \to \mathcal{Q}$. In particular, it collapses the small loops *in each fibre*; it is not the ordinary cofibre that collapses all of $\mathcal{C}_1$ to one point.

Write $\mathbb{S}$ for the sphere spectrum, and

$$\mathbb{S}^L = \Sigma^{\infty}_{BS^1} S^L$$

for the fibrewise suspension spectrum of the one-point compactification of the real rank-two bundle underlying L. Its fibre is $\Sigma^2\mathbb{S}$. Here $\Sigma^{\infty}_{BS^1}$, $\Omega^{\infty}_{BS^1}$, and $\tau_{\le n}$ mean stabilization, infinite-loop space, and Postnikov truncation *in each fibre*; see [MS06] for parametrized spectra. For the pulled-back line $L_c \to X$ define

$$\pi_s^{r+L_c}(X) := \pi_0 \Gamma_X\big(\Omega^{\infty}_X \Sigma^r \mathbb{S}^{L_c}\big), \tag{99}$$

using the derived space of sections, with its zero section. This is an abelian group. If L_c is trivial it is ordinary stable cohomotopy $\pi_s^{r+2}(X)$. Thus $\pi_s^{6+L_c}(X)$ is twisted stable *eight*-cohomotopy; the complex line contributes two real suspension degrees.

Proposition 4.47 (The first two stable layers of the cofibre)**.** *There is an equivalence of parametrized spectra*

$$\tau_{\leq 10}\Sigma^{\infty}_{BS^1}\mathcal{Q} \;\simeq\; \tau_{\leq 10}\Sigma^{7}\mathbb{S}^{L}. \tag{100}$$

It identifies the bottom integral generators after a common orientation is chosen. The oriented family of these two-stage spectra is classified by $\rho_2 t$.

Proof. The fibre and the classification of its families. By Lem. 4.41, the bottom sphere $S^9 \to Q$ is 11-connected. Hence every fibre on the left of (100) is $\Sigma^9 P$, where $P = \tau_{\leq 1}\mathbb{S}$ has $\pi_0 P = \mathbb{Z}$, $\pi_1 P = \mathbb{Z}/2$, and no other homotopy groups. We must identify the family, not just these groups fibre by fibre.

Precomposition with $\mathbb{S} \to P$ identifies the derived mapping spaces

$$\mathrm{Map}_{\mathrm{Sp}}(P, P) \;\simeq\; \mathrm{Map}_{\mathrm{Sp}}(\mathbb{S}, P) \;\simeq\; \Omega^{\infty}P.$$

Indeed, the fibre of the truncation map is 2-connective; maps from it, or its positive suspensions, to the 1-truncated spectrum P vanish. The self-equivalences therefore form the components $+1$ and -1, each with fundamental group $\mathbb{Z}/2$ and no higher homotopy. The simply connected cover of their classifying space is $K(\mathbb{Z}/2, 2)$. Thus oriented families with fibre $\Sigma^9 P$ over the simply connected base BS^1 are classified by $H^2(BS^1; \mathbb{Z}/2) = \mathbb{Z}/2$.

Detecting which family occurs. The second equivariant Morse–Bott attachment identifies the relative cohomology of $(\mathcal{Q}, BS^1)$ in degrees nine and eleven with that of the Thom space of $\bar{\nu}$. Later attachments have rank at least fifteen and do not affect these degrees. Let U be the mod-two reduction of the oriented Thom class, and write $\mathrm{Sq}^2 : H^k(-; \mathbb{Z}/2) \to H^{k+2}(-; \mathbb{Z}/2)$ for the second Steenrod square. The Thom identity [MS74, § 8] gives

$$\mathrm{Sq}^2 U \;=\; w_2(\bar{\nu}) \cup U \;=\; \rho_2 t \cup U. \tag{101}$$

The pullback from $H^2(BS^1; \mathbb{Z}/2)$ to $H^2((K_2)_{hS^1}; \mathbb{Z}/2)$ is an isomorphism, because K_2 is 2-connected. The Thom isomorphism therefore shows that the right-hand side is nonzero.

For the trivial family the bottom Thom class has square zero in this degree. The family $\Sigma^7\mathbb{S}^L$ has square $\rho_2 t \cup U$ by the same Thom identity for L, and so represents the nontrivial class. There are only these two oriented families. Equation (101) identifies the family of $\mathcal{Q}$ with the latter, proving the equivalence. In particular no global choice of an equivariant bottom sphere in $\mathcal{Q}$ has been assumed. □

The classification of lifts. The following fibrewise obstruction map packages both existence and the choices of lift. The connectivity estimate in its proof explains why degree ten, rather than just degree nine, must be retained to classify maps from a nine-dimensional space.

Theorem 4.48 (Lifts form a torsor for twisted stable cohomotopy)**.** *Let X be a CW complex of dimension at most nine and $c : X \to \mathcal{C}$ a map. If $c^*o = 0$, then* Lift(c) *is a torsor for*

$$\pi_s^{6+L_c}(X). \tag{102}$$

Here a torsor is a nonempty set with a free and transitive action of the indicated group; choosing one lift identifies all other lifts with group elements, without giving a preferred choice of zero beforehand.

More precisely, set $\mathcal{P} = \Omega^{\infty}_{BS^1}\tau_{\leq 10}\Sigma^7\mathbb{S}^L$. The collapse, stabilization, truncation, and (100) define a map over BS^1

$$o^{\mathrm{tw}} \;:\; \mathcal{C} \xrightarrow{q} \mathcal{Q} \longrightarrow \Omega^{\infty}_{BS^1}\tau_{\leq 10}\Sigma^{\infty}_{BS^1}\mathcal{Q} \xrightarrow{\simeq} \mathcal{P}. \tag{103}$$

The set $\mathrm{Lift}(c)$ *is identified with the homotopy classes, relative to their endpoints, of paths from the section* $o^{\mathrm{tw}}c$ *to the zero section in* $\Gamma_X(b^*\mathcal{P})$*. Under the natural identification*

$$\pi_s^{7+L_c}(X) \;\cong\; H^9(X;\mathbb{Z}), \tag{104}$$

the component of this obstruction section is c^*o*.*

Proof. Comparison with a homotopy fibre. The collapse has a canonical null-homotopy on $\mathcal{C}_1$. It induces a map to the fibrewise homotopy fibre over the zero section,

$$\mathcal{C}_1 \;\longrightarrow\; \mathrm{hofib}_{/BS^1}(o^{\mathrm{tw}}). \tag{105}$$

This map is 10-connected on every fibre over BS^1. To prove this, work first before taking the Borel construction. Homotopy excision, with connectivities eight for (LS^4, L_1S^4) and two for L_1S^4, compares relative homotopy with the cofibre through degree ten, surjectively in degree eleven. Comparing the homotopy exact sequences therefore makes

$$L_1S^4 \;\longrightarrow\; \mathrm{hofib}(LS^4 \;\to\; Q)$$

10-connected. The space Q is 8-connected, so Freudenthal makes its stable unit $Q \to \Omega^\infty\Sigma^\infty Q$ 17-connected. Postnikov truncation to degree ten is 11-connected. Their composite is thus 11-connected, and passage to homotopy fibres of maps from LS^4 lowers that estimate by one. This proves the asserted 10-connectivity of (105). All these comparisons are fibrewise over the fixed BS^1; the 2-connected space used in excision is L_1S^4, not the total Borel space.

Why this estimate classifies lifts. After pulling back along c, a section of the right-hand side is precisely a null-homotopy of $o^{\mathrm{tw}}c$. The homotopy fibre of the comparison map is 9-connected. Consequently any such section lifts over X by cellular obstruction theory. Two resulting sections are homotopic through sections whenever their images are: lift the given homotopy over $X \times I$ relative to its two ends. This relative CW complex has dimension at most ten, and the possible cell obstructions lie in the vanishing groups π_k of the comparison fibre for $k \le 9$. Thus (105) induces a bijection on the sets of homotopy classes of lifts.

The space $\Gamma_X(b^*\mathcal{P})$ is an infinite loop space. Paths from a fixed point to zero exist exactly when that point has zero component. Once a path is chosen, concatenation by loops at zero acts freely and transitively on the homotopy classes of such paths. The acting group is

$$\pi_1\Gamma_X(b^*\mathcal{P}) \;\cong\; \pi_s^{6+L_c}(X).$$

Indeed, looping the section spectrum lowers the shift from $7 + L_c$ to $6 + L_c$. Removing the truncation changes neither these path components nor this fundamental group: the discarded fibre layers begin in degree eleven, and the source dimensions for points and paths are at most nine and ten, respectively.

Only the bottom integral layer in degree nine contributes to the components of sections of $\Sigma^7\mathbb{S}^{L_c}$ over X. Its orientation makes the coefficient system constant, which proves (104). Finally the bottom Postnikov projection of the collapse evaluates on a nine-cell by the degree of its attaching sphere in the bottom Thom cell. This is exactly the cellular obstruction cochain in the proof of Thm. 4.42, with the same chosen orientation. Hence its class is c^*o. □

Proposition 4.49 (The ordinary-cohomology description of the ambiguity group)**.** *Put* $\tau = \rho_2 f_2$ *and define*

$$\begin{aligned} H^7(X;\mathbb{Z}) &\xrightarrow{\;\delta_\tau\;} H^9(X;\mathbb{Z}/2) \\ a \qquad &\longmapsto\; \mathrm{Sq}^2\,\rho_2 a + \tau \cup \rho_2 a. \end{aligned} \tag{106}$$

For $\dim X \leq 9$ *there is a natural short exact sequence*

$$0 \longrightarrow \operatorname{coker} \delta_\tau \longrightarrow \pi_s^{6+L_c}(X) \longrightarrow H^8(X;\mathbb{Z}) \longrightarrow 0. \tag{107}$$

No splitting is asserted. In this dimension the group depends, up to isomorphism, only on the twisting class τ*, and is isomorphic to ordinary* $\pi_s^8(X)$ *when* $\tau = 0$*.*

Proof. The first two homotopy groups of $\Sigma^6\mathbb{S}^{L_c}$ are $\mathbb{Z}$ in degree eight and $\mathbb{Z}/2$ in degree nine. The first stable Postnikov invariant of the sphere is $\mathrm{Sq}^2 \rho_2$; it records the stable Hopf element in $\pi_1\mathbb{S}$. For an oriented spherical family, the Thom identity adds the operation $w_2 \cup \rho_2$. In the present case this is $\tau \cup \rho_2$ by Lem. 4.45. Equivalently, after the integral Thom identification the Cartan formula reads

$$\mathrm{Sq}^2(\rho_2 a \cup U) = \left(\mathrm{Sq}^2 \rho_2 a + \tau \cup \rho_2 a\right) \cup U;$$

the middle term vanishes since the family is oriented. This proves the asserted twist of the usual stable Postnikov operation, as used in [GSS26, proof of Thm. 3.8, (48)–(50)].

Consequently the fibrewise nine-truncation is the homotopy fibre of the following map of parametrized Eilenberg–MacLane spectra:

$$\tau_{\leq 9}\Sigma^6\mathbb{S}^{L_c} \longrightarrow \Sigma^8(H\mathbb{Z})_X \xrightarrow{(\mathrm{Sq}^2 + \tau\cup(-))\rho_2} \Sigma^{10}(H\mathbb{Z}/2)_X. \tag{108}$$

Here HA represents ordinary cohomology with coefficients A, and the subscript X denotes the constant family. Taking derived sections and their homotopy exact sequence gives

$$H^7(X;\mathbb{Z}) \xrightarrow{\delta_\tau} H^9(X;\mathbb{Z}/2) \longrightarrow \pi_s^{6+L_c}(X) \longrightarrow H^8(X;\mathbb{Z}) \longrightarrow H^{10}(X;\mathbb{Z}/2) = 0.$$

The zero on the right is exactly where the dimension bound enters, and gives (107). Higher fibre layers do not affect components of sections on a nine-complex. The oriented family of the retained two-stage spectrum is classified by τ, by the self-equivalence calculation in Prop. 4.47. This proves the last assertion as well. □

Corollary 4.50 (Noncompact manifolds and manifolds with boundary)**.** *If every component of a smooth nine-manifold* X *is noncompact or has nonempty boundary, then a lift exists for every* $c : X \to \mathcal{C}$*, and* $\mathrm{Lift}(c)$ *is a torsor for* $H^8(X;\mathbb{Z})$*. This statement concerns unrestricted ordinary lifts.*

Proof. Such a manifold has a CW model of dimension at most eight. Hence both $H^9(X;\mathbb{Z})$ and $H^9(X;\mathbb{Z}/2)$ vanish. Apply Thm. 4.42 and (107). □

Example 4.51 (A choice invisible to the Sullivan model)**.** For a constant map $c : S^9 \to \mathcal{C}$, the circle bundle is trivial and the obstruction vanishes. Nevertheless there are two homotopy classes of lifts:

$$\mathrm{Lift}(c) \text{ is a torsor for } \pi_s^8(S^9) = \mathbb{Z}/2.$$

Indeed $H^7(S^9;\mathbb{Z}) = H^8(S^9;\mathbb{Z}) = 0$, whereas $H^9(S^9;\mathbb{Z}/2) = \mathbb{Z}/2$, so this follows from (107). It also follows directly from $\pi_9 F = \mathbb{Z}/2$. Thus one existence obstruction in degree nine does not mean that all choices of lift are classified by ordinary degree-eight cohomology. The additional stable Hopf choice is torsion and is invisible after rationalization.

4.2 Complex projective spaces

We first fix a metric convention that also applies to the real and quaternionic projective spaces used later. It makes the projective lines over $\mathbb{C}$ and $\mathbb{H}$ round spheres of the same

radius.

Definition 4.52 (Compatible projective metric scale)**.** Let $\mathbb{F}$ be one of the associative real normed division algebras $\mathbb{R}, \mathbb{C}, \mathbb{H}$, and put $d = \dim_{\mathbb{R}} \mathbb{F}$. Homogeneous coordinates on $\mathbb{F}P^n$ are taken modulo common right multiplication by a nonzero scalar. Write $g_{\mathbb{F},\mathrm{quot}}$ for the quotient metric of the unit sphere by the right action of $G_{\mathbb{F}} = \{a \in \mathbb{F} : |a| = 1\}$. For $\mathbb{F} = \mathbb{R}$, this is the metric of the antipodal quotient. We use

$$g_{\mathbb{F},R} = 4R^2 g_{\mathbb{F},\mathrm{quot}}, \qquad g_R = g_{\mathbb{C},R} = 4R^2 g_{\mathrm{FS}}. \tag{109}$$

Equivalently, take the quotient of the round sphere $S^{d(n+1)-1}_{2R}$ without further rescaling. Here g_{FS} has holomorphic sectional curvature 4. These choices make $\mathbb{C}P^1$ and $\mathbb{H}P^1$ round spheres of radius R, as proved next. They make $\mathbb{R}P^n$ the antipodal quotient of S^n_{2R}; the factor 2 in this last sphere radius is essential for the common critical-energy scale.

Lemma 4.53 (Hopf coordinates and round metrics)**.** *The map*

$$\Phi_R([q_1 : q_2]) = \frac{R}{|q_1|^2 + |q_2|^2}\Big(2q_1\overline{q}_2,\ |q_1|^2 - |q_2|^2\Big) \tag{110}$$

identifies $(\mathbb{H}P^1, g_{\mathbb{H},R})$ *isometrically with* $S^4_R \subset \mathbb{H}\oplus\mathbb{R}$*. Its restriction to complex homogeneous coordinates identifies* $(\mathbb{C}P^1, g_R)$ *with the equatorial* $S^2_R \subset \mathbb{C}\oplus\mathbb{R}$*.*

Proof. Quaternionic homogeneous coordinates are taken modulo common right multiplication by a nonzero quaternion. Under this multiplication both numerator and denominator in (110) scale by its squared norm, so the formula is well defined. The identity

$$4|q_1|^2|q_2|^2 + (|q_1|^2 - |q_2|^2)^2 = (|q_1|^2 + |q_2|^2)^2$$

places the image on S^4_R. In the affine chart $[w : 1]$, it is inverse stereographic projection:

$$w \longmapsto \frac{R}{1+|w|^2}\Big(2w,\ |w|^2 - 1\Big).$$

The omitted point is $[1 : 0]$, so the map is a diffeomorphism.

For completeness, the quotient norm of a tangent vector v at $[w : 1]$ is obtained by taking the horizontal part of the derivative of $(w, 1)/\sqrt{1+|w|^2}$. Subtracting its component tangent to the quaternionic fiber gives

$$|v|^2_{\mathrm{quot}} = \frac{(1+|w|^2)|v|^2 - |\overline{w}v|^2}{(1+|w|^2)^2} = \frac{|v|^2}{(1+|w|^2)^2}.$$

The stereographic pullback of the round metric is $4R^2|v|^2/(1+|w|^2)^2$, exactly the rescaled quotient metric. The same computation over $\mathbb{C}$ proves the assertion for $\mathbb{C}P^1$. In that case the first coordinate of (110) is complex, which identifies the image as the stated equator. □

We now specialize to $\mathbb{F} = \mathbb{C}$. Linear projective subspaces provide the geodesics needed for the critical-point and index calculations.

Lemma 4.54 (Fubini–Study restriction to a linear subspace)**.** *The standard inclusion* $\mathbb{C}P^k \hookrightarrow \mathbb{C}P^n$ *induced by* $\mathbb{C}^{k+1} \hookrightarrow \mathbb{C}^{n+1}$ *is isometric and totally geodesic for* g_R*.*

Proof. In an affine chart with coordinate $w \in \mathbb{C}^n$, the Fubini–Study norm is

$$(g_{\mathrm{FS}})_w(v, v) = \frac{(1+|w|^2)|v|^2 - |\langle w, v\rangle_{\mathbb{C}}|^2}{(1+|w|^2)^2}. \tag{111}$$

Setting the last $n-k$ coordinates of both w and v to zero gives exactly the corresponding expression on $\mathbb{C}P^k$; multiplying both metrics by $4R^2$ gives the asserted restriction for g_R. For total geodesy, the projectivization of the unitary involution with eigenvalues $+1$ on $\mathbb{C}^{k+1}$ and -1 on its orthogonal complement is an isometry. One component of its fixed locus is precisely this $\mathbb{C}P^k$. Apply Prop. 3.20. □

Theorem 4.55 (Critical levels of complex projective space)**.** *For $n \geq 1$, the critical manifolds of the energy on $(L_\infty \mathbb{C}P^n, g_R)$ are $K_0 = \mathbb{C}P^n$ and $K_m \cong ST\mathbb{C}P^n$, $m \geq 1$. Their energies and lengths are*

$$E(K_m) = 2\pi^2 R^2 m^2, \qquad \ell(K_m) = 2\pi R m. \tag{112}$$

Every nonconstant closed geodesic is an iterate of a primitive geodesic in a projective line.

Proof. Represent a point by a unit vector $u \in \mathbb{C}^{n+1}$. A tangent direction is represented by a unit vector v Hermitian-orthogonal to u. The projective line $\mathbb{P}_{\mathbb{C}}\langle u, v\rangle$ is totally geodesic by Lem. 4.54 and is a round S^2_R by Lem. 4.53. The curve

$$\gamma_{u,v,m}(t) = [\cos(\pi m t)u + \sin(\pi m t)v] \tag{113}$$

is its m-fold great circle, of speed $2\pi R m$. Uniqueness for the geodesic equation shows that every geodesic through the chosen point and direction lies in this line. A general positive-speed solution closes exactly when its trigonometric angle over $[0, 1]$ is an integer multiple of π: the endpoint vector may be the negative of its initial vector, since the coordinates are projective. This proves the complete list of energies. For fixed m, smooth dependence on initial data gives a smooth map $ST\mathbb{C}P^n \to L_\infty \mathbb{C}P^n$. It is injective, and its differential is injective: a variation with zero Jacobi field has zero initial point and velocity variations. Compactness of the unit tangent bundle then makes it an embedding, with image K_m of dimension $4n-1$. □

We proceed to discuss the projective Morse indices, highlighting that the normal holonomy matters.

Lemma 4.56 (Curvature and parallel normal fields)**.** *Let J be the complex structure and let T be tangent to $(\mathbb{C}P^n, g_R)$. Then*

$$\mathsf{R}(V,T)T = \frac{1}{4R^2}\left(|T|^2 V - \langle V, T\rangle T + 3\langle V, JT\rangle JT\right). \tag{114}$$

Along the closed geodesic (113), the fields $T = \dot\gamma$ and JT are parallel and periodic. Parallel transport on the orthogonal complement of their span has holonomy $(-1)^m$.

Proof. We recall the coordinate calculation to fix the scale. For g_{FS}, the Hermitian metric matrix in (111) has expansion at $w = 0$

$$g_{a\bar b}(w) = \delta_{ab} - \delta_{ab}|w|^2 - \overline{w}_a w_b + O(|w|^4).$$

Its first derivatives vanish. Inserting its second derivatives into the curvature formula, and using the real metric associated to this Hermitian norm, gives

$$\mathsf{R}(V,T)T = |T|^2 V - \langle V, T\rangle T + 3\langle V, JT\rangle JT$$

for g_{FS}. Unitary invariance extends the identity from $[1 : 0 : \cdots : 0]$ to every point. Rescaling the metric by $4R^2$ gives (114). The connection preserves J, so T and JT are parallel.

For the holonomy assertion lift the geodesic horizontally to $z(t) = \cos(\pi m t)u + \sin(\pi m t)v$ in the unit sphere. A fixed complex vector $w \perp_{\mathbb{C}} \langle u, v\rangle$ is horizontal along z and has zero covariant derivative there. Its projected field is consequently parallel. At $t = 1$, the lift satisfies $z(1) = (-1)^m z(0)$. Under the identification $T_{[z]}\mathbb{C}P^n = \mathrm{Hom}_{\mathbb{C}}(\mathbb{C}z, z^{\perp})$, the vector w represents the map $z \mapsto w$. Changing z by $(-1)^m$ therefore changes the represented tangent vector by $(-1)^m$. This is the normal holonomy. In the two real tangent directions to the geodesic's projective line, the horizontal representatives themselves also acquire this sign, so the projected fields T, JT are periodic. □

Theorem 4.57 (Morse–Bott index on complex projective space)**.** *The energy on $L_\infty\mathbb{C}P^n$ is Morse–Bott, with*

$$\begin{aligned} \mathrm{ind}(K_0) &= 0, & \mathrm{nul}(K_0) &= 2n, \\ \mathrm{ind}(K_m) &= 2n(m-1)+1, & \mathrm{nul}(K_m) &= 4n-1 \quad (m \geq 1). \end{aligned} \tag{115}$$

In particular the first negative bundle is a trivial real line bundle on $ST\mathbb{C}P^n$.

Proof. Use parallel frames along (113), whose speed is $2\pi Rm$. In the T direction the index form is the nonnegative form $\int |\dot f|^2$ on periodic functions, with one zero mode. In the JT direction, the curvature is $1/R^2$. The scalar operator is $-\mathrm{d}^2/\mathrm{d}t^2 - (2\pi m)^2$ on periodic functions. As in Thm. 4.5, it supplies $2m-1$ negative modes and two zero modes.

The other $2n-2$ real directions have curvature $1/(4R^2)$, so their scalar operators are $-\mathrm{d}^2/\mathrm{d}t^2 - (\pi m)^2$. Because the parallel frames have holonomy $(-1)^m$, the coefficient functions satisfy

$$f(1) = (-1)^m f(0), \qquad \dot f(1) = (-1)^m \dot f(0).$$

Their frequencies are πk with $k \in \mathbb{Z}$ and $k \equiv m \pmod 2$. The negative frequencies satisfy $|k| < m$. Counting real dimensions gives exactly $m-1$: for even m there is the constant mode and the positive even frequencies below m, each with its sine and cosine; for odd m there are the positive odd frequencies below m, each with its sine and cosine. At $|k| = m$ there are two real zero modes. It follows that

$$\mathrm{ind}(K_m) = (2m-1) + (2n-2)(m-1) = 2n(m-1)+1,$$

and $\mathrm{nul}(K_m) = 1 + 2 + 2(2n-2) = 4n-1$. This equals the dimension of $ST\mathbb{C}P^n$, so the periodic Jacobi fields exhaust its tangent space. Constants are handled exactly as in the sphere case. Fredholmness then establishes the Morse–Bott condition.

At $m = 1$ the only negative mode is the constant coefficient in the JT direction. The vector field $J\dot\gamma$ is defined and nonzero for every $\gamma \in K_1$, so it gives a global trivialization of the negative line bundle. □

Remark 4.58. This index formula agrees with the compact rank-one-symmetric-space calculation of [Zil77] and the formula recalled in [Şir24, Thm. 3.2]. Treating every parallel normal frame as periodic would give an incorrect index for odd iterates. The sign holonomy in Lem. 4.56 is the reason no extra negative normal modes occur at the first level.

4.3 Filtration-respecting maps

Every family in this subsection carries the first nontrivial loop stage into the first nontrivial target stage. In fact, these maps preserve every numbered stage. The inclusions below

preserve energy and critical geodesics. The quotient projections in the final subsubsection preserve sublevels by decreasing energy, and need not preserve critical geodesics.

4.3.1 Equatorial inclusions

Proposition 4.59 (Equatorial spheres preserve every stage)**.** *For $1 \le p < q$, the equatorial inclusion $\iota : S^p_R \hookrightarrow S^q_R$ is totally geodesic and isometric. It induces, for every $m \ge 0$,*

$$L_m S^p \hookrightarrow L_m S^q, \qquad (L_\infty \iota)^{-1}(L_m S^q) = L_m S^p. \tag{116}$$

For $m \ge 1$, it sends $K_m(S^p_R)$ into $K_m(S^q_R)$ by the inclusion of Stiefel manifolds, with index difference

$$\mathrm{ind}_{S^q}(K_m) - \mathrm{ind}_{S^p}(K_m) = (q-p)(2m-1), \qquad m \ge 1.$$

At the constant-loop stage both indices are zero.

Proof. The inclusion is induced by a linear isometric inclusion of Euclidean spaces. A great circle in the smaller sphere is still a great circle in the larger one. The formulas for the metric and for the geodesics therefore prove isometry and total geodesy. The critical energy $2\pi^2 R^2 m^2$ is independent of the dimension, and Prop. 3.13 proves the filtration claim. The index difference follows from (19). □

Theorem 4.60 (The inclusion of the complex into the quaternionic line)**.** *The inclusion*

$$\begin{aligned} \mathbb{C}P^1 &\xrightarrow{\iota_{\mathbb{H}}} \mathbb{H}P^1 \\ [z_1 : z_2]_{\mathbb{C}} &\longmapsto [z_1 : z_2]_{\mathbb{H}}, \end{aligned}$$

with the metric scale of Def. 4.52, preserves every critical-energy stage. In particular,

$$L_1 S^2 \hookrightarrow L_1 S^4, \qquad \mathrm{Cyc}_1 S^2 \longrightarrow \mathrm{Cyc}_1 S^4 \quad \text{over } BS^1. \tag{117}$$

For the isometry $\tau(x,y) = (x,-y)$ on $S^4_R \subset \mathbb{R}^3 \oplus \mathbb{R}^2$, the equality of filtered fixed loci is

$$(L_m S^4)^\tau = L_m S^2.$$

Proof. By Lem. 4.53, the displayed map is the equatorial inclusion of equal-radius round spheres. Apply Props. 3.18 and 4.59. The fixed-locus assertion follows from Prop. 3.20 and the common critical values. □

Remark 4.61 (An equality of indices is not a shift of stages). For this inclusion,

$$\mathrm{ind}(K_2(S^2)) = 3 = \mathrm{ind}(K_1(S^4)), \qquad c_2 = 8\pi^2 R^2 \neq 2\pi^2 R^2 = c_1.$$

A twice-traversed great circle stays twice-traversed. It is not carried into the first energy stage of LS^4. The first stage maps to the first stage even though its index increases from 1 to 3.

4.3.2 Projective subspaces

The complex-linear inclusions extend both to subspaces over each of $\mathbb{R}, \mathbb{C}, \mathbb{H}$ and to inclusions obtained by extending the ground division algebra. We first establish a common critical-value scale, including the real and quaternionic cases.

Lemma 4.62 (Horizontal representatives of projective tangents)**.** *For a unit vector $u \in \mathbb{F}^{n+1}$, identify $T_{[u]}\mathbb{F}P^n$ with*

$$u^{\perp_{\mathbb{F}}} = \{v : \langle u, v\rangle_{\mathbb{F}} = 0\}, \qquad \langle u, v\rangle_{\mathbb{F}} := \sum_{\alpha} \overline{u}_\alpha v_\alpha.$$

Under this identification the squared metric norm is $4R^2|v|^2$. A change of representative $u \mapsto ua$, $a \in G_{\mathbb{F}}$, changes the representative of the same tangent vector by $v \mapsto va$. In an affine chart the metric is

$$(g_{\mathbb{F},R})_w(v, v) = 4R^2 \frac{(1 + |w|^2)|v|^2 - |\langle w, v\rangle_{\mathbb{F}}|^2}{(1 + |w|^2)^2}. \tag{118}$$

Proof. At u the vertical tangent space of the unit-sphere quotient is $u \operatorname{Im}\mathbb{F}$. Orthogonality to it, together with tangency to the sphere, is equivalent to $\langle u, v\rangle_{\mathbb{F}} = 0$. For $\mathbb{F} = \mathbb{R}$ the vertical tangent space is zero, and this is the usual tangent space of the sphere. The quotient metric and (109) give the norm and the equivariance statement. Finally differentiate $(w, 1)/(1 + |w|^2)^{1/2}$ and subtract its vertical component. Its squared horizontal norm is the fraction in (118). □

Theorem 4.63 (Critical levels over the three division algebras)**.** *Let $n \geq 1$ and $d = \dim_{\mathbb{R}} \mathbb{F}$. The energy on $(L_\infty\mathbb{F}P^n, g_{\mathbb{F},R})$ is Morse–Bott. Its critical manifolds are $K_0 = \mathbb{F}P^n$ and, for $m \geq 1$, $K_m \cong ST\mathbb{F}P^n$, with*

$$\begin{aligned} c_m &= 2\pi^2 R^2 m^2, & \ell(K_m) &= 2\pi R m, \\ \operatorname{ind}(K_m) &= (d-1)(2m-1) + d(n-1)(m-1), & \operatorname{nul}(K_m) &= 2dn - 1. \end{aligned} \tag{119}$$

At the constants the index is zero and the nullity is dn. Thus the critical-energy stages are $L_m\mathbb{F}P^n = \{E \leq 2\pi^2 R^2 m^2\}$, with the same thresholds for all three ground algebras and all positive projective dimensions.

Proof. Take unit vectors u, v with $\langle u, v\rangle_{\mathbb{F}} = 0$. The great circle $z(s) = \cos(s)u + \sin(s)v$ in the unit sphere is horizontal at every point, since $\langle z, z'\rangle_{\mathbb{F}} = 0$. By Prop. 3.15 its projection is a geodesic. These curves realize every initial point and tangent direction. Moreover $[z(s)] = [u]$ holds exactly when $\sin(s) = 0$: independence of u, v over $\mathbb{F}$ excludes any other possibility. Hence every nonconstant closed geodesic is

$$\gamma_{u,v,m}(t) = [\cos(\pi m t)u + \sin(\pi m t)v]_{\mathbb{F}}. \tag{120}$$

Its speed is $2\pi Rm$, proving the length and energy assertions. For fixed m, the initial-data map from $ST\mathbb{F}P^n$ is a smooth injective immersion, by the Jacobi-field argument in Thm. 4.55. Compactness makes its image an embedded critical manifold, proving $K_m \cong ST\mathbb{F}P^n$.

We spell out the curvature and holonomy needed for the index count. At a point with a chosen unit representative, the tangent maps induced by right multiplication by an orthonormal basis $a_1, \ldots, a_{d-1}$ of $\operatorname{Im}\mathbb{F}$ are denoted I_α. For $d = 1$ this is an empty family. For orthonormal real tangent vectors T, V the quotient-curvature formula is

$$\sec(T, V) = \frac{1}{4R^2}\left(1 + 3\sum_{\alpha=1}^{d-1} \langle V, I_\alpha T\rangle^2\right).$$

Indeed the unit-sphere curvature is 1, and the vertical component of the derivative of a horizontal field has coefficients $\langle V, I_\alpha T\rangle$ in the fiber directions. The submersion curvature identity adds three times the squared norm of this component; rescaling gives the displayed

formula (see [ONe66]). Polarization shows that the Jacobi operator has curvature eigenvalue $1/R^2$ in the $d-1$ directions $I_\alpha T$, and $1/(4R^2)$ in the $d(n-1)$ directions perpendicular to the geodesic's $\mathbb{F}$-projective line. There is also its one-dimensional tangential kernel.

Along (120), put $w(t) = -\sin(\pi m t)u + \cos(\pi m t)v$. The horizontal representatives $w(t)a_\alpha$ project to parallel fields: their derivatives $-\pi m z(t)a_\alpha$ are vertical. At $t = 1$ both z and w have acquired $(-1)^m$, so the projected parallel fields are periodic. The unit tangent is parallel and periodic as well. By contrast, fixed vectors in $\langle u, v\rangle_{\mathbb{F}}^{\perp}$ are horizontal parallel representatives whose projected holonomy is $(-1)^m$. These assertions also follow directly by taking horizontal parts of covariant derivatives on the sphere.

The tangential scalar Hessian is $-\mathrm{d}^2/\mathrm{d}t^2$, with one zero mode and no negative modes. In each of the $d-1$ periodic high-curvature directions it is $-\mathrm{d}^2/\mathrm{d}t^2 - (2\pi m)^2$, with $2m-1$ negative modes and two zero modes. In each of the $d(n-1)$ remaining directions it is $-\mathrm{d}^2/\mathrm{d}t^2 - (\pi m)^2$ with boundary condition $f(1) = (-1)^m f(0)$ (and the same condition on $\dot f$). These are exactly the scalar periodic and sign-twisted problems counted in Thm. 4.57: each low-curvature direction contributes $m-1$ negative modes and two zero modes. Summing their contributions gives the displayed index and

$$\operatorname{nul}(K_m) = 1 + 2(d-1) + 2d(n-1) = 2dn - 1.$$

This equals $\dim ST\mathbb{F}P^n$. Variations of initial data already give that many Jacobi fields, so the Hessian kernel is exactly tangent to K_m. Together with Prop. 3.4, and the analogous constant-loop computation, this proves the Morse–Bott condition. Compare the symmetric-space treatment in [Zil77]. □

Remark 4.64 (The real case and its loop components). For $\mathbb{R}P^n$ the index is $(n-1)(m-1)$; in particular the first nonconstant critical manifold has index zero. When $n \geq 2$, odd m belong to the noncontractible free-loop component, and even m belong to the contractible one: the lift to S^n_{2R} closes exactly for even m. Thus the common list c_m refers to the whole free loop space, not to a reindexing within one component. For $\mathbb{R}P^1$ the two components of each $ST\mathbb{R}P^1$ give winding numbers m and $-m$.

Theorem 4.65 (Projective inclusions preserve every stage)**.** *Let $\mathbb{F} \subseteq \mathbb{K}$ be an inclusion among $\mathbb{R}, \mathbb{C}, \mathbb{H}$, allowing equality, and let $1 \leq k \leq n$. The map*

$$\begin{aligned} \mathbb{F}P^k &\xhookrightarrow{\quad j \quad} \mathbb{K}P^n \\ [x_0 : \cdots : x_k]_{\mathbb{F}} &\longmapsto [x_0 : \cdots : x_k : 0 : \cdots : 0]_{\mathbb{K}}, \end{aligned}$$

with the compatible metrics of Def. 4.52, is an isometric totally geodesic embedding. It induces, for every $m \geq 0$,

$$L_m\mathbb{F}P^k \hookrightarrow L_m\mathbb{K}P^n, \qquad (L_\infty j)^{-1}(L_m\mathbb{K}P^n) = L_m\mathbb{F}P^k,$$

and $\mathrm{Cyc}_m \mathbb{F}P^k \to \mathrm{Cyc}_m \mathbb{K}P^n$ over BS^1. On nonconstant critical manifolds it is the unit-tangent inclusion and preserves the traversal number m. For $\mathbb{F} = \mathbb{K}$ the index difference at level $m \geq 1$ is $d(n-k)(m-1)$, where $d = \dim_{\mathbb{R}} \mathbb{F}$.

Proof. The map is well defined. If two nonzero vectors $x, y \in \mathbb{F}^{k+1}$ satisfy $y = xa$ with $a \in \mathbb{K}^\times$, any nonzero coordinate of x gives $a = x_\alpha^{-1} y_\alpha \in \mathbb{F}$. Thus the map is injective. For vectors with entries in $\mathbb{F}$, the $\mathbb{K}$-Hermitian product equals their $\mathbb{F}$-Hermitian product. A horizontal tangent representative stays horizontal and keeps its norm, so Lem. 4.62 proves

that the inclusion is an isometric immersion. Compactness makes it an embedding. Formula (120) is unchanged by the inclusion, proving total geodesy. The common critical values in Thm. 4.63 and Props. 3.13 and 3.18 give all filtration assertions. Subtracting the index formulas proves the last statement. □

Remark 4.66 (Subspaces and extension of scalars). For equal ground algebras this includes $\mathbb{R}P^k \hookrightarrow \mathbb{R}P^n$, $\mathbb{C}P^k \hookrightarrow \mathbb{C}P^n$, and $\mathbb{H}P^k \hookrightarrow \mathbb{H}P^n$. For proper extensions it includes $\mathbb{R}P^k \hookrightarrow \mathbb{C}P^n$, $\mathbb{R}P^k \hookrightarrow \mathbb{H}P^n$, and $\mathbb{C}P^k \hookrightarrow \mathbb{H}P^n$. At the first critical level their indices are respectively 0, 1, and 3 according to the target ground algebra, independently of projective dimension. The inclusion $\mathbb{C}P^1 \hookrightarrow \mathbb{H}P^1$ of Thm. 4.60 is consequently also a case of the general projective theorem. These statements concern the standard metrics up to constant rescaling. Independent rescalings of source and target can change the numerical energy comparison, but preserve the stage correspondence $m \mapsto m$; see Lem. 4.1.

Corollary 4.67 (The two-sphere in complex projective three-space)**.** *The map*

$$\begin{aligned} \mathbb{C}P^1 &\xhookrightarrow{\ j\ } \mathbb{C}P^3 \\ [z_1 : z_2] &\longmapsto [z_1 : z_2 : 0 : 0] \end{aligned}$$

identifies S^2_R *isometrically with a totally geodesic projective line, and in particular gives*

$$L_1 S^2 \hookrightarrow L_1 \mathbb{C}P^3, \qquad \operatorname{Cyc}_1 S^2 \longrightarrow \operatorname{Cyc}_1 \mathbb{C}P^3 \quad \text{over } BS^1. \tag{121}$$

Both first critical manifolds have index 1*; their dimensions are respectively* 3 *and* 11*.*

Proof. Take $k = 1, n = 3$ in Thm. 4.65 and use the round identification Lem. 4.53. The dimensions and indices are those of Thms. 4.55 and 4.57. □

Remark 4.68 (Stage numbers, normalized energy, and indices). Stage numbers do not count negative Hessian directions. The following comparison is independent of metric scale:

m	c_m/c_1	$\operatorname{ind}(S^2)$	$\operatorname{ind}(S^4)$	$\operatorname{ind}(\mathbb{C}P^3)$
1	1	1	3	1
2	4	3	9	7
3	9	5	15	13

Both $S^2 \hookrightarrow S^4$ and $S^2 = \mathbb{C}P^1 \hookrightarrow \mathbb{C}P^3$ preserve the first nontrivial stage. The different indices describe different attachments at that stage, and do not shift its number. For numerical calculations a common scale R makes $c_m = 2\pi^2 R^2 m^2$ on all three spaces. The quotient convention is $R = 1/2$, while $R = 1$ makes the projective lines unit round spheres. Changing these scales independently leaves every stated stage correspondence unchanged by Lem. 4.1.

4.3.3 Projective quotients

There is a second natural family of projective maps. Instead of including vectors from a smaller coordinate space, regard a fixed $\mathbb{K}$-vector space as an $\mathbb{F}$-vector space and send each $\mathbb{F}$-line to its $\mathbb{K}$-span. This yields quotient fibrations whose loop maps preserve the small-loop stage, and indeed every stage. At a common metric scale this follows from energy decrease and equality of the source and target critical thresholds.

Theorem 4.69 (Projective quotient fibrations respect every stage)**.** *Let $\mathbb{F} \subsetneq \mathbb{K}$ be among $\mathbb{R} \subset \mathbb{C} \subset \mathbb{H}$, put $r = \dim_{\mathbb{F}} \mathbb{K}$, and let $n \geq 1$. Identify the right $\mathbb{F}$-vector space $\mathbb{K}^{n+1}$ isometrically with $\mathbb{F}^{r(n+1)}$. Then*

$$\begin{array}{ccc} \mathbb{F}P^{r(n+1)-1} & \xrightarrow{p_{\mathbb{F},\mathbb{K}}} & \mathbb{K}P^{n} \\ [v]_{\mathbb{F}} & \longmapsto & [v]_{\mathbb{K}} \end{array} \tag{122}$$

is a Riemannian submersion for the common scale R, with totally geodesic fiber $\mathbb{F}P^{r-1}$ in its standard metric. For every $m \geq 0$ it induces maps

$$\begin{aligned} L_m\mathbb{F}P^{r(n+1)-1} &\longrightarrow L_m\mathbb{K}P^{n}, \\ \mathrm{Cyc}_m\,\mathbb{F}P^{r(n+1)-1} &\longrightarrow \mathrm{Cyc}_m\,\mathbb{K}P^{n} \quad \text{over } BS^1. \end{aligned} \tag{123}$$

The energy difference is exactly the vertical energy in (12). In particular the three families are

projection	fiber
$\mathbb{R}P^{2n+1} \longrightarrow \mathbb{C}P^{n}$	$\mathbb{R}P^{1}$
$\mathbb{R}P^{4n+3} \longrightarrow \mathbb{H}P^{n}$	$\mathbb{R}P^{3}$
$\mathbb{C}P^{2n+1} \longrightarrow \mathbb{H}P^{n}$	$\mathbb{C}P^{1}$.

The last is the standard twistor fibration.

Proof. Let $G_{\mathbb{F}} \subset G_{\mathbb{K}}$ be the groups of unit scalars. Both projective metrics are quotients of the same round sphere:

$$S_{2R}^{(\dim_{\mathbb{R}}\mathbb{K})(n+1)-1}/G_{\mathbb{F}} \quad\longrightarrow\quad S_{2R}^{(\dim_{\mathbb{R}}\mathbb{K})(n+1)-1}/G_{\mathbb{K}}.$$

The actions are free, and local trivializations of the $G_{\mathbb{K}}$-bundle identify the fiber with $G_{\mathbb{K}}/G_{\mathbb{F}} \cong \mathbb{F}P^{r-1}$. The horizontal space for the $G_{\mathbb{K}}$-quotient is contained in the horizontal space for the $G_{\mathbb{F}}$-quotient. On that common horizontal space both quotient differentials preserve the sphere metric. This proves that (122) is a Riemannian submersion. No normality of $G_{\mathbb{F}}$ in $G_{\mathbb{K}}$ is required; the fiber is the displayed homogeneous space, not in general a quotient group.

For a fixed right $\mathbb{K}$-line $v\mathbb{K}$, its $\mathbb{F}$-projectivization is a linear $\mathbb{F}P^{r-1}$ inside the source. The metric and total-geodesy assertions therefore follow from Thm. 4.65. By Thm. 4.63, source and target have the common critical values $c_m = 2\pi^2R^2m^2$. Apply Prop. 3.15. The twistor interpretation of the final family uses the description of a point of $\mathbb{C}P^{2n+1}$ as a complex line inside a quaternionic line; see also [Esc75]. □

Corollary 4.70 (The twistor map to the round four-sphere)**.** *The twistor projection with the metric scale of Def. 4.52 induces*

$$L_1\mathbb{C}P^{3} \longrightarrow L_1S^{4}, \qquad \mathrm{Cyc}_1\,\mathbb{C}P^{3} \longrightarrow \mathrm{Cyc}_1\,S^{4} \quad \text{over } BS^1, \tag{124}$$

and similarly at every stage. For a loop in $\mathbb{C}P^3$, equality of its energy with the energy of its image holds exactly when it is horizontal almost everywhere.

Proof. Take $\mathbb{F} = \mathbb{C}$, $\mathbb{K} = \mathbb{H}$, $n = 1$ in Thm. 4.69 and use Lem. 4.53. □

Proposition 4.71 (A filtered triangle and two kinds of projective line)**.** *Fix $\mathbb{C} = \langle 1, i\rangle \subset \mathbb{H}$ and write quaternionic coordinates using the right-$\mathbb{C}$-linear isometry*

$$\begin{array}{ccc} \mathbb{C}^4 & \longrightarrow & \mathbb{H}^2 \\ (z_1, z_2, z_3, z_4) & \longmapsto & (z_1 + jz_3,\ z_2 + jz_4)\,. \end{array}$$

In these coordinates the following diagram commutes:

$$\begin{array}{ccc} \mathbb{C}P^1 & \xrightarrow{j_0} & \mathbb{C}P^3 \\ & \searrow^{\iota_{\mathbb{H}}} & \downarrow{\scriptstyle p} \\ & & \mathbb{H}P^1, \end{array} \qquad j_0[z_1 : z_2] = [z_1 : z_2 : 0 : 0]. \tag{125}$$

The image of j_0 is horizontal for p, and p restricts there to the equatorial isometric inclusion $S^2_R \hookrightarrow S^4_R$. In contrast, the projective line $\{[z_1 : 0 : z_3 : 0]\}$ is a twistor fiber over $[1 : 0]_{\mathbb{H}}$. Consequently, for every $m \geq 0$, the induced maps fit into commuting diagrams

$$\begin{array}{ccc} L_m S^2 & \xrightarrow{L_m j_0} & L_m \mathbb{C}P^3 \\ & \searrow^{L_m \iota_{\mathbb{H}}} & \downarrow{\scriptstyle L_m p} \\ & & L_m S^4 \end{array} \qquad \begin{array}{ccc} \mathrm{Cyc}_m\, S^2 & \xrightarrow{\mathrm{Cyc}_m\, j_0} & \mathrm{Cyc}_m\, \mathbb{C}P^3 \\ & \searrow^{\mathrm{Cyc}_m\, \iota_{\mathbb{H}}} & \downarrow{\scriptstyle \mathrm{Cyc}_m\, p} \\ & & \mathrm{Cyc}_m\, S^4, \end{array} \tag{126}$$

where we identify $\mathbb{C}P^1 \cong S^2$ and $\mathbb{H}P^1 \cong S^4$ with the compatible round metrics, and the cyclified diagram is over BS^1. In particular, taking $m = 1$ exhibits the factorization of the small-loop inclusion through the small-loop space of $\mathbb{C}P^3$: all three maps preserve the first nontrivial filtration stage.

Proof. The composite is $[z_1 : z_2]_{\mathbb{C}} \mapsto [z_1 : z_2]_{\mathbb{H}}$. The identifications of the two included metrics are those of Thm. 4.65. Since both j_0 and pj_0 preserve tangent norms, the submersion norm identity forces every tangent of $j_0(\mathbb{C}P^1)$ to be horizontal. The other projective line consists of all complex lines in $(1, 0)\mathbb{H}$, so is exactly the fiber over $[1 : 0]_{\mathbb{H}}$. The stage maps follow from Thms. 4.65 and 4.69. Composition on loops preserves the commutativity of (125) and commutes with loop rotation; taking Borel constructions gives the second triangle in (126) over BS^1. □

Example 4.72 (A critical twistor loop can project to a noncritical loop)**.** Use the preceding quaternionic description of $\mathbb{C}P^3$ and let $0 < \alpha < \pi/2$. Put $a = \cos\alpha$, $b = \sin\alpha$, and consider

$$\gamma_\alpha(t) = [(\cos(\pi t) + ja\sin(\pi t),\ b\sin(\pi t))]_{\mathbb{C}}. \tag{127}$$

The vectors $u = (1, 0)$ and $v = (ja, b)$ are orthonormal over $\mathbb{C}$, since the complex component of $\langle u, v\rangle_{\mathbb{H}} = ja$ is zero. Thus γ_α is a primitive closed geodesic of $\mathbb{C}P^3$, with energy $c_1 = 2\pi^2 R^2$. For its unit-sphere lift $z(t)$, direct calculation gives

$$|z'(t)|^2 = \pi^2, \qquad \langle z(t), z'(t)\rangle_{\mathbb{H}} = \pi ja.$$

Subtracting the quaternionic vertical component therefore gives

$$E_{\mathbb{H}P^1}(p\gamma_\alpha) = 2\pi^2 R^2(1 - a^2) = c_1 \sin^2\alpha \in (0, c_1). \tag{128}$$

The projected loop is nonconstant, but cannot be critical, since c_1 is the smallest positive critical energy on $\mathbb{H}P^1$. At $\alpha = 0$ the geodesic lies in a twistor fiber and projects to a constant loop; at $\alpha = \pi/2$ it is horizontal and projects to a primitive great circle. This proves explicitly that preservation of the filtration does not imply preservation of its critical manifolds.

Remark 4.73 (Generality and limits of the submersion argument). Every Riemannian submersion respects numerical energy sublevels, regardless of whether its fibers are totally

geodesic. Identifying ordinal stages additionally requires comparing the critical spectra. The Hopf quotients of spheres illustrate the distinction: they require the sharp reindexing $m \mapsto 2m$, as proved in Thm. 4.76 below. This is independent of constant metric rescalings. There is no stage shift for the projective quotient fibrations of Thm. 4.69.

4.4 Filtration-violating maps

The Hopf projections provide natural maps that fail to preserve the number of a critical-energy stage. Their loop maps do satisfy a sharp bound, but with reindexing $m \mapsto 2m$. The reason is geometric: a horizontal great circle upstairs traverses a primitive geodesic downstairs twice. In particular these maps do not preserve the small-loop stage. By Lem. 4.1, changing metric scales cannot remove this failure.

4.4.1 Hopf fibrations

Definition 4.74 (The Hopf projections)**.** Let $\mathbb{F} \in \{\mathbb{R}, \mathbb{C}, \mathbb{H}\}$, $d = \dim_{\mathbb{R}} \mathbb{F}$, and $n \geq 1$. On unit representatives the projection is

$$\begin{array}{ccc} S^{d(n+1)-1} & \xrightarrow{p_{\mathbb{F},n}} & \mathbb{F}P^n \\ x & \longmapsto & [x]_{\mathbb{F}}\,. \end{array} \tag{129}$$

Both spaces have their standard metrics up to scale, as specified at the start of § 4. The fiber is the orbit $xG_{\mathbb{F}}$ of the unit scalars, a great sphere S^{d-1} in the unit representative model. For $\mathbb{F} = \mathbb{R}$ this is the antipodal double covering, with fiber S^0. The three families are

$\mathbb{F}$	projection	fiber
$\mathbb{R}$	$S^n \longrightarrow \mathbb{R}P^n$	S^0
$\mathbb{C}$	$S^{2n+1} \longrightarrow \mathbb{C}P^n$	S^1
$\mathbb{H}$	$S^{4n+3} \longrightarrow \mathbb{H}P^n$	S^3.

Metric scales will enter only the energy calculation below; the stage correspondence in Thm. 4.76 has no scale parameter. The classical complex example is due to Hopf [Hop31]; for the Riemannian-submersion framework see [ONe66; Esc75].

Lemma 4.75 (Exact energy loss in the vertical directions)**.** *For this calculation, realize the source as a round sphere $S^{d(n+1)-1}_{\rho}$ of radius $\rho > 0$ and equip the target with $g_{\mathbb{F},R}$, $R > 0$. The symbols ρ and R are independent metric scales; they do not index filtration stages. The differential of $p_{\mathbb{F},n}$ multiplies horizontal lengths by $2R/\rho$, so this is a Riemannian submersion exactly when $\rho = 2R$. Write $\gamma(t) = \rho z(t)$, $|z(t)| = 1$, and set*

$$a_\gamma(t) = \langle z(t), \dot{z}(t)\rangle_{\mathbb{F}} \in \operatorname{Im}\mathbb{F} \quad \text{for almost every } t.$$

Its vertical energy and the energy of its projection are

$$\begin{aligned} E^{\mathcal{V}}(\gamma) &:= \frac{\rho^2}{2}\int_0^1 |a_\gamma(t)|^2\,\mathrm{d}t, \\ E_{\mathbb{F}P^n}(p_{\mathbb{F},n}\gamma) &= \frac{4R^2}{\rho^2}\Big(E_{S_\rho}(\gamma) - E^{\mathcal{V}}(\gamma)\Big). \end{aligned} \tag{130}$$

In particular equality in $E_{\mathbb{F}P^n}(p\gamma) \leq (4R^2/\rho^2)E_{S_\rho}(\gamma)$ holds exactly for loops horizontal almost everywhere. For $\mathbb{F} = \mathbb{R}$, the vertical energy is zero for every loop.

Proof. Differentiation of $|z|^2 = 1$ shows that the real part of $\langle z, \dot{z}\rangle_{\mathbb{F}}$ vanishes. The vertical and horizontal parts of $\dot{z}$ are

$$\dot{z}^{\mathcal{V}} = z a_\gamma, \qquad \dot{z}^{\mathcal{H}} = \dot{z} - z a_\gamma.$$

Indeed $\langle z, \dot{z} - z a_\gamma \rangle_{\mathbb{F}} = 0$, and multiplication by the unit vector z is isometric on the scalar fiber. Consequently $|\dot{z}^{\mathcal{H}}|^2 = |\dot{z}|^2 - |a_\gamma|^2$. By Lem. 4.62, the squared speed of the projected loop is $4R^2(|\dot{z}|^2 - |a_\gamma|^2)$. Integration proves (130). The equality criterion follows because the subtracted integrand is nonnegative. For the real algebra $\operatorname{Im}\mathbb{R} = 0$. These computations hold for H^1 loops by the almost-everywhere chain rule. □

Theorem 4.76 (Sharp doubling of the Hopf stage number)**.** *For each of the three Hopf families in Def. 4.74, and every $m \geq 0$, composition induces*

$$\begin{aligned} L_m S^{d(n+1)-1} &\longrightarrow L_{2m}\mathbb{F}P^n, \\ \operatorname{Cyc}_m S^{d(n+1)-1} &\longrightarrow \operatorname{Cyc}_{2m} \mathbb{F}P^n \quad \text{over } BS^1. \end{aligned} \tag{131}$$

For every $m \geq 1$, the target stage $2m$ is the smallest numbered stage containing the image of the entire source stage m. More precisely, every horizontal m-fold great circle projects to a $2m$-fold primitive projective geodesic. In particular, the image of $L_1 S^{d(n+1)-1}$ is contained in $L_2\mathbb{F}P^n$ but not in $L_1\mathbb{F}P^n$: the small-loop stage is not preserved. All these assertions are independent of the source and target metric scales, which have been suppressed in the notation.

Proof. The first source and target thresholds are $c_1^S = 2\pi^2\rho^2$ and $c_1^P = 2\pi^2 R^2$. Dividing (130) by c_1^P gives

$$\varepsilon_{\mathbb{F}P^n}(p\gamma) = 4\,\frac{E_{S_\rho}(\gamma) - E^{\mathcal{V}}(\gamma)}{c_1^S} \leq 4\varepsilon_{S_\rho}(\gamma).$$

Thus the source bound $\varepsilon \leq m^2$ implies the target bound $\varepsilon \leq (2m)^2$. This proves the loop-stage map; rotation equivariance gives the cyclified map over BS^1.

To prove sharpness, choose $\mathbb{F}$-orthonormal unit vectors $u, v \in \mathbb{F}^{n+1}$ and put

$$\gamma_m(t) = \rho\Big(\cos(2\pi m t)u + \sin(2\pi m t)v\Big). \tag{132}$$

This is an m-fold great circle and is horizontal: the $\mathbb{F}$-Hermitian product of its normalized position and velocity vanishes. Conversely, for a great circle given by a real orthonormal pair (u, v), horizontality at $t = 0$ forces $\langle u, v\rangle_{\mathbb{F}} = 0$. Thus this describes every horizontal great circle. Its projection is

$$p\gamma_m(t) = [\cos(2\pi m t)u + \sin(2\pi m t)v]_{\mathbb{F}}. \tag{133}$$

The least positive angle closing this projective geodesic is π, as proved in Thm. 4.63. Thus (133) is precisely the $2m$-fold primitive geodesic, of energy c_{2m}^P. It belongs to no stage $j < 2m$. The same witness gives points of the Borel image outside every earlier target Borel sublevel. This proves the minimality assertion.

The formulas prove the result for arbitrary positive ρ, R. Equivalently, its independence of metric scale follows from Lem. 4.1. □

Remark 4.77 (Why energy decrease does not imply stage preservation). In the Riemannian-submersion scale $\rho = 2R$, the Hopf projection decreases energy and preserves every numerical sublevel. Nevertheless, a primitive horizontal geodesic upstairs has length $4\pi R$, while a primitive geodesic downstairs has length $2\pi R$. Their first critical energies therefore differ by a factor of four. The normalized inequality is

$$\frac{E_{\mathbb{F}P^n}(p\gamma)}{c_1^P} \leq 4\,\frac{E_{S_\rho}(\gamma)}{c_1^S}, \tag{134}$$

with equality on horizontal loops, in every scale. Thus the doubling of stage number reflects the double traversal, not a choice of energy units. It also does not mean that every loop in stage m lands in the stratum $L_{2m}\mathbb{F}P^n - L_{2m-1}\mathbb{F}P^n$: constants remain constant, and vertical loops project to constants.

Remark 4.78 (The real covering and the choice of components). For $\mathbb{F} = \mathbb{R}$ every great circle is horizontal. If $n \geq 2$, the projected loop of any closed loop in S^n lies in the contractible component of $L_\infty\mathbb{R}P^n$, since it has a closed lift to the universal cover. The positive critical levels in that component have even traversal numbers. Renumbering only that component would change the meaning of the first stage; the theorem uses the filtration of the whole free loop space, as in Rem. 4.64. For $n = 1$, the covering multiplies the winding number by two, after compatible orientation choices.

Corollary 4.79 (The Hopf maps to round spheres)**.** *With the auxiliary radii ρ, R of Lem. 4.75, for $\mathbb{F} = \mathbb{C}, \mathbb{H}$ and $d = 2, 4$, the projective-line identification of Lem. 4.53 turns $p_{\mathbb{F},1}$ into*

$$\begin{aligned} S^{2d-1}_\rho &\xrightarrow{\ h_{\rho,R}\ } S^d_R \subset \mathbb{F} \oplus \mathbb{R} \\ (q_1, q_2) &\longmapsto \frac{R}{\rho^2}\Big(2q_1\overline{q}_2,\ |q_1|^2 - |q_2|^2\Big). \end{aligned} \tag{135}$$

For $d = 4$ this is the quaternionic Hopf fibration, with fiber S^3. It induces the sharp stage maps

$$L_m S^7 \longrightarrow L_{2m}S^4, \qquad \mathrm{Cyc}_m\, S^7 \longrightarrow \mathrm{Cyc}_{2m}\, S^4 \quad \text{over } BS^1. \tag{136}$$

The analogous complex stage maps have source $L_m S^3$ and target $L_{2m}S^2$, and likewise after cyclification.

Proof. Compose the Hopf projection with the isometry (110); since $|q_1|^2 + |q_2|^2 = \rho^2$, its formula is (135). Apply Thm. 4.76. The sharpness witness can be seen without coordinates on projective space:

$$\begin{aligned} \gamma_m(t) &= \rho(\cos(2\pi m t), \sin(2\pi m t)), \\ h_{\rho,R}\gamma_m(t) &= R(\sin(4\pi m t), \cos(4\pi m t)). \end{aligned} \tag{137}$$

The real first coordinate on the second line is regarded as an element of $\mathbb{F}$. The image is a $2m$-fold great circle of S^d_R. □

Example 4.80 (A first critical loop may project below, at, or above the first threshold)**.** In (135), choose a unit imaginary scalar $I \in \mathbb{F}$, and let $0 \leq a \leq 1$, $b = \sqrt{1-a^2}$. The loop

$$\gamma_a(t) = \rho\Big(\cos(2\pi t) + Ia\sin(2\pi t),\ b\sin(2\pi t)\Big)$$

is a primitive great circle in the source for every a: its defining real two-frame is $u = (1, 0)$, $v = (Ia, b)$. Its normalized vertical coefficient is $\langle z, \dot{z}\rangle_{\mathbb{F}} = 2\pi Ia$. Consequently

$$E(\gamma_a) = c_1^S, \qquad E(h_{\rho,R}\gamma_a) = 4b^2 c_1^P. \tag{138}$$

More explicitly, putting $s = 2\pi t$,

$$\frac{1}{R}h_{\rho,R}\gamma_a(t) = C + A\cos(2s) + B\sin(2s), \quad \begin{cases} C = (Iab, a^2), \\ A = (-Iab, b^2), \\ B = (b, 0). \end{cases}$$

The vectors C, A, B are pairwise real-orthogonal, with $|C| = a$ and $|A| = |B| = b$. Thus for $0 < a < 1$ the image is a twice-traversed round circle of Euclidean radius Rb with

nonzero center RC. Its plane does not pass through the origin, so it is not a geodesic of the round target. It lies in the first target stage exactly when $b \le 1/2$. At $b = 1/2$ its energy equals the first critical value, although the loop itself is not critical. At $a = 0$ it is the twice-traversed great circle from the sharpness proof; at $a = 1$ it is constant. Embedding these two coordinates in $\mathbb{F}^{n+1}$ gives the same examples inside a totally geodesic projective line of $\mathbb{F}P^n$.

Proposition 4.81 (Factoring through projective quotients)**.** *Let $\mathbb{F} \subsetneq \mathbb{K}$ be among $\mathbb{R} \subset \mathbb{C} \subset \mathbb{H}$, and put $r = \dim_{\mathbb{F}} \mathbb{K}$ and $D = (\dim_{\mathbb{R}} \mathbb{K})(n+1) - 1$. Using the coordinate identification from Thm. 4.69, the Hopf projection factors as*

$$\begin{array}{ccc} S^D & \xrightarrow{p_{\mathbb{F},r(n+1)-1}} & \mathbb{F}P^{r(n+1)-1} \\ & \searrow^{p_{\mathbb{K},n}} & \downarrow{\scriptstyle p_{\mathbb{F},\mathbb{K}}} \\ & & \mathbb{K}P^n. \end{array} \tag{139}$$

On loop stages this gives a commuting triangle

$$\begin{array}{ccc} L_m S^D & \longrightarrow & L_{2m}\mathbb{F}P^{r(n+1)-1} \\ & \searrow & \downarrow \\ & & L_{2m}\mathbb{K}P^n, \end{array}$$

and likewise for cyclification over BS^1. In particular the factorization $S^7 \to \mathbb{C}P^3 \to \mathbb{H}P^1 \cong S^4$ consists of a Hopf projection requiring $m \mapsto 2m$ followed by a twistor projection preserving the stage number.

Proof. The composite sends a nonzero vector x first to its $\mathbb{F}$-line and then to its $\mathbb{K}$-span, which is exactly $[x]_{\mathbb{K}}$. Apply Thm. 4.76 to the sphere projections and Thm. 4.69 to the projective projection. Rotation equivariance gives the Borel assertion. □

Example 4.82 (The ordinary Hopf fibrations on the first stage)**.** For the Hopf fibrations over projective lines ($n = 1$), Prop. 4.81 specializes at $m = 1$ as follows. All spheres and projective spaces below have their standard metrics up to independent constant rescaling.

For the quaternionic Hopf fibration $S^7 \to \mathbb{H}P^1 \cong S^4$, the factorization through the twistor space gives

$$L_1 S^7 \xrightarrow{L_\infty p_{\mathbb{C},3}} L_2\mathbb{C}P^3 \xrightarrow{L_\infty p_{\mathbb{C},\mathbb{H}}} L_2\mathbb{H}P^1 \xrightarrow{\cong} L_2 S^4. \tag{140}$$

The first arrow requires stage 2; the twistor arrow preserves stage number. It also restricts to $L_1\mathbb{C}P^3 \to L_1 S^4$, but the image of the preceding sphere map is not contained in that smaller domain. Nor does the composite land in $L_1 S^4$. One may refine the factorization to

$$L_1 S^7 \longrightarrow L_2\mathbb{R}P^7 \longrightarrow L_2\mathbb{C}P^3 \longrightarrow L_2 S^4;$$

again only the initial sphere projection requires the shift.

For the complex Hopf fibration $S^3 \to \mathbb{C}P^1 \cong S^2$, the analogous factorization is

$$L_1 S^3 \xrightarrow{L_\infty p_{\mathbb{R},3}} L_2\mathbb{R}P^3 \xrightarrow{L_\infty p_{\mathbb{R},\mathbb{C}}} L_2\mathbb{C}P^1 \xrightarrow{\cong} L_2 S^2. \tag{141}$$

Here the first map is induced by the antipodal double covering and the second by the projective circle fibration. The second map preserves stage number, while the composite requires target stage 2.

For the real Hopf fibration, the double covering of circles, one obtains

$$L_1 S^1 \xrightarrow{L_\infty p_{\mathbb{R},1}} L_2 \mathbb{R}P^1 \xrightarrow{\cong} L_2 S^1. \tag{142}$$

Identify $\mathbb{R}P^1$ with a circle by

$$\begin{aligned} \mathbb{R}P^1 &\xrightarrow{\cong} S^1 \\ [\cos\theta \,:\, \sin\theta] &\longmapsto e^{2i\theta}. \end{aligned}$$

With the standard projective metric this is a round-circle identification up to scale. The covering doubles the winding number. A once-traversed source circle therefore reaches winding number 2, outside the first target stage. There is no further intermediate quotient by a smaller algebra in $\{\mathbb{R}, \mathbb{C}, \mathbb{H}\}$.

For the complex and quaternionic maps the witness, on unit source and target spheres, is

$$\gamma(t) \,=\, (\cos(2\pi t), \sin(2\pi t)), \qquad h\gamma(t) \,=\, (\sin(4\pi t), \cos(4\pi t)).$$

The image is a twice-traversed great circle, as in (137). This proves the stated failure of first-stage preservation for each composite. All three displays also hold with L_j replaced by Cyc_j, over BS^1.

Remark 4.83 (Scope of the filtration failure). The sharpness statements concern the composition map on the specified energy subspaces. They do not assert an obstruction to replacing that map by a homotopic map factoring through an earlier stage. Such an obstruction would be a further question about the attaching maps and the homotopy class of the induced loop map.

4.4.2 Veronese embeddings

The preceding Hopf maps are quotient projections. A second natural source of filtration failure is provided by the *complex Veronese embeddings*. Their degree determines an exact dilation of the normalized loop energy, hence a sharp change of stage number. Unlike a Hopf projection, a Veronese embedding is injective: the failure here does not come from identifying points of a source geodesic.

Definition 4.84 (Normalized Veronese embedding)**.** Let $n \geq 1$ and $d \geq 1$ be integers, where d now denotes the polynomial degree, and put

$$N_d \,=\, \binom{n+d}{d} - 1.$$

For a multi-index $\alpha = (\alpha_0, \ldots, \alpha_n)$ of nonnegative integers, write $|\alpha| = \sum_j \alpha_j$, $\alpha! = \prod_j \alpha_j!$, and $z^\alpha = \prod_j z_j^{\alpha_j}$. Set

$$V_d(z) \,=\, \left(\sqrt{\frac{d!}{\alpha!}}\, z^\alpha \right)_{|\alpha|=d} \in \mathbb{C}^{N_d+1}.$$

The degree-d Veronese map is

$$\begin{aligned} \mathbb{C}P^n &\xrightarrow{\nu_d} \mathbb{C}P^{N_d} \\ [z] &\longmapsto [V_d(z)]\,. \end{aligned} \tag{143}$$

The square-root multinomial coefficients are part of the metric normalization. We equip the target coordinates with their standard Hermitian inner product. Equivalently, $V_d(z)$ is the symmetric tensor $z^{\otimes d}$, expressed in an orthonormal basis of $\mathrm{Sym}^d \mathbb{C}^{n+1}$, with the metric inherited from $(\mathbb{C}^{n+1})^{\otimes d}$.

Proposition 4.85 (Embedding and metric pullback)**.** *The map (143) is a holomorphic embedding. For the Fubini–Study metrics in the quotient normalization,*

$$\nu_d^* g_{\mathrm{FS}}^{(N_d)} \;=\; d\, g_{\mathrm{FS}}^{(n)}. \tag{144}$$

Here the superscript specifies the projective dimension. The same identity holds for the common scale $g_R^{(k)} := 4R^2 g_{\mathrm{FS}}^{(k)}$ of Def. 4.52. Thus lengths of tangent vectors are multiplied by $\sqrt{d}$. This is the standard metric property of the Veronese map; see, for example, [Ter, Ex. 92].

Proof. The multinomial theorem gives the polarized identity

$$\langle V_d(z), V_d(w)\rangle \;=\; \langle z, w\rangle^d, \qquad |V_d(z)|^2 \;=\; |z|^{2d}. \tag{145}$$

In particular $V_d(z) \neq 0$ for $z \neq 0$. Since $V_d(az) = a^d V_d(z)$, its projectivization is well defined and holomorphic. For unit vectors z, w, collinearity of $V_d(z), V_d(w)$ implies $|\langle z, w\rangle|^d = 1$. Equality in Cauchy–Schwarz then makes z, w collinear. Thus the projective map is injective.

To compute its metric, take $|z| = 1$ and a horizontal tangent representative v with $\langle z, v\rangle = 0$. In the tensor description,

$$DV_d(z)v \;=\; \sum_{a=1}^{d} z^{\otimes(a-1)} \otimes v \otimes z^{\otimes(d-a)}.$$

Every summand is orthogonal to $z^{\otimes d}$; distinct summands are mutually orthogonal, and each has squared norm $|v|^2$. It follows that

$$\langle V_d(z), DV_d(z)v\rangle \;=\; 0, \qquad |DV_d(z)v|^2 \;=\; d|v|^2.$$

Thus $DV_d(z)v$ is horizontal at the unit vector $V_d(z)$. The quotient metric on projective space measures exactly these horizontal norms, proving (144); real polarization gives the bilinear identity. Its positive-definiteness proves that ν_d is an immersion. Together with injectivity and compactness of $\mathbb{C}P^n$, this makes it a holomorphic embedding. Multiplication of both metrics by $4R^2$ proves the statement for g_R. □

Theorem 4.86 (Sharp stage bound for Veronese embeddings)**.** *For the standard projective metrics up to independent constant rescalings, the normalized energy of (15) satisfies*

$$\varepsilon_{\mathbb{C}P^{N_d}}(\nu_d \circ \gamma) \;=\; d\, \varepsilon_{\mathbb{C}P^n}(\gamma). \tag{146}$$

Consequently, for every integer $m \geq 0$, composition induces

$$\begin{aligned} L_m\mathbb{C}P^n \;&\longrightarrow\; L_{\lceil m\sqrt{d}\rceil}\mathbb{C}P^{N_d}, \\ \mathrm{Cyc}_m\,\mathbb{C}P^n \;&\longrightarrow\; \mathrm{Cyc}_{\lceil m\sqrt{d}\rceil}\,\mathbb{C}P^{N_d} \quad \text{over } BS^1. \end{aligned} \tag{147}$$

For $m \geq 1$, the target index $\lceil m\sqrt{d}\rceil$ is the smallest numbered stage containing the entire image of the source stage. In particular, if $d > 1$, the first nontrivial stage is not preserved: its image requires target stage $\lceil\sqrt{d}\rceil \geq 2$.

Proof. First choose a common metric scale R. The metric pullback in Prop. 4.85 and the Sobolev chain rule give the exact identity

$$E_{\mathbb{C}P^{N_d}}(\nu_d \circ \gamma) \;=\; d\, E_{\mathbb{C}P^n}(\gamma).$$

The first critical energy is $c_1 = 2\pi^2 R^2$ on both spaces, by Thm. 4.63. Division by c_1 proves (146) at this scale. Both normalized energies are invariant under constant metric rescalings, proving the identity in general.

Since stage m is the sublevel $\varepsilon \leq m^2$, its image has normalized energy at most dm^2. The least nonnegative integer j with $j^2 \geq dm^2$ is $j = \lceil m\sqrt{d} \rceil$. For sharpness, take the m-fold projective geodesic

$$\gamma_m(t) = [\cos(\pi m t) : \sin(\pi m t) : 0 : \cdots : 0].$$

Its normalized energy is m^2, so its image has normalized energy exactly dm^2 and belongs to no earlier target stage. More precisely, for every $j \geq 0$,

$$(L_\infty \nu_d)^{-1}(L_j \mathbb{C}P^{N_d}) = \{\gamma : \varepsilon_{\mathbb{C}P^n}(\gamma) \leq j^2/d\}. \tag{148}$$

Composition commutes with loop rotation. The maps and the sharpness assertion therefore pass to the Borel constructions over BS^1. □

Proposition 4.87 (Nonconstant critical loops do not remain critical)**.** *For $d > 1$, the image under ν_d of any nonconstant critical loop of $\mathbb{C}P^n$ is not a critical loop of $\mathbb{C}P^{N_d}$. If $d = s^2$ is a square, an m-fold source geodesic has image energy equal to the target critical value c_{sm}, but its image is still not critical.*

Proof. Choose the common scale R. An m-fold primitive projective geodesic has least positive period $1/m$ and energy $m^2 c_1$. Because ν_d is injective, its image has exactly the same least period: equality of image values is equivalent to equality of source values. If the image were a closed geodesic, the classification in Thm. 4.63 would therefore make it an m-fold primitive geodesic, with energy $m^2 c_1$. Its actual energy is $dm^2 c_1$ by Thm. 4.86, a contradiction when $d > 1$. For $d = s^2$, this same energy is c_{sm}; equality with a critical value does not make the loop a critical point. Criticality and the argument are unaffected by constant metric rescalings. □

Example 4.88 (The quadratic two-sphere in $\mathbb{C}P^2$)**.** For $n = 1, d = 2$, the normalized embedding is

$$\begin{aligned} \mathbb{C}P^1 &\xrightarrow{\quad\nu_2\quad} \mathbb{C}P^2 \\ [z_0 : z_1] &\longmapsto [z_0^2 : \sqrt{2}\, z_0 z_1 : z_1^2]\,. \end{aligned} \tag{149}$$

Identifying the source with the round S^2, it gives

$$L_1 S^2 \longrightarrow L_2 \mathbb{C}P^2, \qquad \mathrm{Cyc}_1 S^2 \longrightarrow \mathrm{Cyc}_2 \mathbb{C}P^2 \quad \text{over } BS^1.$$

Neither image is contained in the first target stage. Indeed the primitive source geodesic $\gamma(t) = [\cos(\pi t) : \sin(\pi t)]$ has image

$$\nu_2 \gamma(t) = [\cos^2(\pi t) : \sqrt{2}\cos(\pi t)\sin(\pi t) : \sin^2(\pi t)]$$

of normalized energy 2. This is strictly between the first two target critical values, 1 and 4, so the image is noncritical. It passes beyond the small-loop bound without reaching the second critical energy.

Example 4.89 (Linear and cubic two-spheres in $\mathbb{C}P^3$)**.** The cubic Veronese embedding is

$$\begin{aligned} \mathbb{C}P^1 &\xrightarrow{\quad\nu_3\quad} \mathbb{C}P^3 \\ [z_0 : z_1] &\longmapsto [z_0^3 : \sqrt{3}\, z_0^2 z_1 : \sqrt{3}\, z_0 z_1^2 : z_1^3]\,. \end{aligned} \tag{150}$$

The linear inclusion j of Cor. 4.67 and this cubic embedding have the same source and target, but different first-stage behavior:

$$L_1 S^2 \xrightarrow{L_\infty j} L_1 \mathbb{C}P^3, \qquad L_1 S^2 \xrightarrow{L_\infty \nu_3} L_2 \mathbb{C}P^3. \tag{151}$$

The cubic image of a primitive source geodesic has normalized energy 3, so the second map does not land in $L_1\mathbb{C}P^3$. For degree 1 the Veronese map is linear and preserves all stages; for degrees 2, 3, and 4 the smallest target stage for the first source stage is 2; for degrees 5 through 9 it is 3. These assertions also hold after cyclification.

Remark 4.90 (Making the embedding isometric does not remove the shift). Equipping the source with $d\,g_R^{(n)}$ makes ν_d an isometric embedding into $(\mathbb{C}P^{N_d}, g_R^{(N_d)})$. Its source critical energies then become $d\,c_m$, while the target critical energies remain c_m. The source's first stage is the same subspace as before, by Lem. 4.1; its image still requires target stage $\lceil\sqrt{d}\rceil$. Thus an isometric embedding can fail to preserve numbered stages, even though it preserves numerical energy sublevels. As in Rem. 4.83, the statements here concern the actual composition maps on the specified subspaces; no obstruction to a homotopic factorization through an earlier stage is asserted.

Remark 4.91 (Content established at this stage). The examples determine critical manifolds and indices, the sphere negative bundles, and the first complex-projective negative bundle. For round spheres, Thm. 4.12 also identifies the first attaching map and gives an explicit homotopy model, before and after cyclification. The comparison maps between different targets act on the actual energy subspaces: the inclusions and projective quotients preserve stage number. The Hopf projections require the sharp reindexing $m \mapsto 2m$, and degree-d Veronese embeddings require $m \mapsto \lceil m\sqrt{d}\rceil$. These maps are not asserted to be homotopy equivalences or fibrations of stages. Attaching maps at later sphere stages, corresponding projective-space models, and induced maps on homotopy groups remain for subsequent work.

References

[Bot54] R. Bott. "Nondegenerate Critical Manifolds". In: *Annals of Mathematics*. 2nd ser. 60.2 (1954), pp. 248–261. DOI: 10.2307/1969631 (cit. on pp. 3, 5).

[Bot56] R. Bott. "On the Iteration of Closed Geodesics and the Sturm Intersection Theory". In: *Communications on Pure and Applied Mathematics* 9.2 (1956), pp. 171–206. DOI: 10.1002/cpa.3160090204 (cit. on p. 3).

[Bro10] R. Brown. *Crossed modules and the homotopy 2-type of a free loop space*. 2010. arXiv: 1003.5617 [math.AT] (cit. on p. 34).

[Esc75] R. H. Escobales Jr. "Riemannian Submersions with Totally Geodesic Fibers". In: *Journal of Differential Geometry* 10.2 (1975), pp. 253–276. DOI: 10.4310/jdg/1214432793 (cit. on pp. 4, 64, 67).

[FH17] Y. Félix and S. Halperin. "Rational homotopy theory via Sullivan models: a survey". In: *Notices of the International Congress of Chinese Mathematicians* 5.2 (2017). DOI: 10.4310/ICCM.2017.v5.n2.a3. arXiv: 1708.05245 [math.AT] (cit. on pp. 42, 45, 47, 48).

[GSS26] N. Golub, H. Sati, and U. Schreiber. *On the Derivation of Twisted K-Theory from M-Theory*. 2026. arXiv: 2609.36048 [hep-th] (cit. on pp. 19, 23, 26, 42, 45, 48, 50, 52, 56).

[Hat02] A. Hatcher. *Algebraic Topology*. Cambridge University Press, 2002. URL: pi.math.cornell.edu/~hatcher/AT/AT.pdf (cit. on pp. 28, 36, 51).

[Hop31] H. Hopf. "Über die Abbildungen der dreidimensionalen Sphäre auf die Kugelfläche". In: *Mathematische Annalen* 104 (1931), pp. 637–665. DOI: 10.1007/BF01457962 (cit. on p. 67).

[Hur12] D. E. Hurtubise. "Three Approaches to Morse–Bott Homology". In: *African Diaspora Journal of Mathematics* 14.2 (2012), pp. 145–177. arXiv: 1208.5066 [math.AT] (cit. on p. 4).

[Kli78] W. Klingenberg. *Lectures on Closed Geodesics*. Vol. 230. Grundlehren der mathematischen Wissenschaften. Berlin, Heidelberg: Springer-Verlag, 1978. DOI: 10.1007/978-3-642-61881-9 (cit. on pp. 4, 6, 15, 22, 23, 25).

[KSS26] S. Kallel, H. Sati, and U. Schreiber. *Higher-Dimensional Anyons via Higher Cohomotopy*. Revised manuscript dated August 13, 2026; pinpoint references refer to this revision. 2026. arXiv: 2601.03150 [cond-mat.str-el] (cit. on pp. 37–39, 41, 42).

[Mil63] J. Milnor. *Morse Theory*. Annals of Mathematics Studies 51. Princeton University Press, 1963 (cit. on pp. 3, 5).

[Mor34] M. Morse. *The Calculus of Variations in the Large*. Vol. 18. American Mathematical Society Colloquium Publications. American Mathematical Society, 1934 (cit. on p. 3).

[MS06] J. P. May and J. Sigurdsson. *Parametrized Homotopy Theory*. Vol. 132. Mathematical Surveys and Monographs. American Mathematical Society, 2006. DOI: 10.1090/surv/132. arXiv: math/0411656 (cit. on p. 53).

[MS74] J. W. Milnor and J. D. Stasheff. *Characteristic Classes*. Vol. 76. Annals of Mathematics Studies. Princeton University Press, 1974 (cit. on pp. 53, 54).

[Oan15] A. Oancea. "Morse theory, closed geodesics, and the homology of free loop spaces". In: *Free Loop Spaces in Geometry and Topology*. Vol. 24. IRMA Lectures in Mathematics and Theoretical Physics. European Mathematical Society, 2015. DOI: 10.4171/153/2. arXiv: 1406.3107 [math.DG] (cit. on pp. 4, 6).

[ONe66] B. O'Neill. "The Fundamental Equations of a Submersion". In: *Michigan Mathematical Journal* 13.4 (1966), pp. 459–469. DOI: 10.1307/mmj/1028999604 (cit. on pp. 4, 16, 62, 67).

[Pal63] R. S. Palais. "Morse theory on Hilbert manifolds". In: *Topology* 2.4 (1963), pp. 299–340. DOI: 10.1016/0040-9383(63)90013-2 (cit. on pp. 4, 6, 15).

[Şir24] N. İ. Şirikçi. "The Morse Index for Manifolds with Constant Sectional Curvature". In: *Mediterranean Journal of Mathematics* 21, 139 (2024). DOI: 10.1007/s00009-024-02682-5 (cit. on pp. 22, 59).

[Ter] I. Terek. *Projective spaces, the Fubini–Study metric and a little bit more*. Lecture notes. URL: math-terek.github.io/texts/projective_space.pdf (visited on 10/05/2026) (cit. on p. 72).

[VB85] M. Vigué-Poirrier and D. Burghelea. "A model for cyclic homology and algebraic K-theory of 1-connected topological spaces". In: *Journal of Differential Geometry* 22.2 (1985), pp. 243–253. DOI: 10.4310/jdg/1214439821 (cit. on p. 49).

[VS76] M. Vigué-Poirrier and D. Sullivan. "The homology theory of the closed geodesic problem". In: *Journal of Differential Geometry* 11.4 (1976), pp. 633–644. DOI: 10.4310/jdg/1214433729 (cit. on p. 45).

[Zil77] W. Ziller. "The free loop space of globally symmetric spaces". In: *Inventiones Mathematicae* 41.1 (1977), pp. 1–22. DOI: 10.1007/BF01390161 (cit. on pp. 4, 22, 59, 62).